

(1124)

DEVELOPMENT OF THE
VARIABLE-GAP TECHNIQUE FOR
MEASURING THE THERMAL CONDUCTIVITY
OF FLUORIDE SALT MIXTURES

J. W. Cooke



OAK RIDGE NATIONAL LABORATORY

OPERATED BY UNION CARBIDE CORPORATION • FOR THE U.S. ATOMIC ENERGY COMMISSION

MASTER

RECORDED BY OPTICAL SCANNING SYSTEM

Printed in the United States of America. Available from
National Technical Information Service
U.S. Department of Commerce
5285 Port Royal Road, Springfield, Virginia 22151
Price: Printed Copy \$3.00; Microfiche \$0.95

This report was prepared as an account of work sponsored by the United States Government. Neither the United States nor the United States Atomic Energy Commission, nor any of their employees, nor any of their contractors, subcontractors, or their employees, makes any warranty, express or implied, or assumes any legal liability or responsibility for the accuracy, completeness or usefulness of any information, apparatus, product or process disclosed, or represents that its use would not infringe privately owned rights.

ORNL-4831
UC-80 - Reactor Technology

Contract No. W-7405-eng 26

Reactor Division

DEVELOPMENT OF THE VARIABLE-GAP TECHNIQUE FOR MEASURING
THE THERMAL CONDUCTIVITY OF FLUORIDE SALT MIXTURES

J. W. Cooke

FEBRUARY 1973

NOTICE

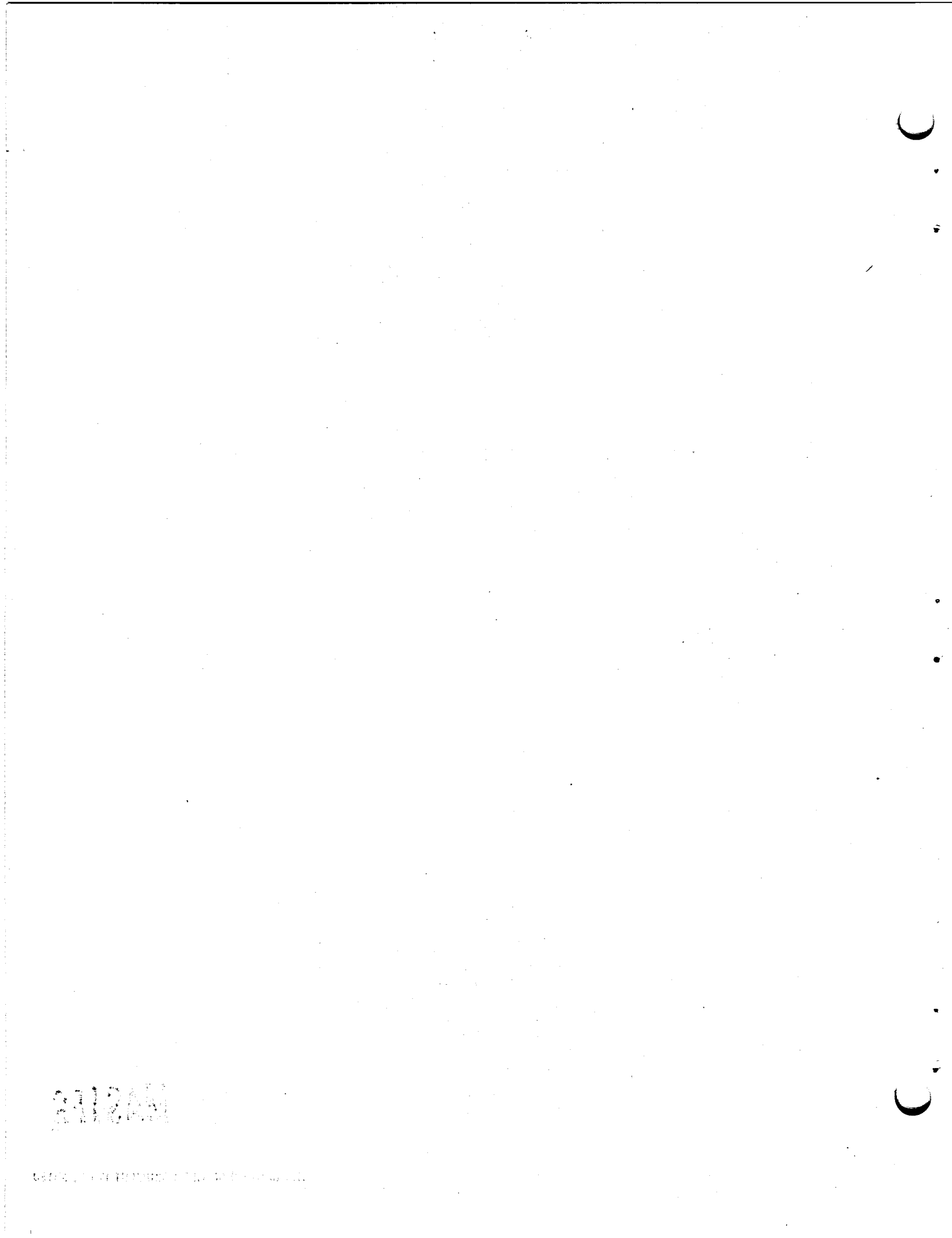
This report was prepared as an account of work sponsored by the United States Government. Neither the United States nor the United States Atomic Energy Commission, nor any of their employees, nor any of their contractors, subcontractors, or their employees, makes any warranty, express or implied, or assumes any legal liability or responsibility for the accuracy, completeness or usefulness of any information, apparatus, product or process disclosed, or represents that its use would not infringe privately owned rights.

OAK RIDGE NATIONAL LABORATORY
Oak Ridge, Tennessee 37830
operated by
UNION CARBIDE CORPORATION
for the
U.S. ATOMIC ENERGY COMMISSION

MASTER

DISTRIBUTION OF THIS DOCUMENT IS UNLIMITED

fey



CONTENTS

	<u>Page</u>
NOMENCLATURE	v
ABSTRACT	1
1. INTRODUCTION	1
2. METHODS FOR MEASURING MOLTEN-SALT THERMAL CONDUCTIVITIES	2
Selected Techniques for Fluids	3
Transient hot wire	3
Transient hot foil	4
Necked-down sample technique	4
Laminar heat flow	5
Parallel wall	5
The Variable-Gap Technique	6
General description	6
Idealized model	7
Effect of radiation	9
Effect of natural convection	12
Effect of heat shunting	16
Method of calculation	19
3. EXPERIMENTAL APPARATUS	22
Thermal Conductivity Cell	22
Furnace	30
Electrical System	30
Instrumentation	32
4. EXPERIMENTAL PROCEDURES	33
Preliminary Procedures	33
Operating Procedure - Fluid Specimen	34
Operating Procedure - Solid Specimen	34
5. EXPERIMENTAL RESULTS	34
Thermal Resistance Curves	35
Thermal Conductivity	40

6. DISCUSSION OF THE RESULTS	40
Comparison with Published Values	40
Comparison with Theory	42
Uncertainties in the Results	43
Adequacy of the Experimental Apparatus	44
7. CONCLUSIONS	45
ACKNOWLEDGMENTS	45
REFERENCES	46
APPENDIX A. ADDITIONAL DETAILS OF THE DESIGN OF THE APPARATUS	51
APPENDIX B. EXPERIMENTAL DATA	55
APPENDIX C. PRECISION AND ERROR ANALYSIS	99

NOMENCLATURE

C_p	Specific heat, constant pressure, cal $\text{g}^{-1} (\text{°C})^{-1}$
D	diameter of main heater assembly, cm
E	ratio of effective to total heater wire length
F	heat shunting factor
G	Guard heater factor
g	Acceleration due to gravity, cm sec^{-2}
h_r	Radiant heat-transfer coefficient, $\text{W cm}^{-2} (\text{°C})^{-1}$
I	Current, amps
k	Thermal conductivity of specimen, k_m is that of the metal cylindrical solid, $\text{W cm}^{-1} (\text{°C})^{-1}$
\bar{n}	Mean index of refraction
Q/A	Heat flux, W cm^{-2}
Q'/A	Measured heat flux uncorrected for heat shunting, W cm^{-2}
R	Radius of cylindrical solid, cm
T	Temperature, °C ; $T_K = \text{°K}$
ΔT	Temperature difference between upper and lower plates of the conductivity cell, °C
$\frac{\Delta T}{(Q/A)_0}$	Thermal resistance at zero specimen thickness, $\text{°C W}^{-1} \text{ cm}^2$
U	Heat-transfer coefficient, $\text{W cm}^{-2} (\text{°C})^{-1}$
V	voltage, volts
v	Integration variable
x, Δx	Specimen or gap thickness, cm
Y	Radiative function defined in Eq. (8)
α	Coefficient of linear expansion, $(\text{°C})^{-1}$
β	Coefficient of bulk expansion, $(\text{°C})^{-1}$
ϵ	Emissivity of cylinder surface
$\bar{\kappa}$	mean absorption coefficient for radiant heat, cm^{-1}
μ	Viscosity, cP
ρ	Density, g cm^{-3}
σ	Stefan-Boltzmann constant, $\text{W cm}^{-2} (\text{°K})^{-4}$
τ	Optical thickness
Ω	Electrical resistance, ohms

Dimensionless Moduli

N_{Gr}	Grashof number, $g\rho^2\beta \Delta T x^3/g_c \mu^2$
N_{Pr}	Prandtl number, $C_p \mu/k$
N_{Ra}	Rayleigh number, $N_{Gr} \cdot N_{Pr}$
N_{Re}	Reynolds number, $\rho V D / \mu$

Subscripts

f	film
c	critical
m	metal
o	at specimen thickness = 0
s	specimen
x	at specimen thickness = x

DEVELOPMENT OF THE VARIABLE-GAP TECHNIQUE FOR MEASURING
THE THERMAL CONDUCTIVITY OF FLUORIDE SALT MIXTURES

J. W. Cooke

ABSTRACT

The development and evaluation of the variable-gap technique for measuring the thermal conductivity of molten fluoride salts is described. A series of measurements were made of the conductivities of several substances (Ar, He, H₂O, Hg, and liquid and solid heat-transfer salt) over a wide range of conductivities [0.4×10^{-3} to $100 \times 10^{-3} \text{ W cm}^{-1} (\text{°C})^{-1}$] and temperatures (40 to 950°C). The deviations of the results from published values averaged $\pm 5\%$. The study demonstrates the accuracy and outstanding versatility of the variable-gap technique.

Key words: thermal conductivity, development, design, measurement, fused salts, high temperature, MSBR.

1. INTRODUCTION

High-temperature operations in the chemical processing and nuclear industries have created a need for economical, efficient heat-transfer media whose thermal properties are superior to those of organic and gaseous coolants. Molten-salt mixtures have good heat-transfer properties compared with organic liquids, and their relative inertness and low vapor pressure give them distinct advantages over liquid metals. They are applied in high-temperature fluxes, heat-treatment baths, and electrolytic fuel cells, and as the fuel carrier and coolant for nuclear reactors, such as the Molten-Salt Breeder Reactor (MSBR) experiments.¹ This report describes an experimental technique for determining a key thermal property of molten salts — thermal conductivity. The study evaluates the method over a broad temperature range using a variety of materials representing a wide range of conductivities.

Very few data on the thermal conductivities of molten salts, in particular, fluoride salts, have been published. Most of the existing measurements for molten fluoride salt mixtures were made by members of the MSBR group at Oak Ridge National Laboratory (ORNL) over 15 years

ago.² To extend the scope of the previous measurements, we have developed an absolute, variable-gap technique to determine the thermal conductivity of fluoride salt mixtures in liquid and solid states at temperatures to 1000°C. This technique is particularly well suited to the measurement of the conductivity of low-conducting, semitransparent fluids that must be contained in inert surroundings at elevated temperatures. Most other applicable methods suffer from one or more deficiencies if used under these conditions.

The variable-gap technique is examined in detail and other techniques are discussed briefly. The development of an experimental apparatus is described, and experimental results are presented for the conductivities of several calibrating fluids: Ar, He, heat-transfer salt* (HTS), H₂O, and Hg. These fluids represent a very wide range of conductivities [0.4×10^{-3} to $100 \times 10^{-3} \text{ W cm}^{-1} (\text{°C})^{-1}$] which were measured over a large temperature range (40 to 950°C). The thermal conductivities of molten fluoride salts will be presented in a separate report to be published.

2. METHODS FOR MEASURING MOLTEN-SALT THERMAL CONDUCTIVITIES

Thermal conductivity is one of the most difficult of all thermo-physical properties to determine experimentally. The difficulties primarily are due to the unreliability of temperature measurements, the inadequacy of thermal insulation, and the simultaneous transfer of heat by mechanisms other than conduction. Conductivity can be measured by either steady-state, quasi-steady-state, or transient-state heat flow systems. Experimental determinations using the steady-state methods depend upon the attainment of suitable boundary conditions that will allow the Laplace equation to be solved for the temperature distribution. The conductivity is then calculated from the Fourier heat-transfer equation. The transient method requires the solution of the diffusion equation with suitable initial and boundary conditions for the thermal diffusivity coefficient; the density and heat capacity must be known to calculate the conductivity. The quasi-steady-state methods are based on a solution of

* KNO₃-NaNO₂-NaNO₃ (44-49-7 mole %).

the diffusion equation for unique initial and boundary conditions such that the thermal conductivity can be directly determined.

In addition to conduction, radiation also may be present with transparent substances, and the experimental technique must be capable of identifying and separating these two mechanisms. In the case of fluids, convection may also be present. Thus, only a limited number of experimental techniques are available for the determination of the conductivity of fluids. Several techniques found in published investigations are described briefly in the following section, and the technique used in the present studies is described in a later section.

Selected Techniques for Fluids

We will describe briefly each technique and discuss its advantages and disadvantages for the measurement of conductivity of molten salts.

Transient hot wire

In this technique, the rate of change of temperature of a line heat source situated in an infinite medium is used to determine the conductivity of the medium. The line heat source consists of a wire (1 to 5 mils diam) placed axially in a cylinder (2 to 4 cm diam) filled with the specimen. The wire is heated by a steady current, and its temperature is determined by the change in its electrical resistivity. After an initial transient heating period, the log temperature becomes a linear function of time until natural convection begins to occur. The slope of this linear function of temperature with time can be related directly to the conductivity of the specimen. Thus, this technique is a quasi-steady-state technique rather than a transient technique. It is a common technique for determining conductivity of liquids and has been described in many publications.³⁻⁵

Its simplicity, quickness, precision, and accuracy make this technique useful for most liquids. With molten salts, however, a significant amount of current can be shunted through the salt itself due to the relatively high electrical conductivity of the molten salts at elevated temperatures. Since the degree of current shunting is very difficult to

predict, molten salt conductivity results obtained by this technique are subject to questions which have not been sufficiently resolved to make it suitable for this application.⁶

Transient hot foil

This technique^{7,8} is similar to the transient hot-wire technique except in two respects: (1) a thin foil is substituted for the fine wire to provide a plane heat source instead of a line source, and (2) the temperature is measured with a front-wave-shearing laser interferometer. Because this temperature measuring technique is extremely sensitive, the heat flux from the foil can be greatly reduced. However, the fluid specimen must be transparent as well as compatible with the material used in the cell window.

The transient hot-foil method is more difficult to apply than the transient hot-wire technique. Its primary advantage is in the reduction in the molten-salt ionization that results from a lower voltage along the heat source. Consequently, the interface between the heated foil and the molten salt remains polarized and the flow of current into the salt is minimized. In practice, however, other voltage potentials may exist within the cell, and some current will flow into the salt even though the surfaces are polarized. Moreover, operation at elevated temperatures presents formidable problems in the design and choice of materials for the cell windows. Diamond is the only transparent material suitable for use with molten fluoride salts at high temperatures, but its high cost and fabrication difficulties would restrict its use to very small apertures.

Necked-down sample technique

This method⁹ is based on the measurement of the steady-state change in resistance caused by electrical heating of a narrow bridge of the sample material which joins two larger bodies of the same material. The theory describing this phenomenon shows that the change in resistance expressed by the voltage drop caused by the heating current does not depend on the detailed shape of the narrow region. A necessary condition, if this is to be true, is that no significant flow of heat occur outside of the boundaries of the sample. For liquids, the narrow bridge is

maintained by containing the liquid in a vessel separated into two parts by a thin wall with a small aperture. The material of the wall must have both a high thermal and a high electrical resistance. The technique is classified as a quasi-steady-state method.

Several uncertainties are associated with the method, the first of which is the loss of heat by conduction along the thin separating wall. A second major problem arises from the possibility of convection. Moreover, with molten salts the possibility of polarization effects also would need to be considered. The important advantages of the technique are the simplicity of the apparatus, the rapidity with which the measurements can be made, and the reduction in the uncertainties in radiation by the small size of the heated region.

Laminar heat flow

The laminar flow method determines the conductivity of a fluid flowing in a circular tube under carefully defined conditions. The wall temperature of the tube is maintained uniform while the inlet and outlet temperatures of the fluid are measured. In this method, radiation losses can be neglected and the troublesome measurement of heat flux eliminated. The main problems concern the prediction of velocity and temperature profiles of the fluid at the entrance section of the tube and maintaining a uniform wall temperature. Furthermore, the assumption of constant physical properties of the fluid over the temperature range can introduce significant error. Most of the published results of this technique differ from the accepted values for thermal conductivity because the hydrodynamic and thermal entry lengths were not properly assessed.¹⁰

Parallel wall

With this method, the steady heat flow through the specimen and the temperature drop across it are measured.¹¹⁻¹³ The specimen is contained between two parallel walls of plane, cylindrical, or spherical geometry. This method is the most commonly used technique for measuring thermal conductivity. Its simplicity with regard to the analytic model and experimental setup make it most attractive; however, the uncertainties caused by convection, radiation, and stray heat flow at high temperatures

can be considerable. Reducing the heat flow uncertainties by decreasing the specimen thickness and temperature drop can lead to large errors in these two measurements as well as in the heat flow. Thus, although the method is simple, it requires care in application and may be unsuitable for low-thermal conductivity fluids at high temperatures.¹²

The Variable-Gap Technique

The variable-gap technique for measuring conductivity is a significant improvement over the parallel wall method in that it takes advantage of the fluidity of the specimen. By use of this technique the specimen thickness can be varied continuously during the operation with a minimum disturbance to the specimen composition or to the system temperature distribution. Also by varying the specimen thickness, the undesirable effects of several factors, including the errors caused by specimen voids or inhomogeneities, natural convection, radiative heat transfer, corrosion, deposit formation, radial heat flow, thermocouple location, and thermocouple drift, can be greatly reduced. Since only the change in the specimen thickness and the change in the temperature across the specimen is measured, the potential errors of these measurements are smaller and the influence of convection, radiation, and heat losses can be detected and minimized. In addition, the apparatus can be used with little or no modification to measure the conductivities of solids and gases as well as liquids. Considering the advantages of the method, it is surprising that only limited use has been made of the variable-gap technique.^{12,14,15}

General description

The experimental apparatus is shown schematically in Fig. 1. Heat from the main heater travels downward through the liquid sample region (labeled "variable gap" in the figure) to a heat sink. Heat flow in the upward and radial directions is minimized by appropriately located guard heaters, and the heat flux into the sample is measured by the voltage and current of the dc power to the main heater. The temperature drop across the gap is determined by thermocouples located on the axial center line in the metal surfaces defining the sample region. The sample thickness is varied by moving the assembly containing the main heater and is measured

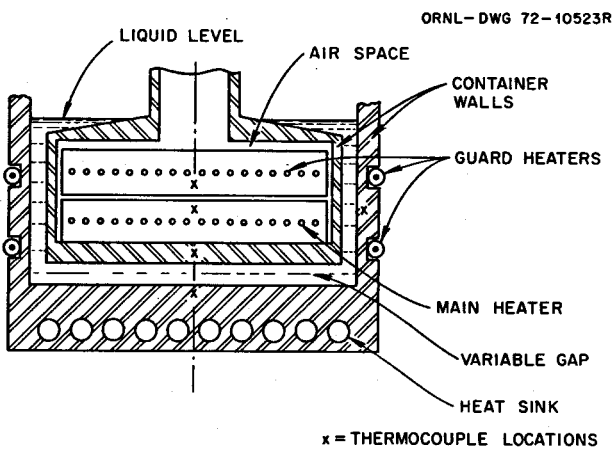


Fig. 1. Schematic drawing of a variable-gap thermal conductivity cell.

by a precision dial indicator. The system temperature level is maintained by a surrounding zone-controlled furnace.

Idealized model

The measured temperature difference can be resolved into the temperature drop across the sample gap; the temperature drops in the metal walls defining the test region; the temperature drops in any solid or gaseous films adhering to the metal surfaces; and errors associated with thermocouple calibration, lead-wire inhomogeneities in thermal gradient regions, and instrument malfunctions. Neglecting the error term, we can write

$$\Delta T = \Delta T_s + \Delta T_m + \Delta T_f , \quad (1)$$

where subscripts are sample, metal, and surface film, respectively.

For the sample region, the temperature difference is

$$\Delta T_s = (Q/A) \Delta x_s / k_s , \quad (2)$$

where Q/A is the heat flux, Δx_s is the gap width, and k_s is the thermal conductivity of the liquid sample. It is assumed that no natural convection exists in the sample region.

Similarly, the temperature drop in the confining horizontal metal walls can be written

$$\Delta T_m = (Q/A) \Delta x_m / k_m , \quad (3)$$

where Δx_m is the heat-flow path length in the metal walls, and k_m is the wall conductivity. The heat flux Q/A is the same as in Eq. (2), assuming that no radial heat flow and no bypass heat flow through the side (vertical) walls of the sample cup. Since k_m is a function of temperature, Eq. (3) can be written separately for the upper and lower metal walls; however, for the purposes of this analysis, the two regions are combined.

The film temperature difference is of the same form as the ΔT 's given in Eqs. (2) and (3). If surface films are present but of constant and known thickness, Δx_f , during the experiment, there is no effect on the derived sample conductivity or on the associated error. However, a film that grows or decays in an unknown way during the course of the measurement introduces an error in Δx_s .

Combining the above expressions, we obtain:

$$\Delta T = \frac{Q}{A} \left(\frac{\Delta x_s}{k_s} + \frac{\Delta x_m}{k_m} + \frac{\Delta x_f}{k_f} \right) ,$$

or

$$\frac{\Delta T}{Q/A} = \left(\frac{1}{k_s} \right) \Delta x_s + \left(\frac{\Delta x_m}{k_m} + \frac{\Delta x_f}{k_f} \right) , \quad (4)$$

or, simplifying the notation,

$$\frac{\Delta T}{Q/A} = \left(\frac{1}{k} \right) \Delta x + \left(\frac{\Delta T}{Q/A} \right)_0 , \quad (5)$$

where $[\Delta T/(Q/A)]_0$ combines all the fixed resistances. This is of the form,

$$y = ax + b , \quad (6)$$

where a is the slope of this linear expression and is the reciprocal of the sample conductivity. The intercept b combines all other resistances. In operating the apparatus, Q/A is kept constant and ΔT is recorded as Δx is varied. If other modes and paths of heat transfer exist within the specimen, the thermal resistance will not be a linear function of the

specimen thickness. However, the effect of these other forms of heat transfer will be reduced as the specimen thickness is decreased. Thus, the conductivity can be determined from the reciprocal slope evaluated at zero specimen thickness.

Another approach to the determination of the sample conductivity can be obtained by rearranging Eq. (6) as:

$$k = \frac{1}{a} = \frac{x}{y - b} . \quad (7)$$

Again, if other modes and paths of heat transfer exist within the specimen, the value of conductivity obtained from Eq. (7) will be the effective value which will approach the true value only as the specimen thickness approaches zero.

Effect of radiation

Many investigators consider only the radiation emitted by the wall surfaces when evaluating the heat transfer through a medium separating the walls. This assumption may be correct when the medium is a gas whose mean absorption coefficient $\bar{\kappa}$ is small and whose mean refraction index \bar{n} is near unity. Many media, however, absorb and emit significant amounts of radiation. This internal radiation can contribute more to the heat transfer from wall to wall than the radiation emitted by the wall surfaces. Indeed, even at room temperature, the heat transferred by radiation can approach 5% of that transferred by conduction in some organic fluids whose specimen thickness is as small as 0.1 cm.

If some simplifying assumptions are made, an expression for the radiant heat transfer can be derived. These assumptions are the existence of a constant temperature gradient within the medium and the use of mean values \bar{n} and $\bar{\kappa}$ independent of wavelength. The following equation was derived by Poltz^{16,17} for the radiant heat flux:

$$\frac{Q_r}{A} = \frac{16}{3} \frac{\bar{n}^2}{\bar{\kappa}} \sigma T^3 \left(\frac{\Delta T}{\Delta x} \right) Y , \quad (8)$$

where

$$Y = \frac{3}{\tau} (2 - \epsilon) \int_0^1 \frac{1 - \exp [-(\tau/v)]}{1 + (1 - \epsilon) \exp [-(\tau/v)]} v^3 dv ,$$

and

τ = optical thickness of the medium = $\kappa \Delta x$,

T = average medium temperature, °K,

ϵ = emissivity of the wall surface,

σ = Stefan-Boltzmann constant, $5.71 \times 10^{-12} \text{ W cm}^{-2} (\text{°K})^{-4}$,

v = dummy integration variable.

In Fig. 2, where Y is plotted as a function of τ for various values of ϵ , the curve for $\epsilon = 0$ represents the hypothetical case in which the radiation heat transfer between the walls is accomplished solely by the inner radiation within the medium. The distance between the curve for $\epsilon = 0$ and one of the upper curves (the appropriate plate emissivity

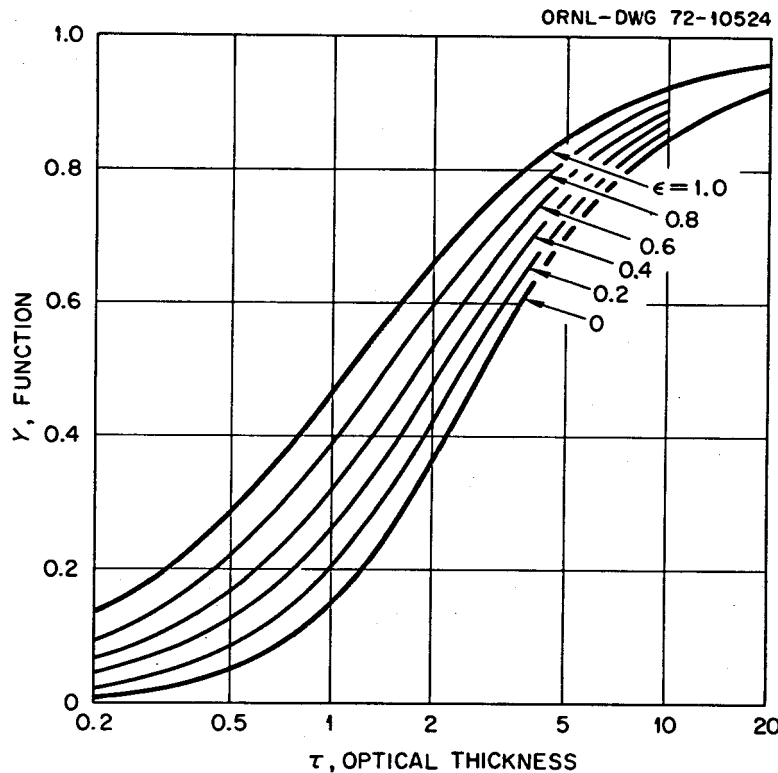


Fig. 2. Radiative function (Y) vs plate emittance and optical thickness of the specimen.

curve) represents the contribution of the radiation emitted by the wall surfaces to the total radiated heat flow from wall to wall.

Equation (8) can be combined with the previously derived Eq. (5) to obtain an expression for the total thermal resistance across a medium separated by two parallel walls when the heat is being transferred simultaneously by conduction and radiation. That is,

$$\frac{\Delta T}{Q/A} = \left(\frac{1}{k + \frac{16}{3} \bar{n}^2 \sigma T^3 Y} \right) \Delta x + \left(\frac{\Delta T}{Q/A} \right)_0 . \quad (9)$$

In the limiting case where the optical thickness τ approaches zero (i.e., very small infrared-absorbing medium),

$$Y_{\tau \rightarrow 0} = \frac{3}{4} \epsilon_r \tau \quad (\text{Ref. 16}) ,$$

where

$$\epsilon_r = \left(\frac{1}{\epsilon_1} + \frac{1}{\epsilon_2} - 1 \right)^{-1} = \frac{\epsilon}{2 - \epsilon}$$

for

$$\epsilon = \epsilon_1 = \epsilon_2 .$$

Thus, Eq. (9) simplifies to

$$\frac{\Delta T}{Q/A} = (k + 4 \bar{n}^2 \epsilon_r \sigma T^3 \Delta x)^{-1} \Delta x + \left(\frac{\Delta T}{Q/A} \right)_0 . \quad (10)$$

Figure 3 is a plot of the thermal resistance as a function of specimen thickness for various values of the absorptivity coefficient for a specimen assumed to have a $k = 0.0034 \text{ W cm}^{-1} (\text{°C})^{-1}$, $\bar{n} = 1.5$, $\epsilon_{\text{wall}} = 0.5$, and $T = 1000^\circ\text{C}$. For these values of conductivity and temperature, the percentage of heat transferred by radiation is quite large. As the absorption coefficient \bar{k} decreases from $\bar{k} = \infty$ (pure conduction) to $\bar{k} = 0$, the percentage of radiated heat increases to a maximum at about $\bar{k} = 2$ and decreases until $\bar{k} = 0$. Within the interval $\infty > \bar{k} > 0$ these curves have

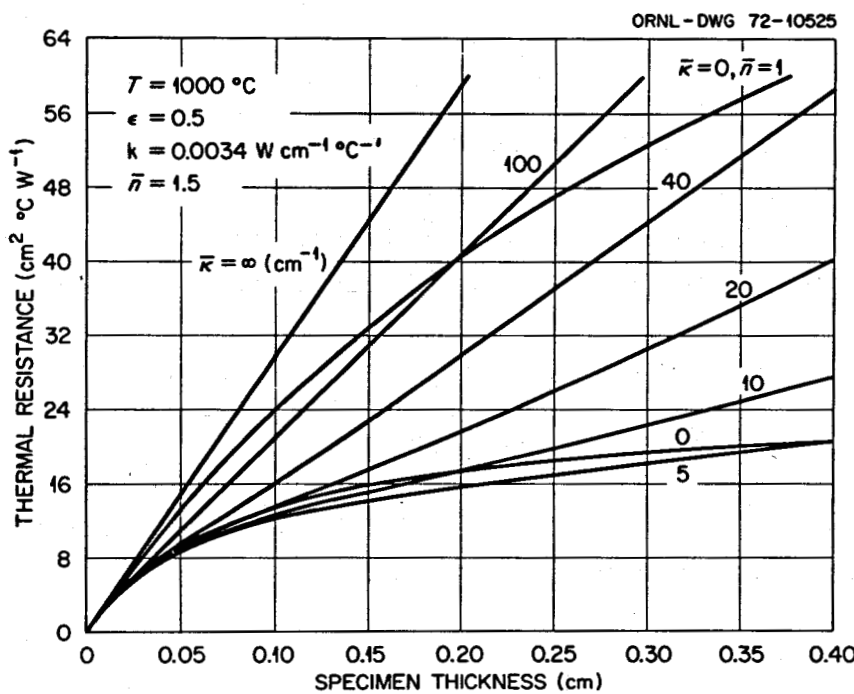


Fig. 3. Thermal resistance of an infrared absorbing fluid having assumed properties at various values of absorptivity, κ (cm^{-1}) vs specimen thickness.

an inflection point producing what could be described as "lazy S" curves. Also shown in Fig. 3 is the resistance curve for a gas whose absorptivity is near zero and whose index of refraction is near one. If the optical properties of a specimen are known, Eq. (9) can be fitted to the experimental data to obtain the slope (and thus the conductivity) at a specimen thickness approaching zero; however, the mean optical properties must be used and the temperature gradient within the specimen must be nearly linear.

Effect of natural convection

Under ideal conditions, no natural convection would be expected in a fluid enclosed between two horizontal, parallel plates with one-dimensional downward heat flow. In the real situation, however, small departures from the ideal conditions can initiate and sustain convection currents within the fluid. If the plates are not horizontal or parallel or if a temperature gradient exists in the horizontal direction, convection cells can

occur. If, in addition, the vertical temperature distribution within the specimen is not linear, but distorted by interfluid infrared absorption, the natural convection can be enhanced. Finally, vibrations, especially those in resonance with the natural frequency of the enclosed fluid, can induce and enhance natural convection.

In order to initiate and sustain buoyancy convection cells within enclosed spaces, certain instability criteria must be satisfied. Rayleigh was one of the first investigators to recognize that the instability criterion could be related to certain limiting values of the dimensionless moduli N_{Ra} known as the Rayleigh number, which is

$$N_{Ra} = N_{Gr} N_{Pr} = \left(\frac{g \rho^2 \beta \Delta T \Delta x^3}{g_c \mu^2} \right) \left(\frac{C_p \mu}{k} \right), \quad (11)$$

where

- g = local acceleration due to gravity, cm/sec^2
- g_c = dimensional constant = $1.0 \text{ g cm dyne}^{-1} \cdot \text{sec}^{-2}$,
- ρ = density of fluid, g/cm^3 ,
- μ = viscosity, cP,
- x = gap distance, cm,
- k = thermal conductivity, $\text{W cm}^{-1} (\text{°C})^{-1}$,
- C_p = (specific) heat at constant pressure, cal $\text{g}^{-1} (\text{°C})^{-1}$,
- β = coefficient of bulk expansion, $(\text{°C})^{-1}$

The Rayleigh number, in essence, is the ratio of the product of the buoyancy and inertial forces to the viscous forces. The limiting value of the Rayleigh number to initiate and sustain convection cells has been calculated to be 1700 when the fluid layer is bound on both sides by solid parallel and horizontal walls and is heated from below.¹⁸ Recent experimental studies by Norden and Usmanov¹⁹ using an interferometer technique show, however, that the departure from conductive to convective mode of heat transfer can occur at $N_{Ra} < 1700$ for small specimen thicknesses.

Figure 4 shows a portion of the data taken from the above experimental studies in which the critical temperature difference, ΔT_c (the temperature difference above which convection occurs), is plotted as a

ORNL-DWG 72-10526

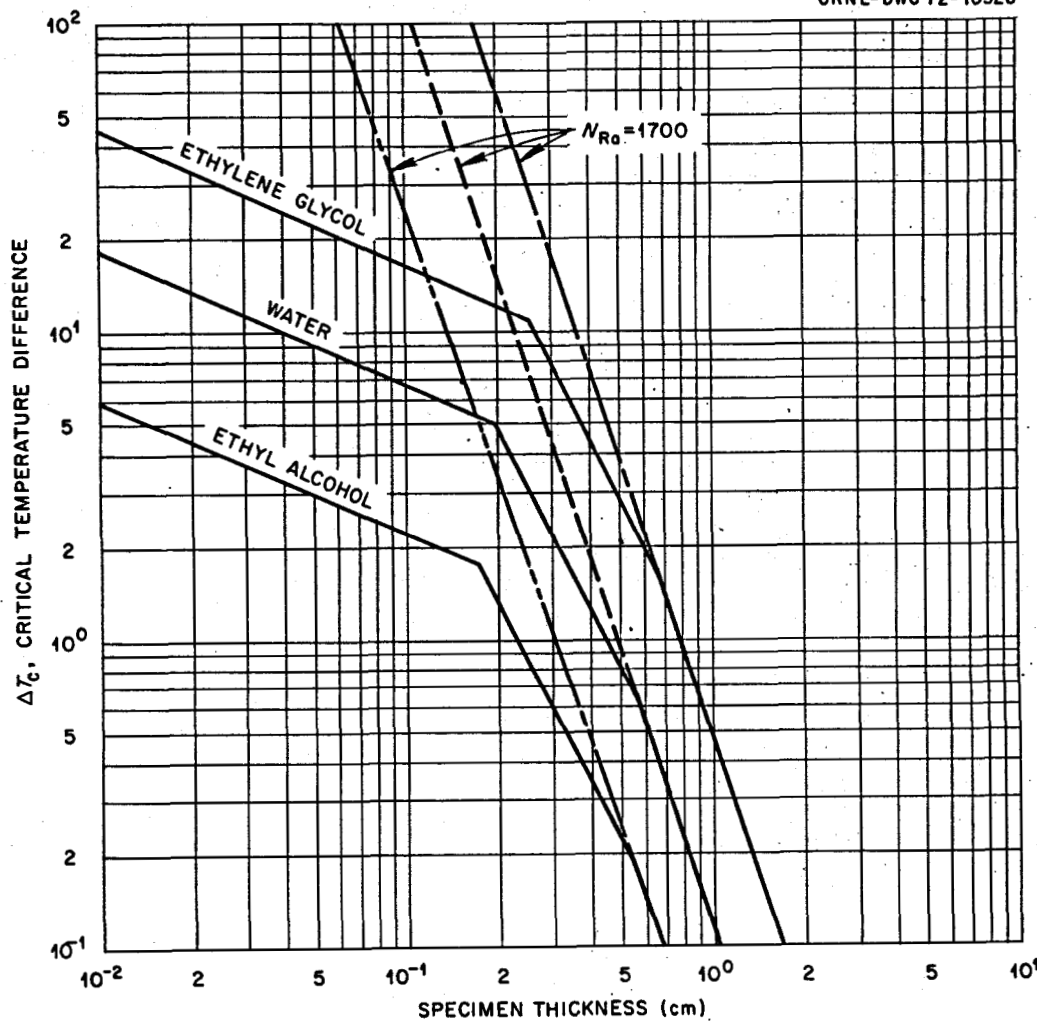


Fig. 4. Critical temperature above which convection occurs as a function of specimen thickness for three liquids showing the departure from theoretical criteria, $N_{Ra} = 1700$.

function of the specimen thickness for three liquids: ethylene glycol, water, and ethyl alcohol. Also shown plotted are the curves for the theoretical values of $N_{Ra} = 1700$. The area below each of the curves plotted in Fig. 4 is stable (i.e., conduction only) and above the curves is unstable (i.e., convection occurs). The experimental data can be seen to have two linear slopes ($n = 0.45$ and 2.0) which merge with the theoretical curve ($n = 3$) where

$$\Delta T_c \Delta x^n = \text{constant} .$$

The $N_{Ra} = 1700$ criteria could lead to a gross overestimate of ΔT_c for small specimen thicknesses.

Heat-transfer measurements made during Norden and Usmanov's studies showed the ratio of the effective conductivity to the true conductivity for water to be 1.10 at a specimen thickness of 0.15 cm and an N_{Ra} of only 260. Thus, considerable care must be exercised to prevent natural convection in fluids contained between parallel plates heated from below as well as inclined, cylindrical, and spherical annuli heated from either side.

A similar experimental study by Berkovsky and Fertman²⁰ was made recently in which the specimen was heated from above and had a non-uniform upper plate temperature distribution. This study showed that when the nonuniformity of the temperature ($T_{max} - T_{min}$) exceeded a certain value with respect to the lower plate temperature T_o , no convection occurred. It was found that if

$$\frac{T_{max} - T_{min}}{T_{max} - T_o} \approx 1 ,$$

no significant convection occurs at a Rayleigh number of less than 10^4 .

No experimental results are reported for the amount of convection taking place when the specimen is heated from above and the plates are not exactly parallel or are slightly tilted. If we consider this case analogous to the Berkovsky and Fertman study, convection would be avoided at an N_{Ra} of less than 10^4 if the ΔT of the tilted layer above that of the horizontal layer did not exceed that of the average ΔT across the plates. Since $\Delta T \propto \Delta x$, the difference in the edge-to-edge separation distance between the plates with respect to each other, or with respect to the horizontal, should not exceed their average separation distance.

To minimize convection due to vibrations, the conduction cell should be well isolated from all sources of vibrations, particularly those within the resonance frequency of the cell.

Effect of heat shunting

Some shunting of heat around the specimen is unavoidable even for the most carefully designed thermal conductivity cells. The percent of shunted heat as compared to heat flow through the specimen can be minimized by careful use of insulating materials, by guard heating, by using large cell diameter to thickness ratios, and by using zoned heat sources and sinks. The shunting problems becomes most acute for low-conductivity specimens at elevated temperatures.

The apparatus described in the present report is designed to minimize the shunting error with specimens having estimated thermal conductivities in the range of 0.05 to $0.10 \text{ W cm}^{-1} (\text{ }^{\circ}\text{C})^{-1}$. The cell wall thickness and the ratio of cell diameter to sample thickness are optimized to reduce the heat shunted to less than 1% of the total heat flow in the absence of heat guards. Unfortunately, the conductivities of the salts of interest to the MSBR program were found to be an order of magnitude lower than the range for which the apparatus was designed. As a result, the radial guard heating was not adequate in a few cases to prevent some heat shunting, and corrections were required.

Figure 1 shows the complexity of the possible heat-transfer modes and paths within the conductivity cell. Since neither the temperature distribution along the cell wall nor the heat-transfer coefficients are well known, the simplified model shown in Fig. 5 was selected as an appropriate model for calculating the amount of heat shunting in the system.

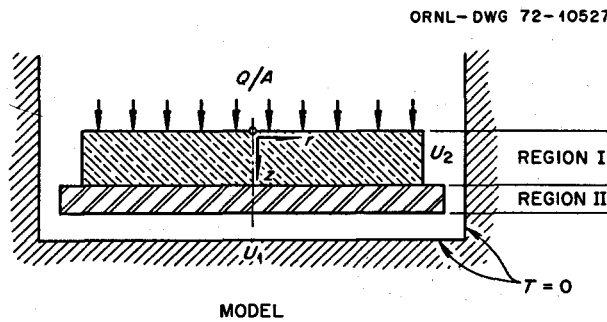


Fig. 5. Model of the conductivity cell for heat shunting calculation.

By assuming a uniform heat flux and a uniform sink and wall temperature equal to 0°C, an easy solution for the center-line heat flux may be obtained from the generalized heat conduction equation [Eq. (12)]. The radial heat-transfer coefficient U_2 may then be decreased to account for the guard heating.

The temperature distribution within the cylindrical solid can be described by the general heat conduction equation,

$$\frac{\partial^2 T}{\partial r^2} + \frac{1}{r} \frac{\partial T}{\partial r} + \frac{\partial^2 T}{\partial z^2} = 0 , \quad (12)$$

where T is the temperature (°C) and r and z are the radial and axial coordinates (cm) measured as shown in Fig. 5. Dividing the model into two regions, the boundary conditions for either region can be written:

$$k' \frac{\partial T(r,0)}{\partial z} = -C , \quad (13)$$

$$k' \frac{\partial T(r,L)}{\partial z} = -U_1 [T(r,L)] , \quad (14)$$

$$k' \frac{\partial T(R,z)}{\partial r} = -U_2 [T(R,z)] , \quad (15)$$

where k' is the conductivity [$\text{W cm}^{-1} (\text{°C})^{-1}$] of the cylindrical solid within the region, L is the thickness of the solid (cm), R is the radius (cm), C is a constant, and U_1 and U_2 are the axial and radial overall heat-transfer coefficients respectively.

The solution of Eq. (12) for the ratio of the axial center-line heat fluxes entering and leaving region I, using the above boundary conditions, is

$$F_I \equiv \frac{Q/A(0,0)}{Q/A(0,L)} = \sum_n \frac{2a_n J_1(a_n)}{(N_2 + a_n^2) J_o^2(a_n)} \times \left(\cosh \frac{a_n L}{R} - D_n \sinh \frac{a_n L}{R} \right) , \quad (16)$$

where

$$D_n = \frac{N_1 \sinh (a_n L/R) + a_n \cosh (a_n L/R)}{N_1 \cosh (a_n L/R) + a_n \sinh (a_n L/R)}, \quad (17)$$

and a_n are the roots of

$$a_n J_1(a_n) - N_2 J_0(a_n) = 0, \quad (18)$$

and

$$N_1 = \frac{R U_1}{k'}, \quad N_2 = \frac{R U_2}{k'}. \quad (19)$$

There is a similar equation for F_{II} .

The heat-transfer coefficients U_1 and U_2 were calculated assuming series and parallel paths of all three heat-transfer modes (convection, conduction, and radiation). The ratio F of the heat flux entering region I to the heat flux leaving region II was calculated as

$$F = F_I F_{II}. \quad (20)$$

To account for various degrees of guard heating a factor G was defined as

$$G = \frac{T_{heater} - T_{wall}}{T_{heater} - T_{sink}}, \quad (21)$$

such that

$$N_2 = \frac{R G U_2}{k'} . \quad (22)$$

Plots of the percentage of heat shunted around the specimen, $1 - F$, vs the specimen thickness, Δx , for various specimen conductivities as determined by a computer solution of Eq. (16) are shown in Figs. 6 and 7 for temperature levels of 300 and 900°C, respectively. Both of these plots assume partial guard heating; $G = 0.5$ was employed. The dashed curves assume the specimen to be transparent to infrared radiation and the wall emissivities to be 0.5. From these plots, it can be seen that the amount of heat shunted around the specimen can approach 100% for large Δx and very small specimen conductivities. In our conductivity

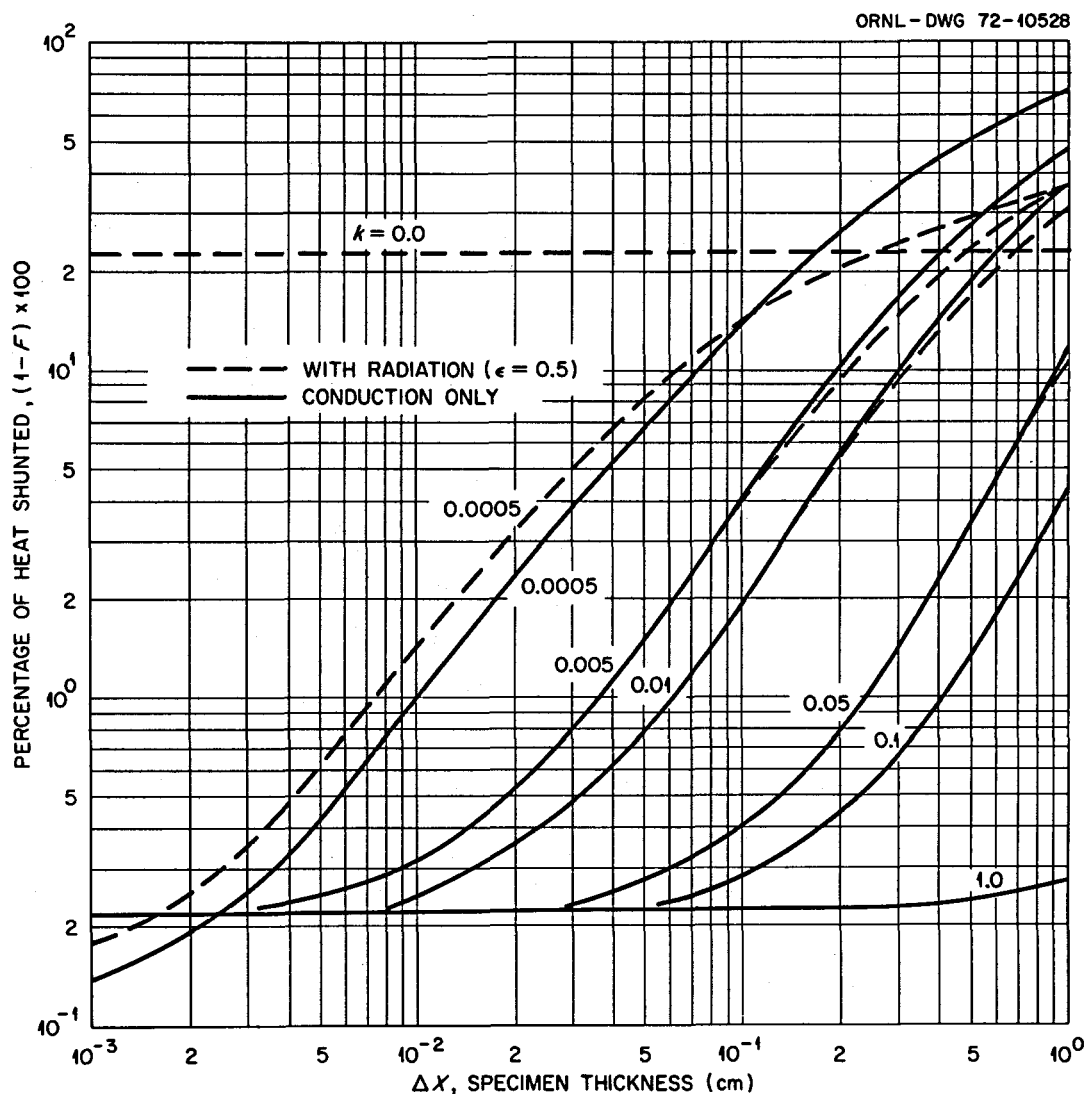


Fig. 6. Percent of heat shunted around specimen vs specimen thickness for various specimen conductivities with and without radiative heat transfer at 300°C for $G = 0.5$.

measurements, the guard heating factor G was near zero and a specimen thickness of <0.1 cm was used in determining the conductivity.

Method of calculation

In the variable-gap technique, the thermal conductivity coefficient can be determined (1) from the reciprocal slope of the total thermal resistance across the specimen (including metal walls, deposits, etc.)

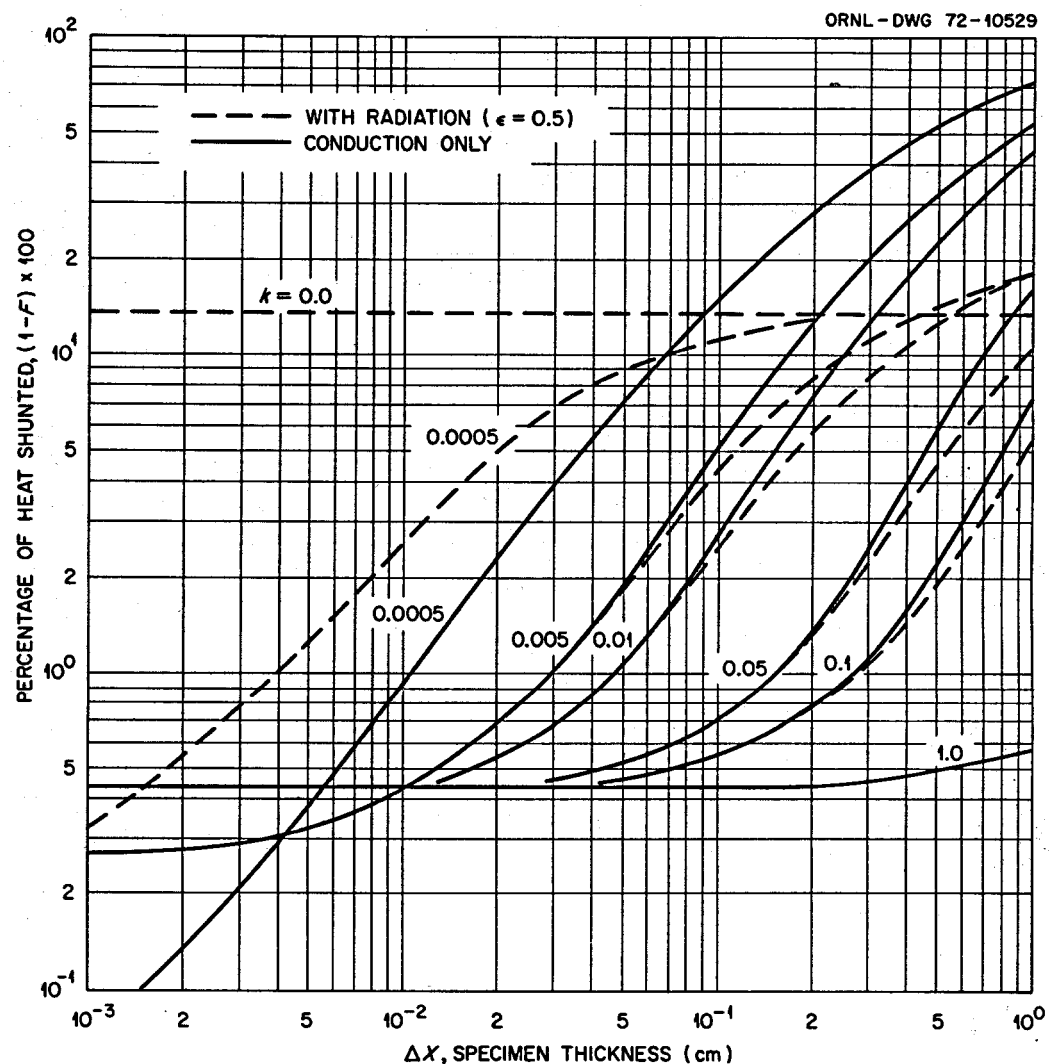


Fig. 7. Percent of heat shunted around specimen vs specimen thickness for various specimen conductivities with and without radiative heat transfer at 900°C for $G = 0.5$.

as a function of specimen thickness as it approaches zero or (2) from the effective conductivity as the specimen thickness approaches zero. Except for a few spot checks, method (1) was used to reduce the data in this report. The thermal resistance is calculated from the measured heat flux Q'/A and from the measured temperature difference, where

$$\frac{Q'}{A} = \frac{4EIV}{\pi D^2},$$

and

I = heater current, amps,

V = heater voltage, V,

D = diameter of upper heater plate, cm,

E = ratio of effective to total heater wire length.*

The heat flux Q/A is obtained from the measured heat flux by correcting for the heat shunting. If the guard heating factor G [see Eq. (21)] is greater than about 0.01, a heat shunting factor F is interpolated from the plots of $1 - F$ vs Δx (Figs. 6 and 7) obtained from computer solutions of Eq. (16). From these solutions, the percentage of shunted heat, $1 - F$, is found to be very nearly proportional to $G^{0.8}$. Thus, the heat shunting factor for any degree of guard heating is calculated using the results from only one heat shunting factor at $G = 0.5$:

$$(1 - F)_G = (G/0.5)^{0.8} (1 - F)_{G=0.5} . \quad (23)$$

The heat flux is then calculated as $Q/A = F (Q'/A)$ and the total thermal resistance is $\Delta T/(Q/A)$, where ΔT is the previously defined total temperature difference across the specimen.

The total thermal resistance is then plotted as a function of the specimen thickness for a given specimen temperature. The specimen temperature is defined as the average of the upper and lower plate temperature and both the specimen temperature and the measured heat flux are kept nearly constant as the specimen thickness is varied (see Experimental Procedures).

Three methods were used to determine the slope of the resistance curve at $\Delta x = 0$. First, visual inspection of the curve gave good results when the data were smooth and the resistance curve was linear. Second, when the curve was not linear, numerical finite-difference techniques were used to obtain the slope at $\Delta x = 0$. In the third method the data were fitted to Eq. (9) [or Eq. (10) if $\bar{\kappa} = 0$] if adequate information of the optical properties of the specimen were known.

*The total wire length between voltage taps includes two 0.875-in.-long lead wires.

Most of the data reported in this study were analyzed by visual inspection or the third method mentioned above. The data were fitted to Eq. (9) in the following way. The fixed resistance,

$$\left(\frac{\Delta T}{Q/A} \right)_0 ,$$

is found by extrapolating the thermal resistance vs Δx to $\Delta x = 0$; the plate emissivities are determined by carrying out the experimental procedure with the conductivity cell evacuated; and the index of refraction is taken from the literature, an average \bar{n} over the range of infrared-wavelengths. From an estimate of the conductivity by visual inspection of the data for $\Delta x < 0.1$, the absorptivity, $\bar{\kappa}$, can then be found from fitting Eq. (9) to the larger values of Δx . Using these values of the fixed resistance, the plate emissivities, the average index of refraction, and the calculated absorptivity, the thermal conductivity is determined by the best fit of the data over the complete range of Δx .

3. EXPERIMENTAL APPARATUS

The design and construction of the apparatus and auxiliary equipment are discussed here. The description of the thermal conductivity cell itself is sufficiently complete to permit duplication; however, only unusual auxiliary equipment is discussed in detail. Additional details and illustrations are given in Appendix A.

The complete system can be considered to consist of four parts: the thermal conductivity cell, the furnace, the electrical system, and the instrument network. The connections and relationships between the various components are shown schematically in Fig. 8. Photographs of the apparatus are shown in Figs. 9 and 10.

Thermal Conductivity Cell

The thermal conductivity cell is shown in Fig. 11 and in detail in Figs. A-1 and A-2 in Appendix A. The cell is made up of two components: the cylindrical-shaped component, which consists of a sink and the radial

ORNL-DWG 72-10530

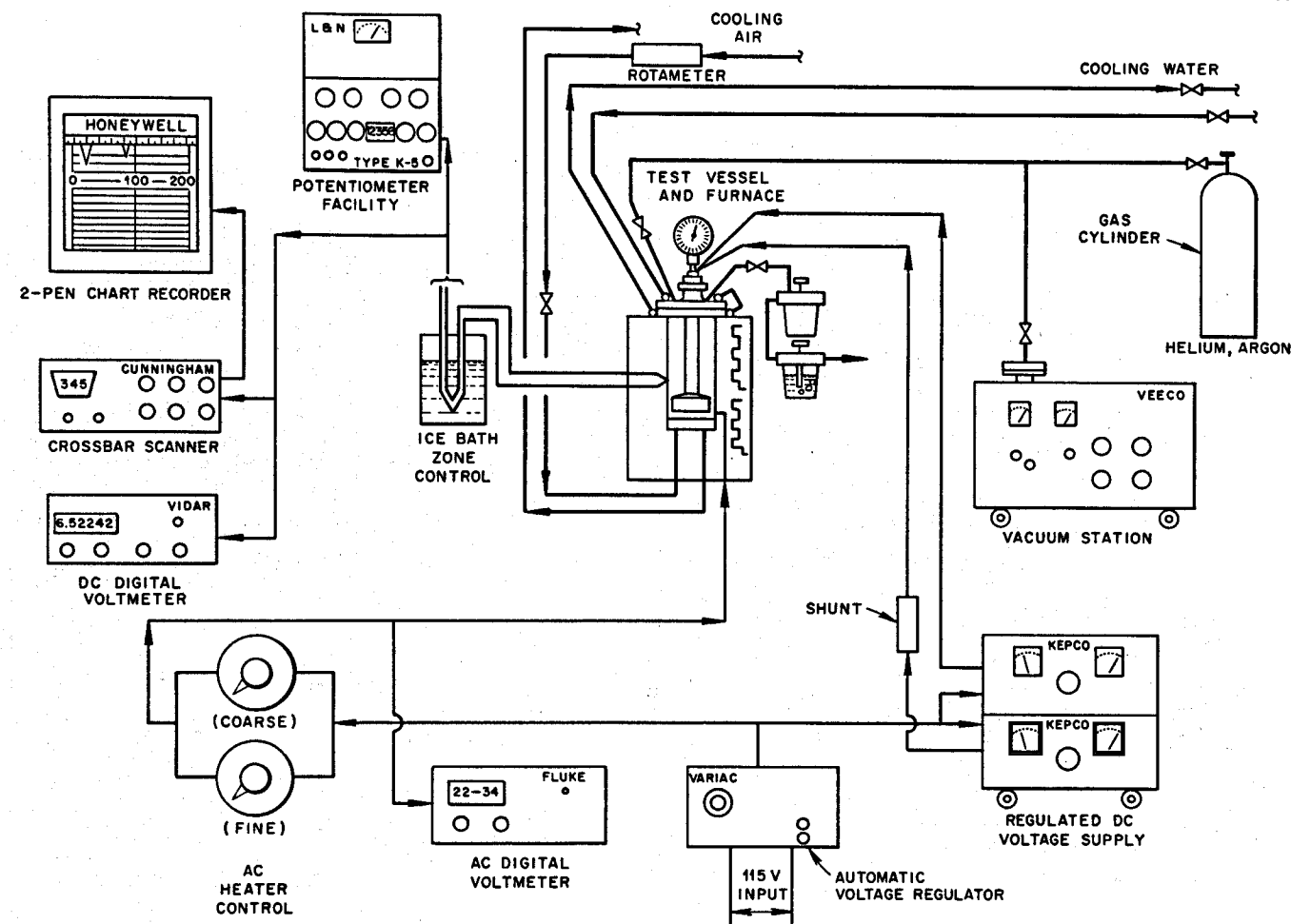
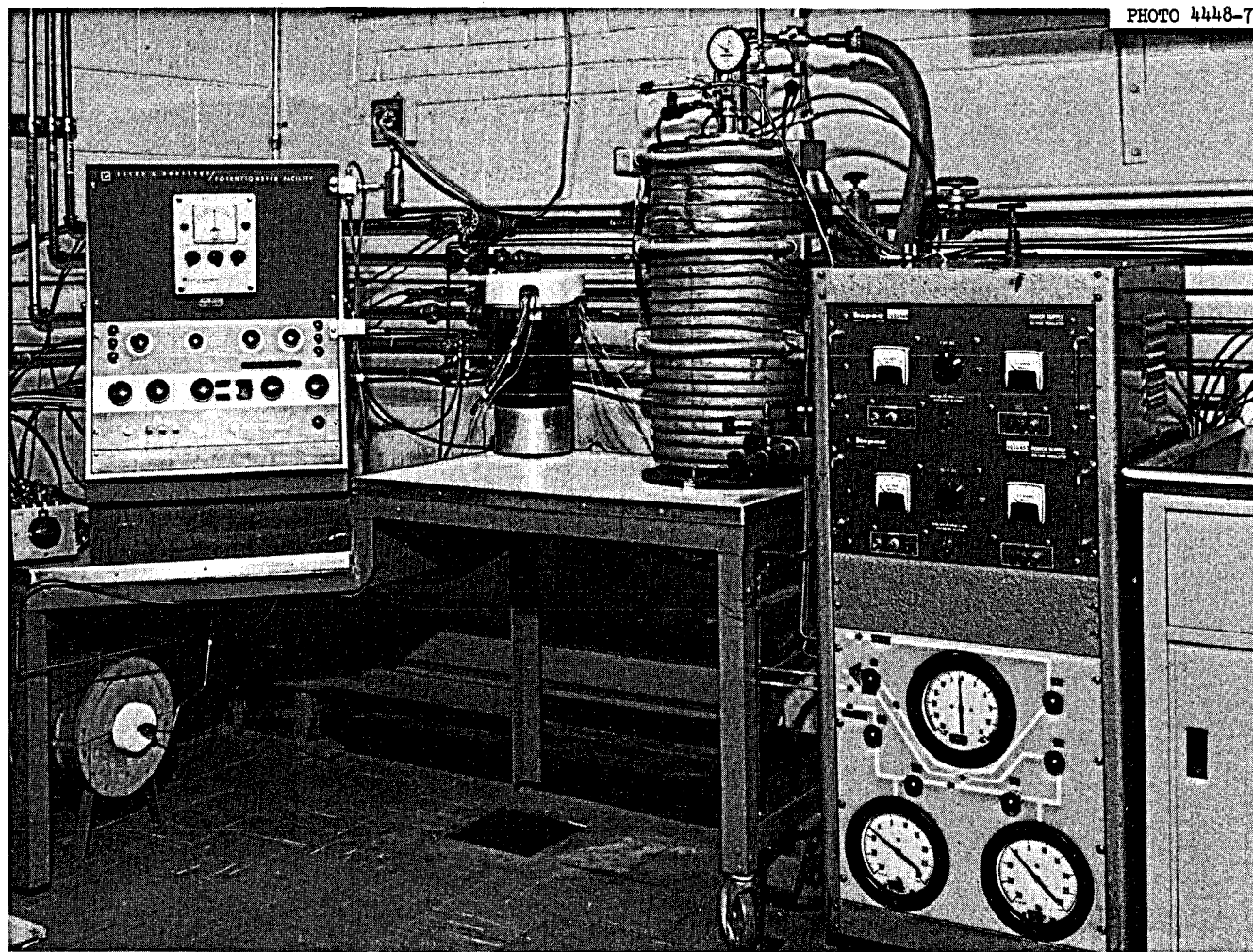


Fig. 8. Schematic illustration of the complete system for thermal conductivity measurements.

PHOTO 4448-72



214

Fig. 9. Photograph of the apparatus, front view.

PHOTO 4447-72

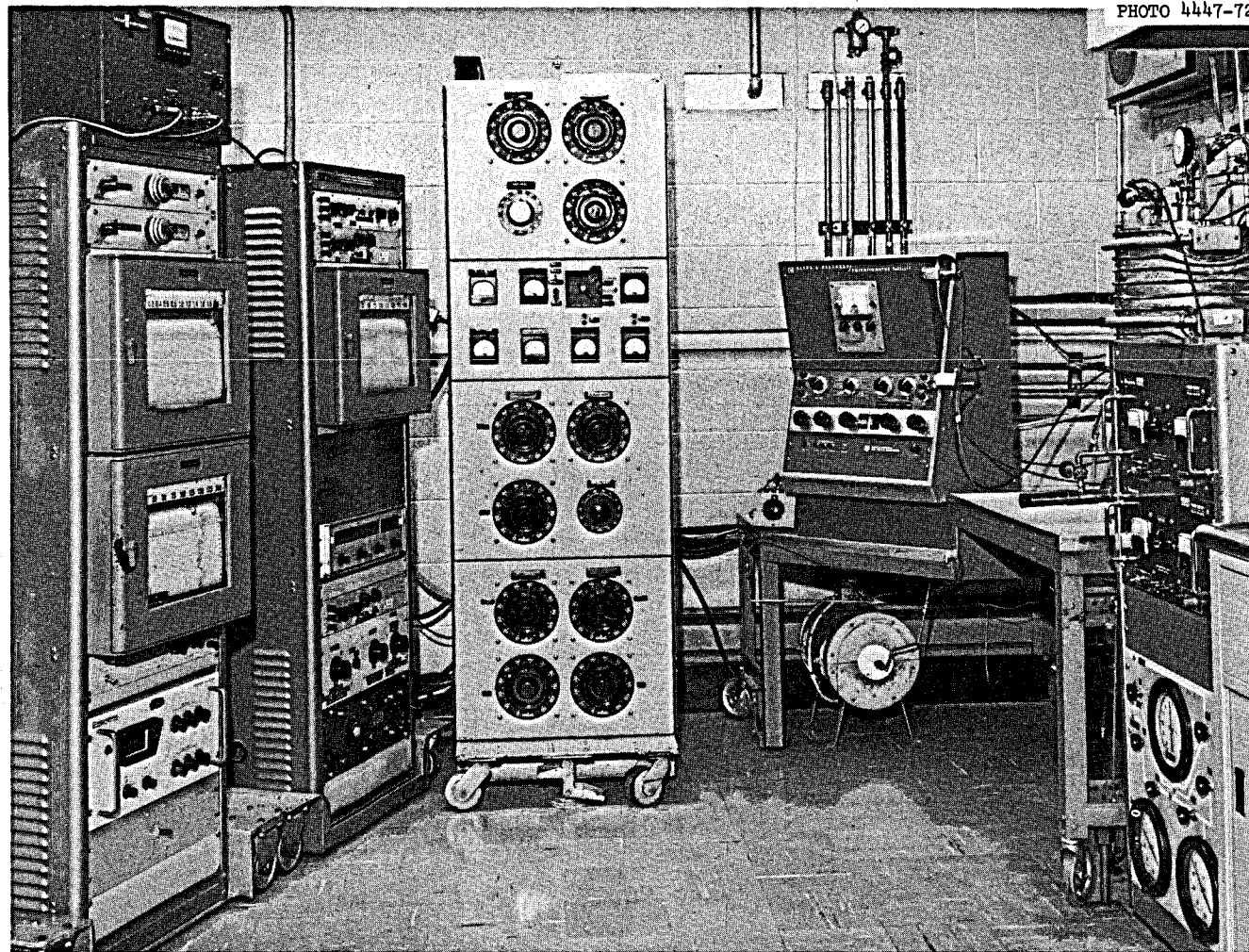


Fig. 10. Photograph of the apparatus, side view.

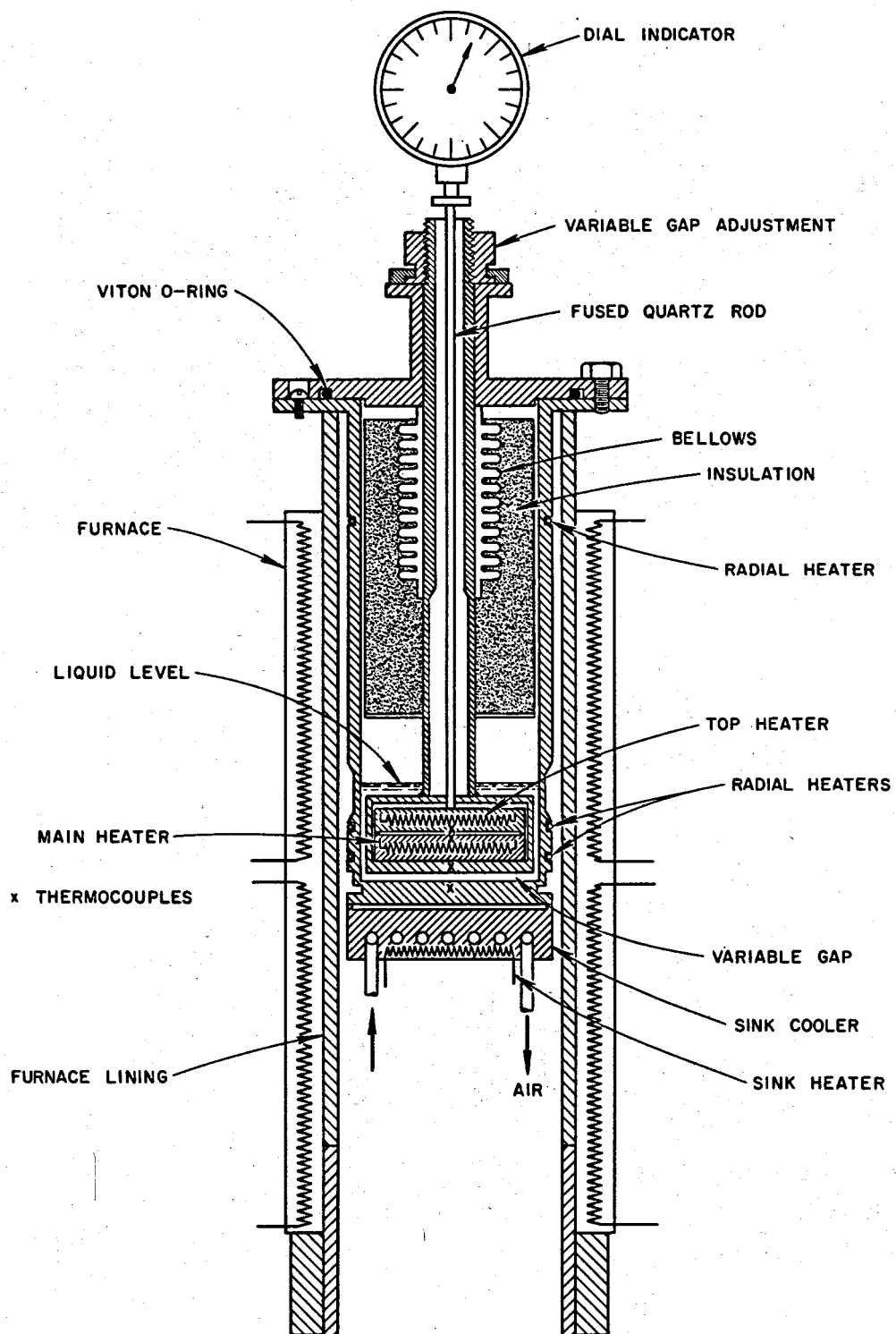


Fig. 11. Schematic cross section of the conductivity cell.

heaters and contains the salt, and the piston-shaped component, which is mobile in the vertical direction and contains the main heater and the guard heater assemblies.

The cylindrical component was machined from three pieces of stainless steel type 304 and welded together as shown. The lower section, which contains the molten salt, has holes drilled through the component for cooling air passages, and a sink heater which is a 1/8-in.-diam Calrod sheath-type element pressed into grooves machined in the lower section. Similar heaters are placed around the cylinder at the level of the salt for the radial guard heaters. Figure 12 shows the location and designations of the thermocouples and heaters. Several dimensions of the cylinder component are maintained in close tolerances to insure that the specimen thickness is uniform across the diameter (Fig. A-1). The cylinder is about 4 in. OD x 3.5 in. ID, and 12 in. long. The final machining of these surfaces was made after the entire cylinder had been dimensionally stabilized by heat treatment.

The mobile piston component containing the main heater assembly is shown in detail in Fig. A-2 in Appendix A. The main heater is constructed with 10-mil Pt-10% Rh wire, wound, embedded, and buried in a high-density Al_2O_3 insulator. A duplicate heater, the main guard heater, sits above the main heater. Between these two heaters is a 1/16-in. gap containing three platinum-foil radiation shields. The temperature across this gap is monitored by two thermocouples and balanced with the guard heater to prevent axial heat loss. A gold foil provides high contact conductance between the main heater and the bottom of the piston container. All the electrical wiring, the platinum wire, and the thermocouples extend through a hollow rod connecting the piston with the upper plate and support. A flexible bellows welded to the piston rod and the upper flange allows mobility of the piston while providing a vacuum tight seal. The vertical movement of the piston is adjusted by a threaded nut whose microthreads are precision machined. The vertical movement of the piston is measured with a dial indicator connected to the bottom of the piston with a fused quartz rod to minimize the effect of thermal expansion. Several dimensions of the mobile piston component are also

ORNL-DWG 72-10531

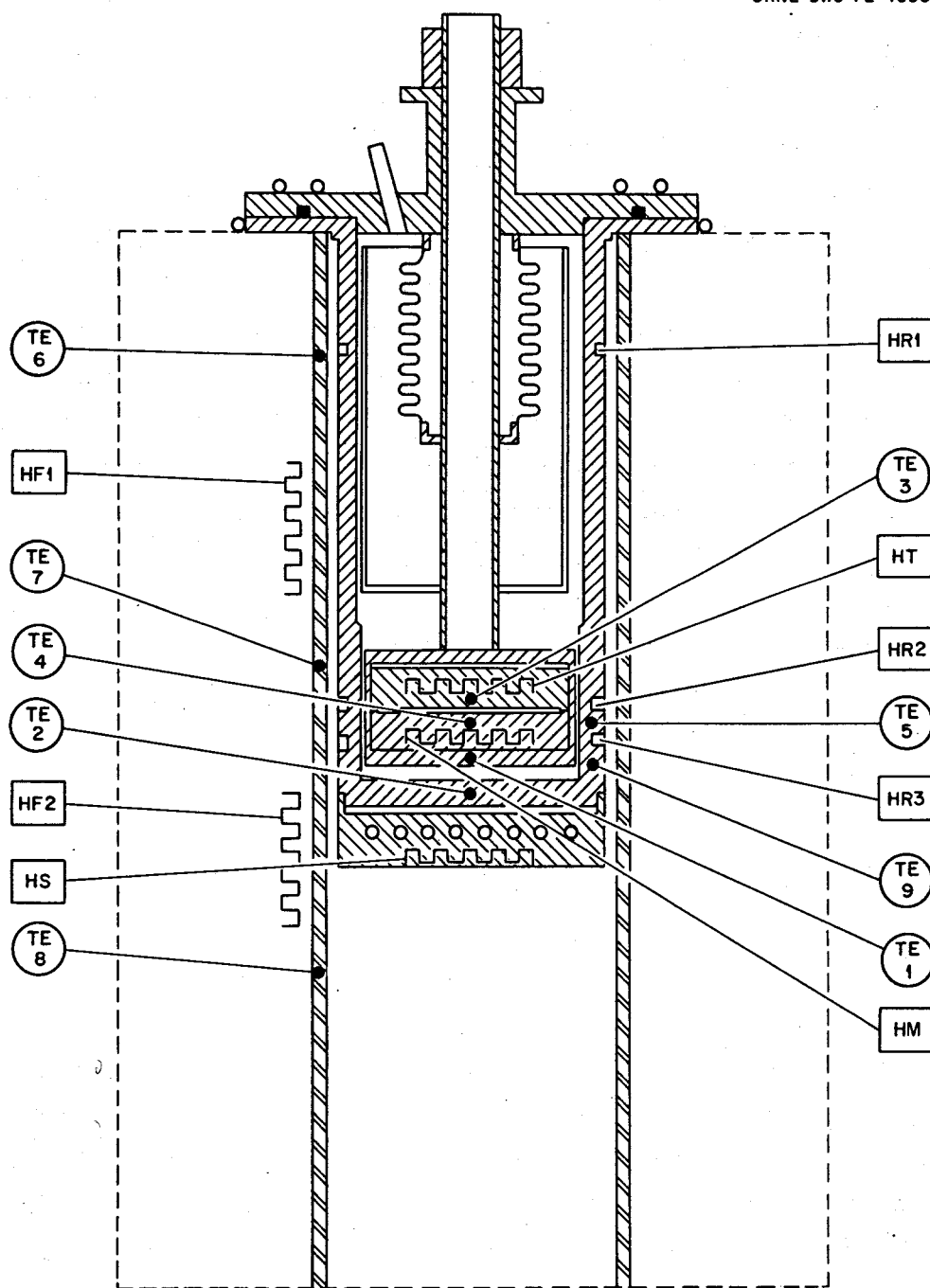


Fig. 12. Position of thermocouples and heaters.

maintained in close tolerances (See Fig. A-2). The specifications of these tolerances insure that the parallelism of the two plate surfaces does not vary by more than 0.005 in. This tolerance was measured *in situ* by placing a ball bearing in the gap of the specimen, rotating the apparatus in an inclined position, and measuring the variation in the gap setting with the dial indicator. A typical plot of this variation around the edge of the cell is shown in Fig. 13. The maximum edge-to-edge variation of the thickness in this case of 0.0017 in. demonstrates excellent conformity to the 0.005-in. tolerance.

The test cell described here and in considerably more detail in Appendix A is the final design (Model III-B) of the conductivity cell. Several modifications were made in the course of the development of this apparatus. The notation, description, and chronological appearance of these modifications are listed in Table 1.

The locations of the thermocouples used in the conductivity cell are shown in Fig. 12. Initially, the thermocouples were 1/16-in.-OD sheathed Chromel-Alumel thermocouples; later Pt vs Pt-10% Rh thermocouples were used. Thermocouples 1, 2, 5, and 6 are arc welded to the bottom of their respective thermal wells to insure that they remain fixed during the measurements.

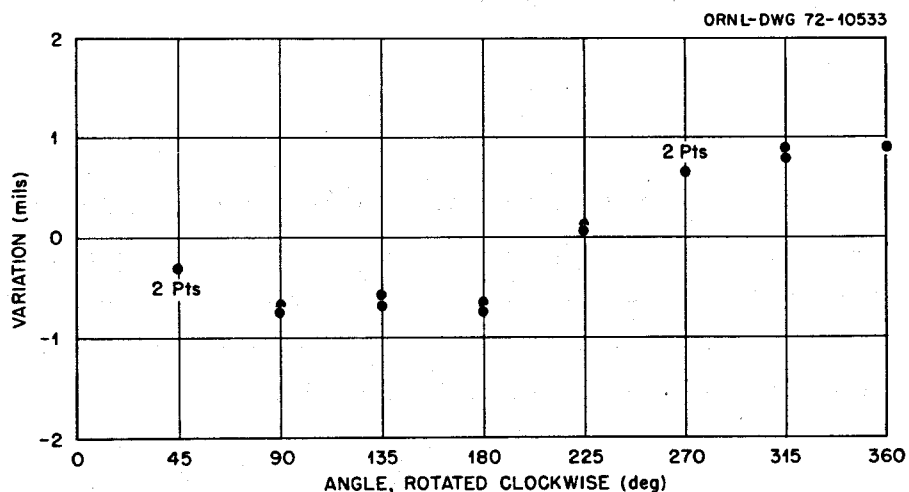


Fig. 13. Variation in the gap thickness around the circumference of the conductivity cell.

Table 1. Cell modifications

Model	Heater assembly ^a	Cylinder	Thermocouples
I-A	Thick one-piece heater core; D = 8.572 cm, E = 0.969	Original cylinder	1/16-in.-OD SS-sheathed, Chromel-Alumel grounded junctions, MgO insulation
II-A	Thinner two-piece heater core with 1/32-in. air gap between main and guard heaters; E = 0.971	Original cylinder	1/16-in.-OD SS-sheathed, Pt vs Pt-10% Rh ungrounded junctions, MgO insulation
II-B	"	Wall of the original cylinder was undercut and grooved to reduce heat flow down the wall; TC 9 added	"
III-B	New heater with 1/16-in. air gap with three Pt foil baffles; E = 0.966	"	"

^aD = diameter of heater assembly and E = ratio of effective-to-total heater wire length, where the total wire length between the voltage taps includes two 0.875-in.-long lead wires.

Furnace

The furnace consists of two 6-in.-ID × 8-in.-long individually controlled clamshell heaters of the embedded wire type. The annular space between the heater and the 12.5-in.-OD water-cooled furnace shell was filled with Fiberfrax insulation. This furnace is capable of raising the ambient temperature of the molten salt to 1000°C.

Electrical System

The heater electrical system is diagrammed in Fig. 14. The ac supply voltages to the sink, guard, and furnace heaters are regulated with a

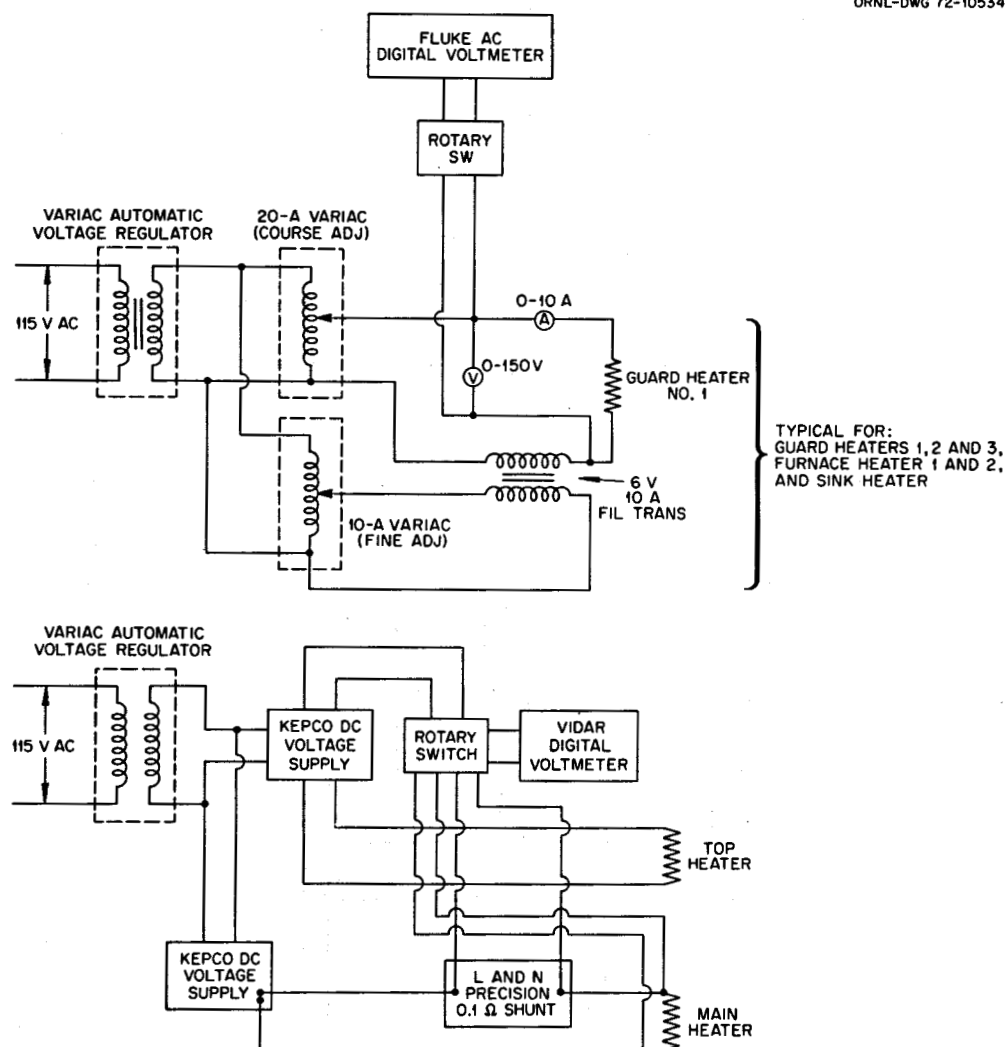


Fig. 14. Diagram for electrical heater system.

Variac automatic voltage regulator. The voltage through each of the heaters is adjusted by two Variacs, coarse and fine, and by a filament transformer. The fine adjustment extends the coarse Variac setting with the addition of 6 V of increased sensitivity (0.038 V). A Fluke ac digital voltmeter is used for setting and reading the voltages.

Two Kepco dc voltage supplies provide the electrical power to the main and top guard heaters. The supply voltage to the two Kepco units is also regulated by the Variac automatic voltage regulator. The power

to the main heater is determined from measurements of the voltage and the current with a Vidar digital microvoltmeter and a Leeds and Northrup precision resistor. Specifications of these instruments are given in Table A-1 in Appendix A.

Instrumentation

The thermocouple circuit diagram is shown in Fig. 15. The temperature measurements are made with grounded 1/16-in.-OD Chromel-Alumel

ORNL - DWG 72-10535

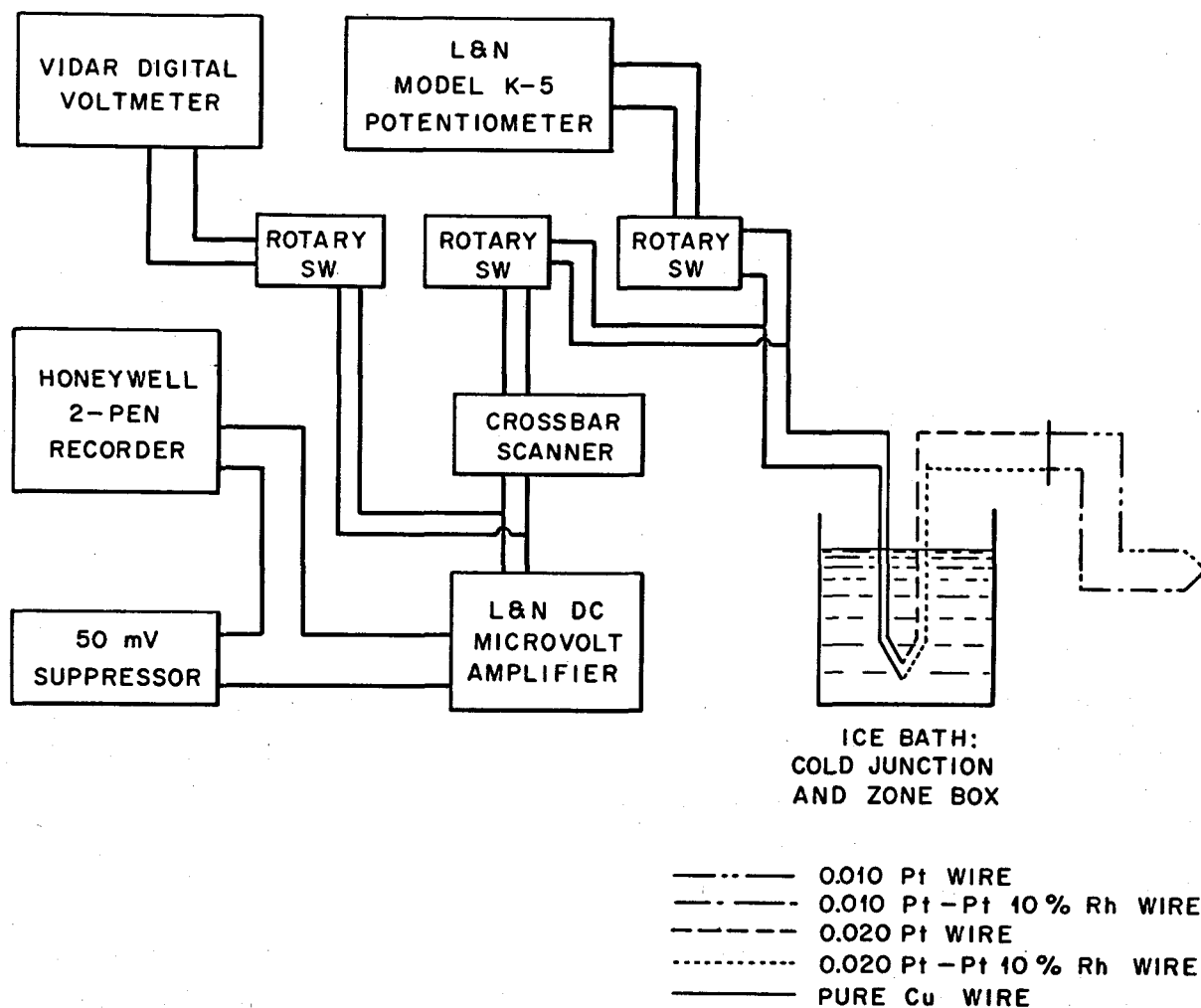


Fig. 15. Thermocouple circuit diagram.

thermocouples or with ungrounded 1/16-in.-OD Pt vs Pt-10% Rh thermocouples; both are sheathed in 304 type stainless steel. Lead wires from each thermocouple are joined by arc welding to high-purity copper circuitry wire. To minimize and cancel extraneous thermal emf's, each of these junctions is contained in a mineral-oil-filled glass tube inserted in a hole drilled into a high-purity copper block, 3 X 2 in. diameter, and the whole assembly is immersed in a distilled water ice bath. Low thermal emf holder is used in other circuitry junctions.

Each thermocouple emf can be read by either a Vidar digital microvoltmeter, a Honeywell pen recorder, or a Leeds and Northrup K-5 potentiometer facility. The specifications of these instruments are given in Table A-1, Appendix A.

4. EXPERIMENTAL PROCEDURES

Preliminary Procedures

The conductivity cell surfaces are cleaned with detergent, rinsed with demineralized water, and dried with filtered air. After use, the corrosion products are removed by polishing with rotary stainless steel brushes, 600-grit cloth, and crocus cloth to restore the surfaces. In assembling the apparatus, the parallelism of the plates is checked for the specified tolerance (0.005 in.), and the thermocouple readings at room temperature match within $<0.2\mu\text{V}$. The purity of the specimens used in the determinations meet the ACS specifications for reagent-grade chemicals: 99.997% pure argon, 99.995% pure helium, doubly deionized and triple distilled water, triple distilled mercury, and reagent-grade KNO_3 , NaNO_2 , and NaNO_3 salts dried in vacuum.

The specimen is introduced into the cell, the apparatus leveled and leak tested with a helium leak detector. The system is then outgassed by heating overnight at about 150°C . Voids in the specimen are removed by alternately increasing and decreasing the specimen thickness after it has been melted under vacuum. For liquid and solid samples, an argon cover gas is introduced into the cell at slightly above atmospheric pressure.

Operating Procedure - Fluid Specimen

The furnace heat is applied to the system to reach the desired temperature level. The main heater is adjusted to obtain the required heat flux through the specimen (0.02 to 0.7 W cm^{-2}), and the guard heaters are adjusted to maintain a close temperature balance between thermocouples three and five ($< \pm 0.5^\circ\text{C}$) and thermocouples three and four ($< \pm 1^\circ\text{C}$)^{*} to minimize heat losses (see Fig. 12). After steady-state conditions are reached, the measurements are recorded; the criterion for the steady-state condition is a temperature drift of less than $1^\circ\text{C}/\text{hr}$. Recordings are made of all thermocouple readings, air flow rate in the cooling sink, dial indicator reading, and voltages and currents from power panelmeters and digital voltmeters at each gap distance. The gap is then changed, steady-state conditions are reestablished, and the recordings repeated. A number of gap spacings are used (0 to 0.4 cm) depending on the linearity of the data. The heat flux and average specimen temperature are kept constant for each gap spacing ($> \pm 0.005 \text{ W cm}^{-2}$, $> \pm 1^\circ\text{C}$).

The above procedure is repeated for each specimen temperature level.

Operating Procedure - Solid Specimen

If the measurements are made with the specimen in the solid state, the specimen is melted before each gap spacing is selected, and then the gap spacing is fixed by cooling the specimen to the desired temperature.

5. EXPERIMENTAL RESULTS

The experimental results from this study demonstrate the successful development of the variable-gap technique for the measurements of molten-salt thermal conductivities. Concurrently with the development of the method, we measured conductivities of several molten fluoride salt mixtures which will be presented in a subsequent report.

* In some cases the radial guard heating was inadequate to reduce the radial ΔT to $< \pm 1^\circ\text{C}$, and a correction for heat shunting was necessary (Chapter 2).

The thermal conductivities of five materials were determined over a temperature range from 38 to 946°C for a total of 31 series of measurements. Argon, helium, water, HTS,* and mercury were selected to calibrate the apparatus because their conductivities are well established and cover a wide range of values: 0.4×10^{-3} to $100 \times 10^{-3} \text{ W cm}^{-1} (\text{°C})^{-1}$. The conductivity of HTS is not as well established a value as those of the other substances. However, HTS can be heated to temperatures required to melt the fluoride salt mixtures. Nearly 350 measurements were made of the thermal resistance as a function of specimen thickness to obtain the 31 determinations of conductivity. In addition, another 50 measurements of resistance vs thickness were made with the system evacuated to evaluate the surface emissivities.

The original and reduced data are presented in Tables B-1 to B-22 in Appendix B. The data were reduced as indicated in the method of calculation in Chapter 2. The total thermal resistance is plotted as a function of the specimen thickness, and the thermal conductivity is determined from the reciprocal slope as the specimen thickness approaches zero.

Thermal Resistance Curves

Several representative plots of total thermal resistance as a function of specimen thickness are shown in Figs. 16 to 20. At the lower temperature the thermal resistance is a linear function, as shown in Figs. 16 and 17 for mercury at 60.8°C and HTS at 197°C. At the higher temperatures, the influence of infrared radiation on the heat transfer can be seen by the curvature of the resistance curve for HTS and argon at 526°C and helium at 946°C (Figs. 18 to 20).

The fixed thermal resistance of the conductivity cell,

$$\left(\frac{\Delta T}{Q/A} \right)_0 ,$$

varies from 5 for mercury to 30 for argon. Model changes in the main

* HTS: $\text{KNO}_3\text{-NaNO}_2\text{-NaNO}_3$ (44-49-7 mole %).

ORNL-DWG 72-10536

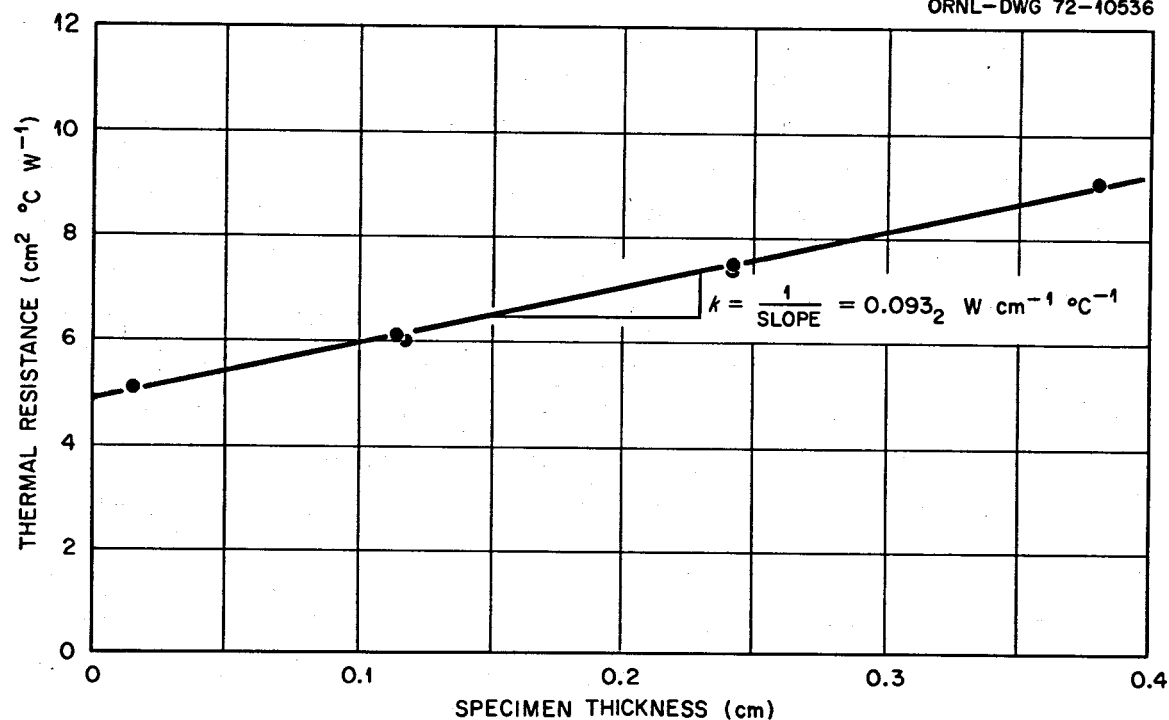


Fig. 16. Total thermal resistance vs specimen thickness of mercury at 60.8°C (Run 2, Apparatus I-A).

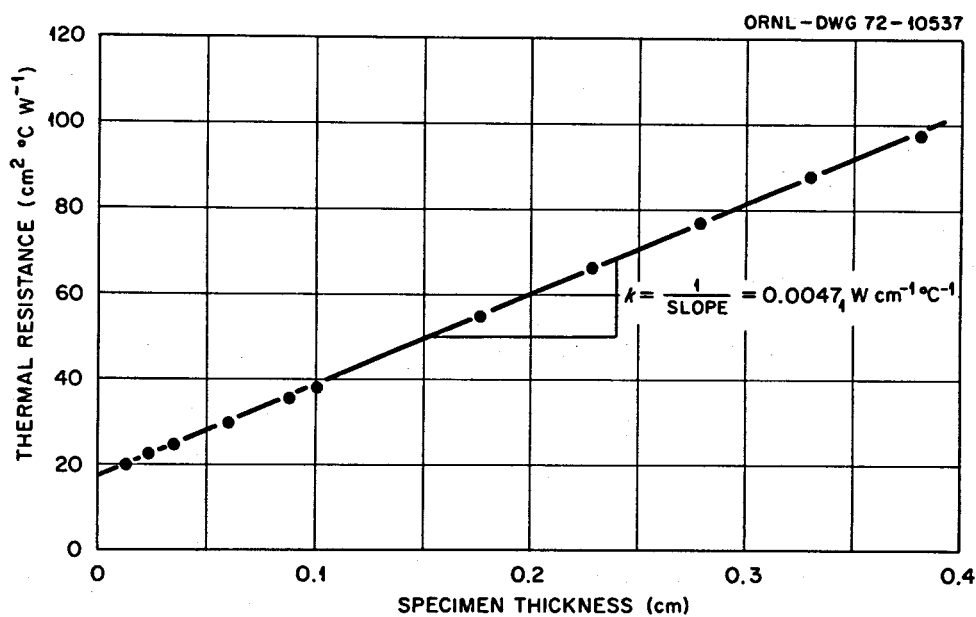


Fig. 17. Total thermal resistance vs specimen thickness of HTS at 197°C (Run 10, Apparatus I-A).

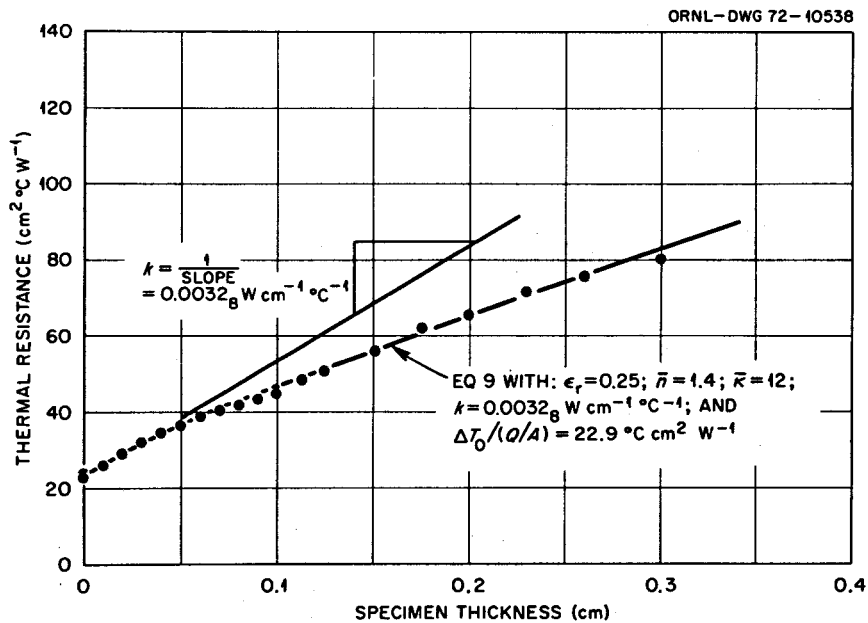


Fig. 18. Total thermal resistance vs specimen thickness of HTS at 526°C (Run 1, Apparatus II-B).

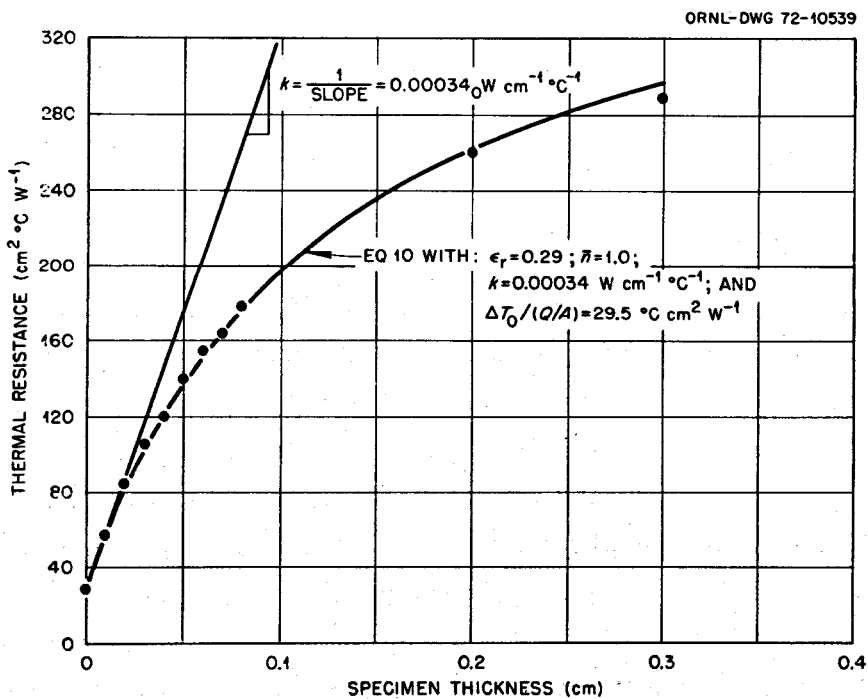


Fig. 19. Total thermal resistance vs specimen thickness of argon at 503°C (Run 1, Apparatus II-B).

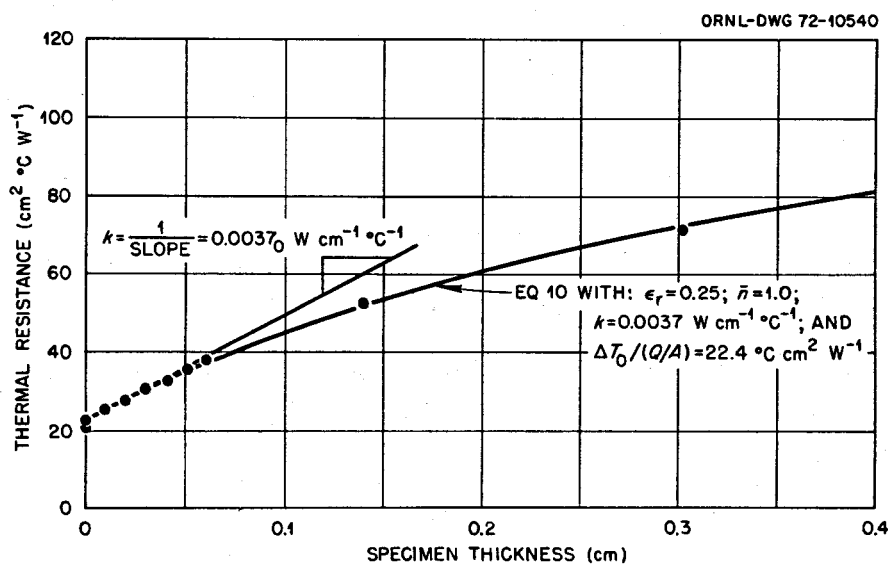


Fig. 20. Total thermal resistance vs specimen thickness of helium at 946°C (Run 2, Apparatus II-B).

heater assembly (Table 1) account for most of the variation in fixed thermal resistance. Model I-A was operated several months at temperatures up to 800°C with fluoride salt mixtures during a time between mercury and HTS calibration runs. The Chromel-Alumel thermocouples of model I-A would be expected to show significant emf drift under these conditions.

Thermal resistance as a function of gap spacing with the cell evacuated is shown in Fig. 21 for two temperature levels (200 and 510°C) and two values of heat flux (0.100 and 0.224 W cm^{-2}). The values of the specimen resistance (i.e., total minus fixed resistance) were used for the evacuated runs. The expected lack of variation of the resistance as a function of the gap spacing can be seen in the figure. A slight change in the emissivity of the plate surfaces will account for the small difference in the resistance between the two heat flux values at 200°C . The total hemispherical emissivity ϵ , calculated from the thermal resistance using Eq. (10) in Chapter 2 (assuming equal emissivity for the two plates), varied from 0.4 to 0.5 .

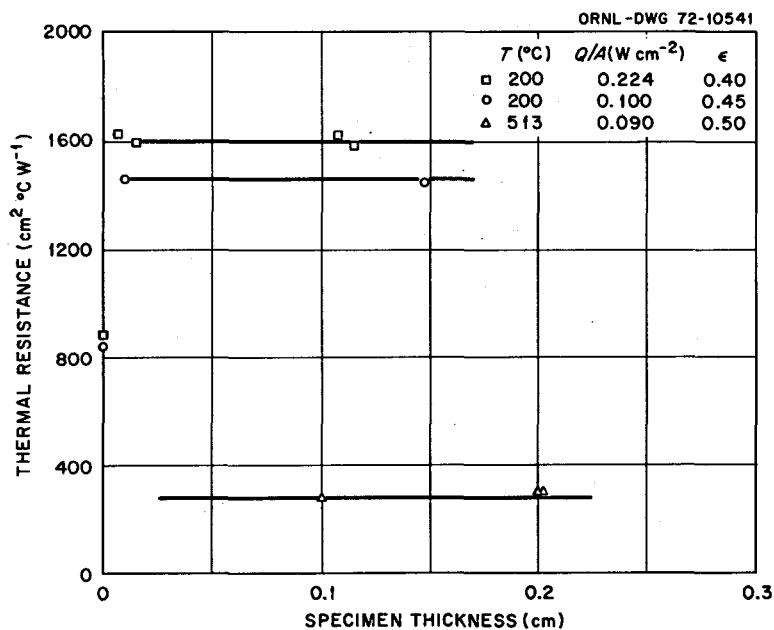


Fig. 21. Thermal resistance vs gap spacing with the conductivity cell evacuated.

The inflection in the slope of the resistance curve for HTS at 526°C (Fig. 18) is similar to those shown in Fig. 3 for small infrared absorbing materials. The solid curve drawn through the data was derived from Eq. (9), using the procedure outlined in Chapter 2. A value of $\bar{n} = 1.4$ was derived from the Molten Salts Handbook²¹ for the eutectic composition of $\text{NaNO}_3\text{-KNO}_3$ (47-53 mole %) at 525°C and the previously measured value of $\epsilon = 0.45$ was used for the plate emissivities. Incorporating these values in Eq. (9), a best fit of the experimental data over the entire range of specimen thicknesses ($0 < \Delta x < 0.3$ cm) gave values of the specimen conductivity and mean absorbtivity of $3.28 \times 10^{-3} \text{ W cm}^{-1} (\text{°C})^{-1}$ and 12 cm^{-1} , respectively.

The thermal resistance curves shown in Figs. 19 and 20 resemble those shown in Fig. 3 for nonabsorbing gases ($\bar{n} = 1$, $\bar{\kappa} = 0$). Using the previously determined plate emittance, the values of the conductivity were found from a best fit of the resistance data to Eq. (9) to be 0.34×10^{-3} and $3.3 \times 10^{-3} \text{ W cm}^{-1} (\text{°C})^{-1}$ for argon and helium at 503 and 946°C , respectively.

Thermal Conductivity

The experimental results for the thermal conductivity for the different calibration specimens used with the various apparatus models are presented in Table 2. One value for the conductivity of solid HTS at 120°C is 14% larger than a published value.⁵ The maximum deviation of the other results from published values are +9.6% and -12%. The average of the 18 positive deviations is 4.9%, and the average of the 12 negative deviations is -4.4%.

6. DISCUSSION OF THE RESULTS

The accuracy of the results, comparison with previously published values, and theoretical correlations are discussed in this chapter.

Comparison with Published Values

The values of the conductivity of the substances used to calibrate the variable-gap apparatus were well established with the exception of HTS. Touloukian's recommended values²² for argon and helium and Powell's values^{13,23} for water and mercury are representative of accepted conductivities for these materials. Of the two studies on the conductivity of HTS, we selected the more recent results of Turnbull⁵ over those of Vargaftik²⁴ because, as Turnbull points out, Vargaftik's calibration tests with "Dowtherm A" do not agree with other published values. However, Turnbull employed the transient-hot-wire technique with its attendant current-shunting problems (Chapter 2); consequently, the conductivity of HTS cannot be regarded to be as well established as that of the other specimens measured.

The individual deviations between the experimental results and the published values were examined as a function of the specimen type, specimen conductivity, specimen temperature, and apparatus model. No obvious correlation could be found.

Table 2. Experimental results

Model	Specimen	Run No.	Temperature (°C)	Thermal conductivity [W cm⁻¹ (°C)⁻¹]		Difference (%)	Reference
				Exptl.	Literature		
I-A	H₂O	1	45.2	6.7 ₁	6.38	5.2	13
		2	51.9	6.7 ₁	6.47	3.7	13
		3	38.0	6.7 ₈	6.30	7.6	13
	Hg	1	60.2	83. ₁	93.2	-10.8	23
		2	60.8	93. ₂	93.2	0.0	23
	HTS	1	307	4.2 ₄	4.30	-1.4	5
		2	308	4.1 ₅	4.30	-3.5	5
		3	546	3.4 ₅	3.24	6.5	5
		4	545	3.3 ₄	3.24	3.1	5
		5	197	4.7 ₈	4.80	-0.4	5
		6	277	4.4 ₃	4.38	1.1	5
		7	549	3.4 ₇	3.22	7.7	5
		8	285	4.6 ₄	4.40	5.5	5
		9	199	4.8 ₃	4.80	0.6	5
		10	198	4.7 ₁	4.80	1.9	5
		11	552	3.0 ₇	3.21	-4.4	5
		12	554	3.4 ₈	3.20	8.7	5
II-A	He	1	172	2.0 ₅	1.93	6.2	22
		2	509	3.0 ₄	3.02	0.7	22
II-B	He	1	519	2.7 ₀	3.04	-11.2	22
		2	946	3.7 ₀	4.21	-12.1	22
	Ar	1	503	0.34 ₀	0.361	-5.8	22
		2	860	0.49 ₃	0.463	6.5	22
		3	859	0.45 ₂	0.463	-2.4	22
	HTS	1	526	3.2 ₈	3.33	-1.5	5
III-B	He	1	525	3.2 ₀	3.07	4.2	22
		2	527	3.0 ₀	3.07	-2.3	22
		3	105	1.9 ₄	1.77	9.6	22
	HTS	1	517	3.3 ₄	3.37	-0.9	5
		2	317	4.4 ₉	4.26	5.4	5
		3	120	6.2 ₇	5.5	14.0	5

The average deviation of $\pm 5\%$ from the published values for the thermal conductivities is considerably less than expected considering the specialized design of the apparatus.

Comparison with Theory

The experimental results for HTS at 526°C (Fig. 18) are an example of a test of the theory of Chapter 2 for infrared absorbing materials. Equation (9) in conjunction with the values of \bar{k} , \bar{n} , ϵ , and k (selected in the manner previously described) agrees well with the experimental thermal resistance data over the range of specimen thicknesses examined. In addition, the inflection point of Eq. (9) and the apparent inflection point in the thermal resistance data both occur in the vicinity of $x = 0.1$ cm. Such agreement gives us confidence in the use of Eq. (9) to represent the thermal resistance data of mildly infrared absorbing specimens like HTS at 500°C ($\bar{k} = 12 \text{ cm}^{-1}$). However, as Poltz¹⁷ points out, the Kirchoff theory ceases to be valid if the reciprocal of the absorption coefficient is of the same magnitude as the wavelength in some regions of the absorption spectrum. Fortunately, when this condition occurs, the thermal resistance is very nearly a linear function of the specimen thickness.

From a theoretical standpoint, the disruption of the lattice continuity by melting should lower the conductivity significantly. If we extrapolate our one result for the conductivity of solid HTS at 120°C to the melting point at 142°C by assuming that thermal conductivity is proportional to the inverse of the absolute temperature $k \propto 1/T$ (°K) (according to the Debye phonon-scattering theory), a ratio of the liquid-to-solid thermal conductivity at the melting point is found to be 0.85. Turnbull²⁵ reports the average ratio of liquid-to-solid conductivities at the melting point for a large number of salts to be 0.86 ± 0.13 . However, Turnbull's reported values for HTS⁵ do not show a discontinuity at the melting point. Accordingly, our value of the conductivity of solid HTS, 14% higher than Turnbull's, appears to be the more reasonable one.

Uncertainties in the Results

A detailed error analysis of the system is given in Appendix C, and the result of this analysis is shown in Fig. 22. The estimated maximum and standard error limits in the conductivity measurements using apparatus III-B are plotted as a function of the specimen conductivity. The effects of the specimen temperature range (300 to 900°C) and of the degree of radiation effects (zero to maximum radiation at 900°C) do not contribute greatly to the error and are shown by the areas included within the small bands in Fig. 22. It is apparent from the figure that the error is sensitive to the magnitude of the specimen conductivity except at larger values of the conductivity. Much of the increase in error at low values of conductivity results from an increased uncertainty in the measurement of the change in the specimen thickness. This uncertainty, caused by the thermal expansion of the conductivity cell as the guard heating is adjusted, can be minimized by a dual quartz rod, dial indicator system. Such a system was not considered necessary for the present apparatus since the conductivities of the molten fluoride salts were found to be in the vicinity of $0.01 \text{ W cm}^{-1} (\text{°C})^{-1}$.

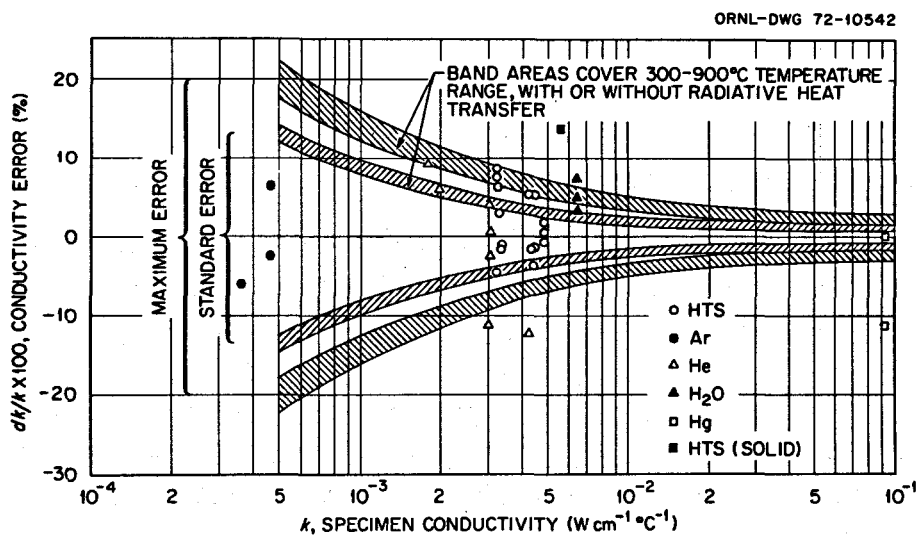


Fig. 22. Estimated standard and maximum error limits in the conductivity measurements for Apparatus III-B vs specimen conductivities with and without radiative heat transfer over 300 to 900°C range. Also shown are experimental deviations from published values.

Figure 22 shows also the deviations of each of the experimental results from the published values. Several points are outside of the estimated error limits (the conductivity of solid HTS was discussed in the previous section). Data for water and mercury were obtained using Apparatus I-A, in which Chromel-Alumel thermocouples were used. Since the uncertainty of the temperature measured with the Chromel-Alumel thermocouples is four times of that from Pt vs Pt-10% Rh thermocouples, the error limits for Apparatus I-A are considerably larger than for III-B, especially at the higher specimen conductivities. Excluding these points, 93% of the data lies within the maximum error limits and 68% within the standard error limits.

Adequacy of the Experimental Apparatus

The experimental apparatus proved extremely durable despite its complex design. Model I-A endured 500 hr of operation with a fluoride salt mixture at temperatures ranging from 500 to 800°C and for 850 hr with HTS at temperatures from 200 to 500°C before failure of a thermocouple required the replacement of the heater assembly. Model II-A suffered a weld failure in the heater assembly after 1000 hr of operation with helium and argon at temperatures from 200 to 950°C and 800 hr with fluoride salt mixtures from 500 to 850°C. Model III-B is still in operating condition after nearly 3000 hr with fluoride salt mixtures at temperatures from 500 to 960°C.

We previously noted that a dual quartz-rod dial-indicator system would be able to account for thermal expansion of the cell in measuring specimen thicknesses at low conductivity. For such measurements, the upper and lower plate surfaces should be polished to a mirror finish also.

The accuracy and precision of the conductivity values could possibly be improved by measuring the heat flux departing from the specimen. This heat flux can be determined by the usual means of measuring the temperature drop along a well-insulated rod of known conductivity. By measuring both the heat flux entering and leaving the specimen, the effect of heat shunting on the determination should be reduced.

7. CONCLUSIONS

Designed as it is for specialized thermal conductivity measurements with molten fluoride salt mixtures from 500 to 1000°C, the variable-gap apparatus has demonstrated remarkable versatility. Experimental results agree with published results within an average deviation of $\pm 5\%$ for a wide variety of specimens (solids, liquids, and gases), specimen conductivities [0.4×10^{-3} to $100 \times 10^{-3} \text{ W cm}^{-1} (\text{°C})^{-1}$], and temperature levels (40 to 950°C). In addition, the variable-gap apparatus has demonstrated its ability to distinguish and evaluate the internal radiation within small infrared absorbing fluids.

Considering the wide range of application and the accuracy of the variable-gap method, it is surprising to find so few references to it in the literature. The experimental measurements of the conductivity of several fluoride salt mixtures made concurrently with the present study will be reported in a later publication.

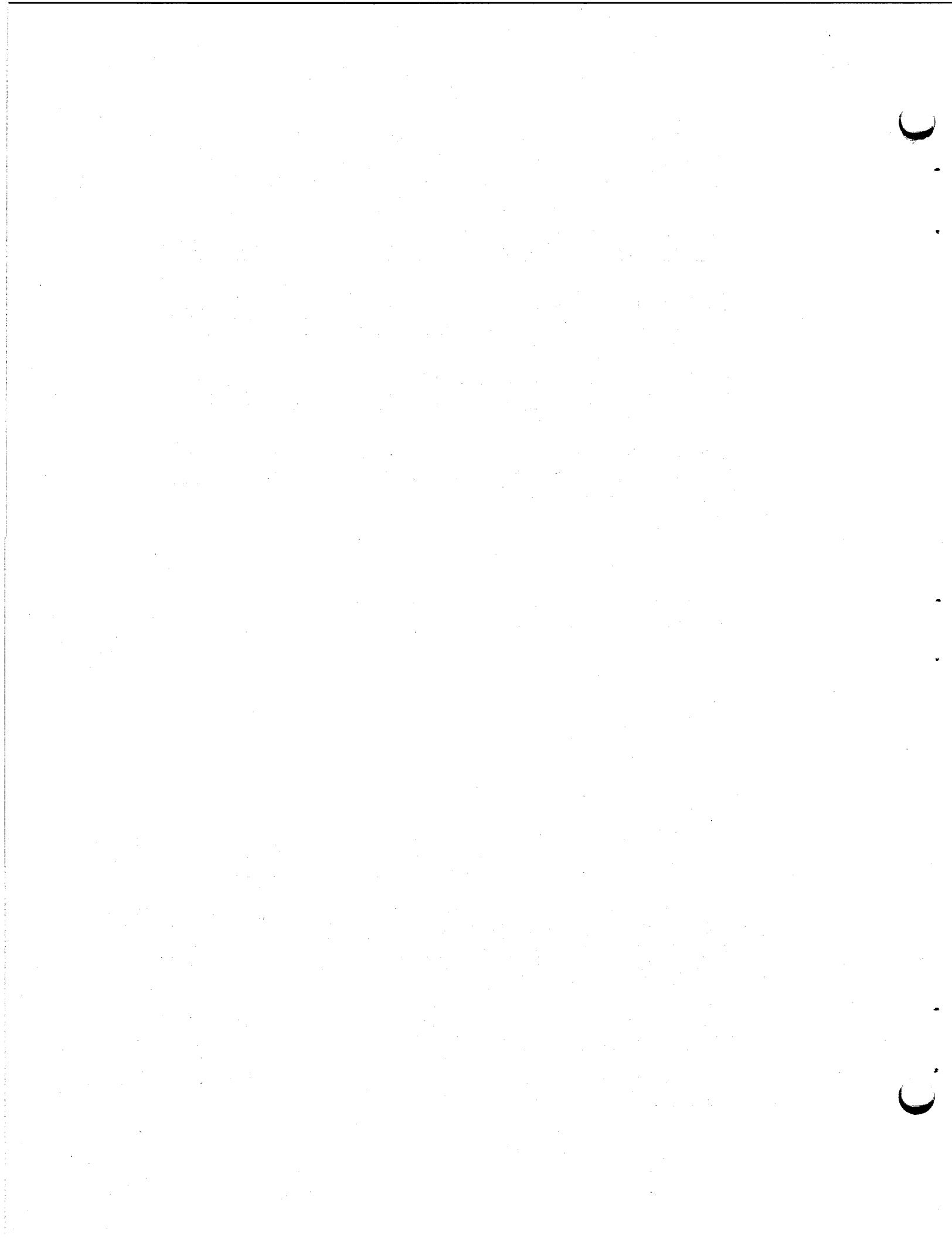
ACKNOWLEDGMENT

The author is grateful for the invaluable assistance of many of his associates who contributed to this investigation. In particular, the author wishes to express his appreciation to the following persons: S. J. Claiborne, Jr., for his valuable assistance in assembling and operating the apparatus, W. K. Sartory for his patient advice, J. W. Krewson and W. A. Bird for their design of the instrumentation, J. W. Teague for his expediting the fabrication of the apparatus, Roberta Shor and M. R. Sheldon for assistance with the final editing, and Margie Adair and Dolores Eden for their typing of the report.

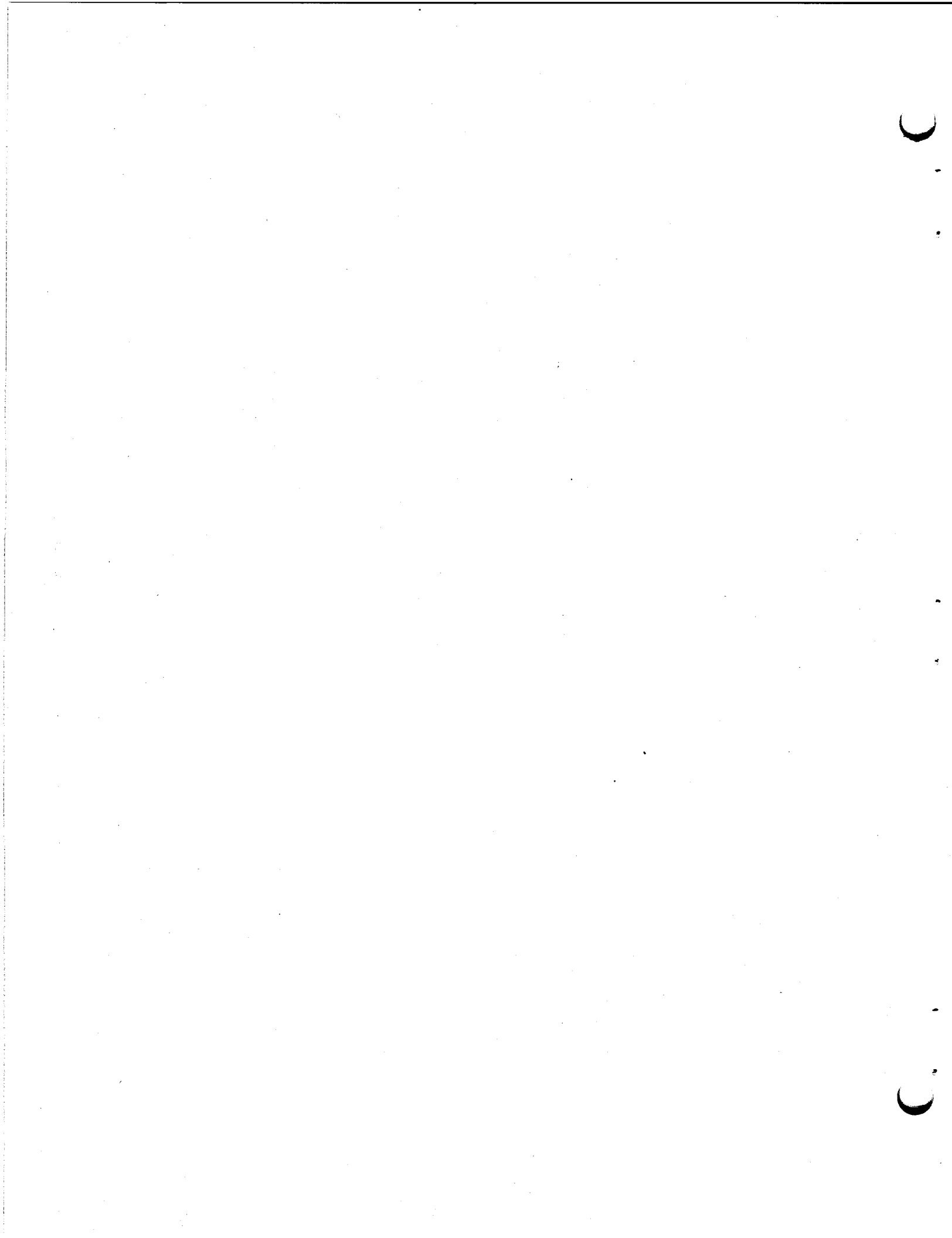
REFERENCES

1. E. S. Bettis and W. B. McDonald, "Molten-Salt Reactor Experiment," Nucleonics, 22(1): 67-70 (1964).
2. W. D. Powers, S. I. Cohen, and N. D. Greene, "Physical Properties of Molten Reactor Fuels and Coolants," Nucl. Sci. and Eng., 17(2): 200-211 (1963).
3. Narayanaswamy Mani, "Precise Determination of the Thermal Conductivity of Fluids Using Absolute Transient Hot-Wire Technique," PhD Dissertation, Calgary, Alberta, August 1971.
4. P. Grassmann, W. Straumann, F. Widmer, and W. Jobst, "Measurement of Thermal Conductivities of Liquids by an Unsteady State Method," Progr. Intern. Res. Thermodyn. Transport Properties, Papers Symp. Thermophys. Properties, 2nd, Princeton, N. J., pp. 447-53, Academic Press, New York, 1962.
5. A. G. Turnbull, "The Thermal Conductivity of Molten Salts," Australian J. Appl. Sci., 12(1): 30-41 (1961).
6. L. R. White and H. T. Davis, "Thermal Conductivity of Molten Alkali Nitrates," J. Chem. Phys., 47(12): 5433-5439 (1967).
7. S. E. Gustafsson, "A Non-Steady-State Method of Measuring the Thermal Conductivity of Transparent Liquids," Z. Naturforschg., 22a(7): 1005-1011 (1967).
8. S. E. Gustafsson, N. O. Halling, and R. A. E. Kjellander, "Optical Determination of Thermal Conductivity with a Plane Source Technique (II Molten LiNO₃, RbNO₃, and Cs(NO₃)₂)," Z. Naturforsch., 23a(5): (1968).
9. C. E. Mallon and M. Cutler, "Thermal Conductivity of Electrically Conducting Liquids," The Rev. of Sci. Instr., 36(7): 1036-1040 (1965).
10. P. Y. Achener and J. T. Jouthas, "Alkali Metals Evaluation Program, Thermodynamic and Transport Properties of Cesium and Rubidium, Thermal Conductivity of the Vapor," AGN-8192, Vol. 2, Aerojet General Corp., October 1968.
11. J. E. S. Venart, "A Simple Radial Heat Flow Apparatus for Fluid Thermal Conductivity Measurements," J. Sci. Instr., 41: 727-731 (1964).
12. W. Fritz and H. Poltz, "Absolutbestimmung Der Wärmeleitfähigkeit von Flüssigkeiten - I," Intern. J. Heat Mass Transfer, Vol. 5, pp. 307-316, Pergamon Press (printed in Great Britain), 1962.

13. A. R. Challoner and R. W. Powell, "Thermal Conductivities of Liquids: New Determinations for Seven Liquids and Appraisal of Existing Values," Proc. Roy. Soc. (London), A238(1212): 90-106 (1956).
14. J. Matolich and H. W. Deem, "Thermal Conductivity Apparatus for Liquids; High Temperature, Variable-Gap Technique," Proc. 6th Conf. on Thermal Conductivity, Oct. 19-21, 1966, Dayton, Ohio, pp. 39-51.
15. J. W. Cooke, "Thermal Conductivity of Molten Salts," Proc. 6th Conf. on Thermal Conductivity, Oct. 19-21, 1966, Dayton, Ohio, pp. 15-27.
16. H. Poltz, "Die Wärmeleitfähigkeit von Flüssigkeiten II, Erschienen in der Zeitschrift," Intern. J. Heat Mass Transfer, 8: 515-527 (1965).
17. H. Poltz and R. Jugel, "The Thermal Conductivity of Liquids - IV. Temperature Dependence of Thermal Conductivity," Intern. J. Heat Mass Transfer, 10: 1075-88 (1967).
18. H. Gröber and S. Erk, Fundamentals of Heat Transfer, 3rd ed., rev. by U. Grigull, Trans. by J. R. Moszynski, p. 315, McGraw Hill, New York, 1961.
19. P. A. Norden and A. G. Usmanov, "The Inception of Convection in Horizontal Fluid Layers," Heat Transfer - Soviet Research, 4(2): 155-161 (1972).
20. B. M. Berkovsky and V. E. Fertman, "Advanced Problems of Free Convection in Cavities," 4th Intern. Heat Transfer Conference, Paris, September 1970, Vol. 4, Paper NC 2.1, E. L. Seiver Publishing Co., Amsterdam, 1971.
21. G. J. Jantz, Molten Salts Handbook, p. 92, Academic Press, New York, 1967.
22. Y. S. Touloukian, P. E. Liley, S. C. Saxena, Thermal Conductivity; Nonmetallic Liquids and Gases (Vol. 3 of Thermophysical Properties of Matter; the TPRC Data Series), Plenum Press, New York, 1970.
23. R. W. Powell and R. P. Tye, "The Thermal and Electrical Conductivity of Liquid Mercury," Proc. Heat Transfer Conf., 1961-62; University of Colorado, 1961 [and] Westminster, England, 1961-62, Intern. Developments in Heat Transfer, Paper 103, pp. 856-862, ASME, 1963.
24. N. B. Vargaftik, B. E. Neimark, and O. N. Oleshchuck, "Physical Properties of High Temperature Liquid Heat Transfer Medium," Bull. All-Un. PWR Eng. Inst., 21: 1 (1952).
25. A. G. Turnbull, "The Thermal Conductivity of Molten Salts," Australian J. Appl. Sci., 12(3): 324-329 (1961).



APPENDICES



APPENDIX A

ADDITIONAL DETAILS OF DESIGN OF THE APPARATUS

Sufficient detail is given in this section of the Appendix that the thermal conductivity cell can be duplicated. Details of the various components are shown in Figs. A-1 and A-2.

The discussion of the methods in Chapter 2 and Appendix C suggests that the geometry of the apparatus exerts considerable effect of the accuracy of the conductivity determination. However, in most cases, the consequences of gross size, corrosion, and high-temperature strength counteract other changes which might improve its accuracy. We concentrated on minimizing stray heat flow because the heat-transfer model is unidimensional.

The cylinder containing the specimen is constructed from stainless steel (304) and is illustrated in Fig. A-1. The dimensions of the cylinder were selected to minimize heat shunting around the specimen without sacrificing its structural integrity. The length of the cylinder was chosen to fit a standard furnace, 5 in. ID \times 18 in. long, so that the specimen would occupy its center. A uniform air gap, 3/32 in., between the cylinder and the sink provides an even heat flux distribution to the sink.

The mobile heat assembly, shown in Fig. A-2, is designed to reduce the upward flow of heat from the specimen area. The most important part of the assembly is the Al_2O_3 heater core machined from a high-purity, high-density Al_2O_3 ceramic. The core is fabricated in two pieces and is designed so that a 60-in. length of 0.010-in.-diam Pt-10% Rh wire could be uniformly wound on each piece forming the main and guard heaters. The grooves containing the wires were then filled with Al_2O_3 cement and fired. The surface of the main heater was ground flat and smooth. Several dimensions of the mobile heat assembly were closely controlled to insure a uniform specimen thickness. These are shown in Fig. A-2.

Other considerations contributing to the design of the apparatus include the ease of assembly and disassembly and the convenience of filling,

ORNL-DWG 72-10543

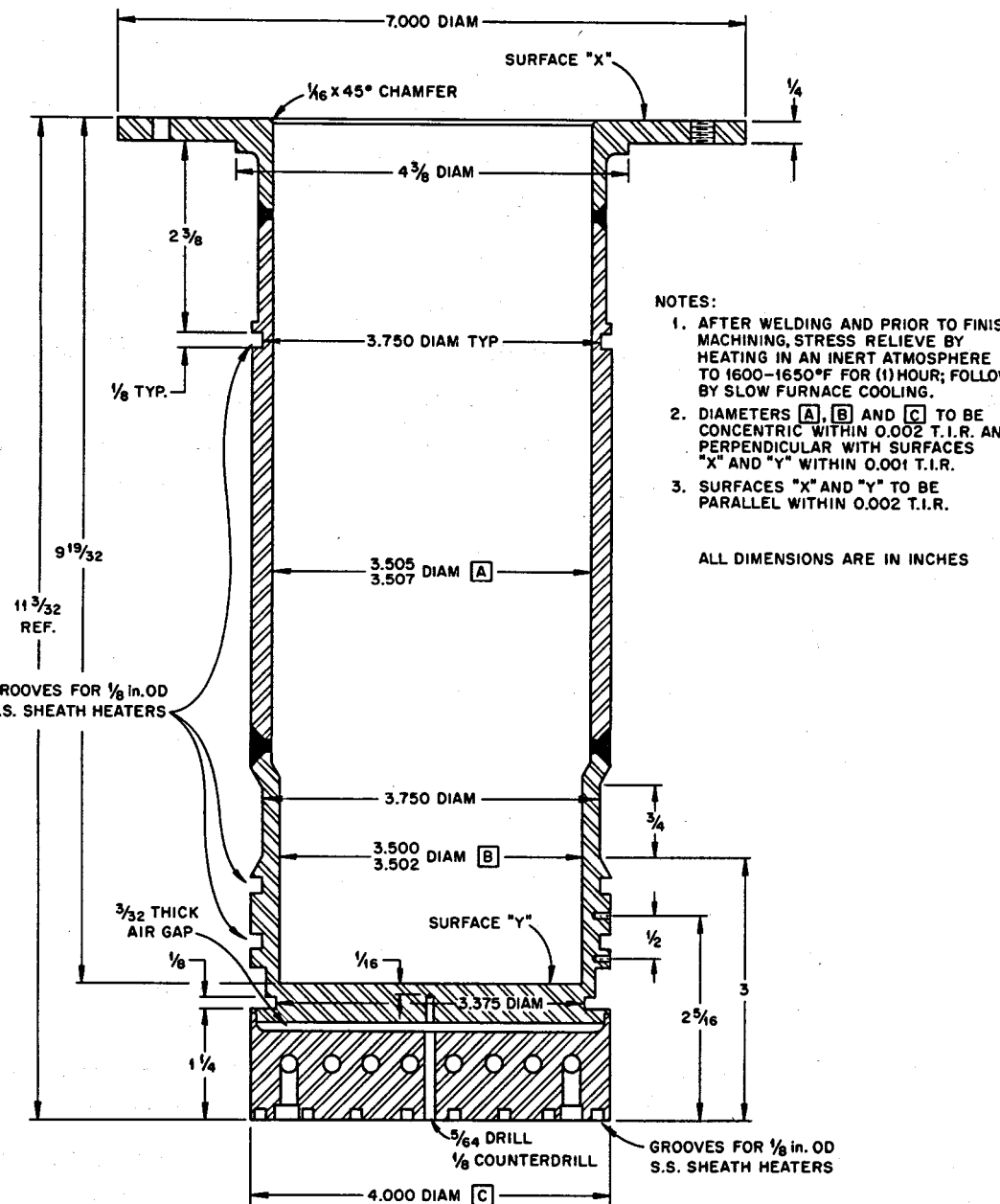


Fig. A-1. Detail of the conductivity cell cylinder.

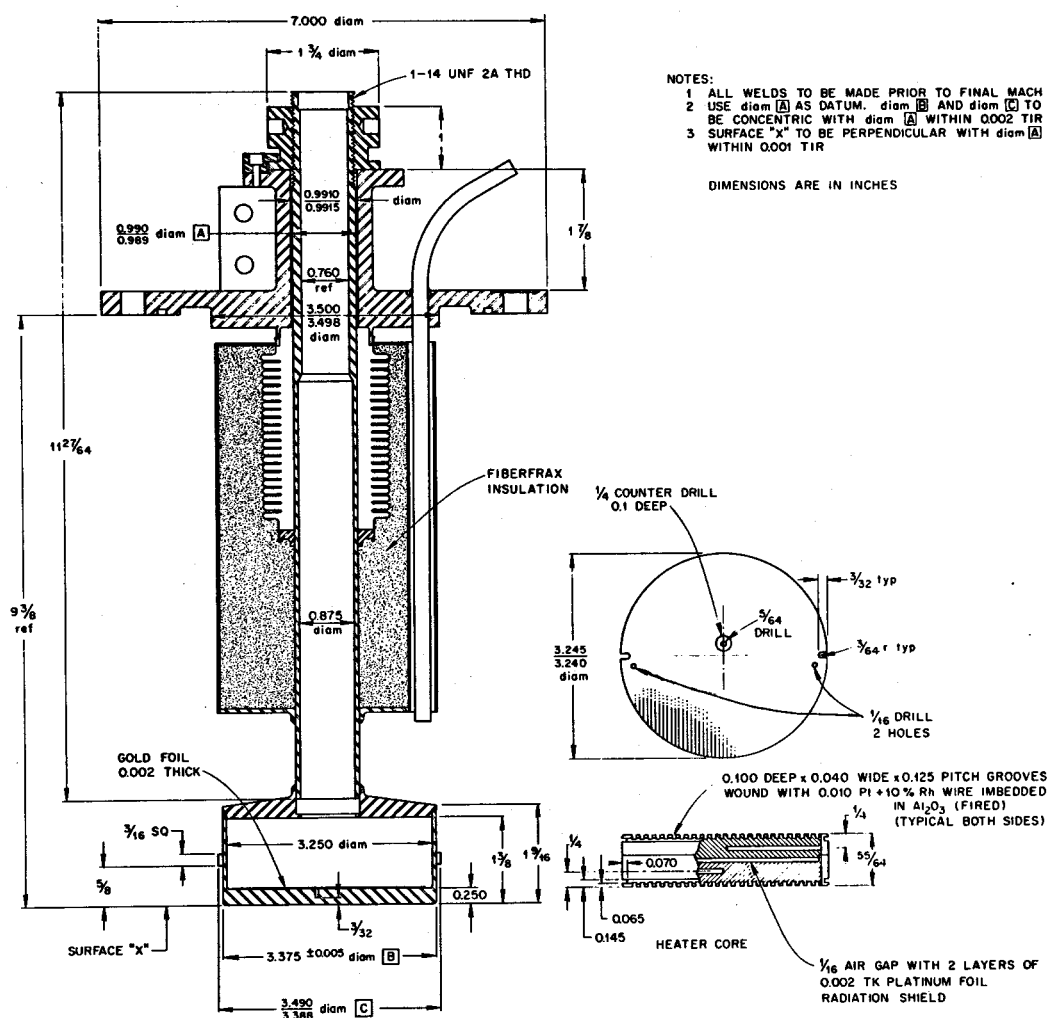


Fig. A-2. Detail of movable piston assembly of the conductivity cell.

draining, and cleaning the apparatus. In addition, the specimen volume and the total heated mass of the apparatus were made as small as possible.

The more important experimental equipment used in the present investigation is listed in Table A-1. Model and serial numbers, capacities, accuracies, and least count are given when known or applicable.

Table A-1. List of Pertinent Experimental Equipment
(heading values are given if known)

Equipment	Capacity or range	Accuracy	Least Count
<u>Potentiometer</u>			
L&N 7555 type K-5, 177362, Leeds & Northrup	0 - 1.6 V	±(0.001% of reading + 2 µV)	2.0 µV
	0 - 0.16 V	±(0.003% of reading + 0.02 µV)	0.2 µV
	0 - 0.016 V	±(0.003% of reading + 0.1 µV)	0.02 µV
<u>Voltage regulator</u>			
Variac, automatic Model 1581-A	Output 115 V, adj. ±10%, 50 A	±0.25%	
<u>Null detector</u>			
Leeds & Northrup 9834-1	0.07 µV/mm for source resistances up to 2000 Ω		0.1 µV
<u>DC digital voltmeter</u>			
Vidar 521 integrating voltmeter	±10 µV to ±1000 V in six-decade stages	±0.01% of full scale	1.0 µV
<u>Thermocouples</u>			
Pt vs Pt-10% Rh		±0.2	
Chromel-Alumel		±0.75	
<u>Precision resistor</u>			
Leeds & Northrup Model 4360	0.1 Ω, 15 A	±0.04%	
<u>DC voltage supply</u>			
Kepco Model SM 75-8MX	Input 105-125 V, 60 cps, 9.6 A max; output 0-75 V, 0-8 A	Line: <0.01% voltage variation or 0.002 V, which- ever greater after stabilizing	
<u>Dial indicator</u>			
Federal Model E3BS-R1	20 revolutions (0.4 in.)	one-half of one division	0.0001 in.

APPENDIX B

EXPERIMENTAL DATA

The uncorrected, raw data, experimental thermocouple emfs, heater current and voltage, and gap-dial indicator readings are given in Tables B-1 through B-11. The reduced experimental results, which include specimen thickness, the average temperature level, temperature drop, heat flux, and total thermal resistance are tabulated in Tables B-12 through B-22. All these data are grouped by specimen and apparatus model numbers (Table 1), and appear in chronological order.

The guard and shunting factors are determined as indicated in the method of calculation given in Chapter 2, where the guard factor is specifically defined as (see Fig. 12):

$$G \equiv \frac{T_3 - T_5}{T_3 - T_2} .$$

The heat flux is determined as

$$\frac{Q}{A} = \frac{4FEIV}{\pi D^2} .$$

The data for vacuum runs were reduced in a slightly different way from the other runs. The plate-to-plate temperature drop was determined from the total drop minus the estimated wall temperature drops and was used to calculate the thermal resistance. If the average temperature level varied significantly in the vacuum runs, the calculated thermal resistances were normalized to a mean average temperature by the ratio

$$\left(\frac{T_{\max}}{T_{\text{mean}}} \right)^3 ,$$

where T is in °K.

Table B-1. Experimental Data for H₂O Using Apparatus I-A

Table B-1 (Continued)

Table B-2. Experimental Data for Hg Using Apparatus I-A

Run →	1-A	1-B	1-C	1-D	1-E	2-A	2-B	2-C	2-D	2-E	2-F
Date	9-14-65	9-14-65	9-14-65	9-14-65	9-14-65	9-15-65	9-15-65	9-15-65	9-15-65	9-15-65	9-15-65
Time Begun	12:55	2:05	3:50	4:06	6:05	10:40	12:10	1:25	2:45	4:45	6:40
Dial Zero (in.)	-0.00050	-0.00050	-0.00050	-0.00050	-0.00050	0.00000	0.00000	0.00000	0.00000	0.00000	0.00000
Dial Reading (in.)	0.19469	0.09462	0.09451	0.04446	0.02237	0.09500	0.04480	0.14975	0.09508	0.04484	0.00578
TC 1 (mv)	2.5855	2.5774	2.5800	2.5498	2.4645	2.5861	2.5673	2.6130	2.5707	2.5312	2.5167
TC 2 (mv)	2.2959	2.3658	2.3585	2.3648	2.3048	2.3815	2.3989	2.3620	2.3626	2.3621	2.3766
TC 3 (mv)	3.0665	2.9982	3.0192	2.9771	2.8796	3.0324	2.9891	3.0881	2.9889	2.9476	2.9216
TC 4 (mv)	3.0351	2.9842	3.0069	2.9658	2.8766	3.0190	2.9827	3.0662	2.9773	2.9423	2.9228
TC 6 (mv)	-	-	-	-	-	-	-	-	-	-	-
TC 5 (mv)	3.0348	2.9830	3.0136	2.9956	2.8535	3.0285	2.9849	3.0652	2.9751	2.9517	2.9128
TC 7 (mv)	1.0832	0.8723	0.8765	-	-	0.8735	0.8389	0.8820	0.8505	-	-
TC 8 (mv)	-	-	-	-	-	-	-	-	-	-	-
TC 9 (mv)	-	-	-	-	-	-	-	-	-	-	-
TC 1 (final)	2.5841	2.5728	2.5793	2.5438	2.4638	2.5862	2.5657	2.6143	2.5498	2.5291	2.5181
TC 2 (final)	2.2941	2.3612	2.3579	2.3639	2.3038	2.3815	2.3971	2.3635	2.3441	2.3600	2.3776
Time Finish	1:12	2:16	3:55	4:46	6:15	10:50	12:20	1:35	3:35	4:50	6:46
HT {v}	0.0 (a)	0.0 0.0									
HM {v}	16.62 (a)	16.60 2.265	17.08 2.326	17.02 2.326	17.06 2.333	17.03 2.330	17.00 2.330	17.00 2.331	16.96 2.317	16.96 2.323	16.96 2.332
HS {v}	0.0 (a)	- 7.3	0.0 0.0	- 2.2	- -	0.0 0.0	- 5.5	0.0 0.0	- 3.7	- -	- -
HR 1 {v}	- (a)	8.2 7.5	- 7.6	- 7.5	- -	7.9 7.5	7.5 7.8	7.8 7.6	7.6 7.3	7.6 7.3	7.6 7.3
HR 2 {v}	- (a)	8.0 7.6	- 7.6	- 7.5	- -	7.9 7.6	7.6 7.6	7.6 7.3	7.3 7.3	7.3 7.3	7.3 7.3
HR 3 {v}	- (a)	8.0 7.6	- 7.6	- 7.5	- -	7.9 7.6	7.6 7.6	7.6 7.3	7.3 7.3	7.3 7.3	7.3 7.3
HF 1 {v}	0.0 (a)	0.0 0.0									
HF 2 {v}	0.0 (a)	0.0 0.0									

Table B-3. Experimental Data for HTS Using Apparatus I-A

Table B-3 (Continued)

Run No. →	2-E	2-F	3-A	3-B	3-C	3-D	3-E	3-F	3-G	3-H	3-I	3-J	3-K	3-L
Date	7-11-66	7-11-66	7-12-66	7-12-66	7-12-66	7-13-66	7-13-66	7-13-66	7-13-66	7-13-66	7-13-66	7-13-66	7-14-66	7-14-66
Time Begun	2:35	4:05	2:10	3:15	4:05	9:20	10:45	11:50	1:10	2:15	3:20	4:17	8:50	10:25
Dial Zero (in.)	0.00280	0.00280	0.00645	0.00645	0.00645	0.00645	0.00645	0.00645	0.00645	0.00645	0.00645	0.00645	0.00645	0.00645
Dial Reading (in.)	0.11650	0.14027	0.15656	0.14649	0.12648	0.11410	0.09417	0.07421	0.05418	0.03422	0.01415	0.02422	0.04443	0.06411
TC 1 (mv)	12.804	12.826	22.846	22.856	22.824	22.858	22.820	22.807	22.777	22.760	22.712	22.734	22.686	22.748
TC 2 (mv)	12.244	12.185	22.244	22.285	22.307	22.384	22.395	22.433	22.456	22.476	22.503	22.492	22.381	22.404
TC 3 (mv)	12.940	12.963	23.019	23.025	22.989	23.020	22.979	22.961	22.944	22.922	22.888	22.906	22.851	22.915
TC 4 (mv)	12.913	12.935	22.985	22.996	22.960	22.993	22.952	22.939	22.911	22.889	22.850	22.871	22.816	22.883
TC 5 (mv)	12.921	12.948	23.023	23.027	22.990	23.020	22.977	22.963	22.941	22.921	22.906	22.918	22.852	22.913
TC 6 (mv)	14.139	14.144	24.329	24.313	24.299	24.251	24.224	24.205	24.196	24.176	24.154	24.157	24.094	24.124
TC 7 (mv)	-	-	-	-	-	-	-	-	-	-	-	-	-	-
TC 8 (mv)	13.486	13.458	24.059	24.069	24.074	24.053	24.040	24.045	24.053	24.056	24.060	24.058	23.947	23.965
TC 9 (mv)	-	-	-	-	-	-	-	-	-	-	-	-	-	-
TC 1 (Final)	12.805	12.826	22.843	22.856	22.825	22.857	22.819	22.806	22.777	22.758	22.711	22.734	22.684	22.749
TC 2 (Final)	12.244	12.185	22.247	22.286	22.305	22.383	22.394	22.431	22.455	22.476	22.503	22.492	22.380	22.405
Time Finish	2:45	4:10	2:20	3:20	4:15	9:25	10:50	12:00	1:15	2:25	3:32	4:20	9:00	10:30
HT (v) (a)	0 0													
HM (v) (a)	8.72 0.8872	8.72 0.8868	9.62 0.7946	9.62 0.7942	9.62 0.7947	9.62 0.7946	9.62 0.7948	9.62 0.7949	9.62 0.7954	9.62 0.7959	9.62 0.7963	9.62 0.7959	9.60 0.7956	9.68 0.8009
HS (v) (a)	0 0													
HR 1 (v) (a)	4.0 3.9	4.0 3.9	4.7 4.0	4.7 4.0	4.7 4.0	4.6 3.9	4.6 3.9	4.6 3.9	4.6 3.9	4.0 3.3	4.0 3.3	4.0 3.3	4.0 3.3	4.0 3.3
HR 2 (v) (a)	5.6 6.0	5.8 6.2	3.8 3.7	3.7 3.5	3.1 3.0	2.8 2.6	2.3 2.1	2.0 1.5	1.2 0.8	- 0.2	0 0	1.0 0.5	- 0.5	1.7 1.2
HR 3 (v) (a)	5.5 5.9	5.8 6.2	3.7 3.5	3.7 3.5	3.1 3.0	2.8 2.5	2.3 2.1	2.0 1.6	1.2 0.8	- 0.2	0 0	1.0 0.5	- 0.5	1.7 1.2
HF 1 (v) (a)	- 3.7	- 3.7	6.1 6.1											
HF 2 (v) (a)	- 3.8	- 3.8	6.1 6.1											

Table B-3 (Continued)

Run No. →	3-M	3-N	3-O	4-A	4-B	4-C	4-D	4-E	4-F	5-A	5-B	5-C	5-D	5-E
Date	7-14/66	7-14-66	7-14-66	7-14-66	7-15-66	7-15-66	7-15-66	7-15-66	7-15-66	7-18-66	7-18-66	7-18-66	7-19-66	7-19-66
Time Begun	11:30	1:00	2:42	4:10	9:10	10:50	12:40	2:20	3:33	12:45	2:30	3:50	9:20	11:10
Dial Zero (in.)	0.00645	0.00645	0.00645	0.00645	0.00645	0.00645	0.00645	0.00645	0.00645	0.05269	0.05269	0.05269	0.05269	0.05269
Dial Reading (in.)	0.08432	0.10430	0.13669	0.03915	0.03891	0.01910	0.01188	0.02239	0.03054	0.20243	0.18253	0.16240	0.14226	0.12232
TC 1 (mv)	22.774	22.778	22.845	22.695	22.672	22.671	22.691	22.690	22.691	8.3190	8.2950	8.2555	8.2980	8.2450
TC 2 (mv)	22.378	22.335	22.316	22.418	22.385	22.448	22.495	22.457	22.433	7.6417	7.6902	7.7421	7.8495	7.8653
TC 3 (mv)	22.936	22.947	23.006	22.861	22.828	22.834	22.856	22.854	22.856	8.4584	8.4351	8.3871	8.4301	8.3772
TC 4 (mv)	22.907	22.916	22.979	22.828	22.800	22.802	22.822	22.822	22.824	8.4406	8.4171	8.3732	8.4159	8.3625
TC 5 (mv)	22.932	22.951	23.015	22.858	22.821	22.838	22.866	22.854	22.853	8.4288	8.3976	8.3381	8.3832	8.3315
TC 6 (mv)	24.143	24.146	24.166	24.083	24.013	24.017	24.035	24.033	23.027	9.2262	9.2213	9.1900	9.2147	9.2005
TC 7 (mv)	-	-	-	-	-	-	-	-	-	-	-	-	-	-
TC 8 (mv)	23.961	23.929	23.930	23.941	23.903	23.925	23.943	23.925	23.909	8.8046	8.7530	8.7556	8.8065	8.8067
TC 9 (mv)	-	-	-	-	-	-	-	-	-	-	-	-	-	-
TC 1 (final)	22.772	22.780	22.843	22.694	22.673	22.672	22.690	22.689	22.690	8.3193	8.2942	8.2551	8.2975	8.2438
TC 2 (final)	22.375	22.330	22.317	22.418	22.386	22.447	22.493	22.455	22.432	7.6417	7.6882	7.7410	7.8495	7.8652
Time Finish	11:40	1:10	2:50	4:15	9:20	11:00	12:50	2:34	3:43	12:50	2:35	3:55	9:35	11:20
HT (v) (a)	0 0													
HM (v) (a)	9.68 0.8008	9.68 0.8008	9.67 0.7987	9.64 0.7983	9.68 0.8022	9.68 0.8023	9.68 0.8018	9.68 0.8018	9.68 0.8018	9.59 1.0995	9.59 1.1003	9.59 1.1016	9.59 1.1016	9.59 1.1016
HS (v) (a)	0 0													
HR 1 (v) (a)	4.0 3.3	4.0 3.3	4.0 3.3	2.4 2.0	2.4 2.0	2.4 1.9	2.4 1.9	2.4 1.9	2.4 1.9	1.9 1.7	1.9 1.7	1.9 1.7	1.9 1.7	1.9 1.7
HR 2 (v) (a)	2.0 1.7	2.6 2.3	3.3 3.2	<1.0 0.3	<1.0 0.2	0 0	0 0	0 0	1.0 0.5	5.6 6.2	5.4 6.0	5.1 5.5	4.9 5.4	4.7 5.2
HR 3 (v) (a)	2.0 1.7	2.6 2.4	3.3 3.1	<1.0 0.4	<1.0 0.3	0 0	0 0	0 0	1.0 0.5	5.5 6.2	5.3 6.0	5.0 5.5	4.9 5.2	4.7 5.2
HF 1 (v) (a)	6.1 6.1	6.1 6.1	6.1 6.1	6.1 6.1	6.1 6.1	6.1 6.0	6.1 6.1	6.1 6.1	6.1 6.1	2.8 2.7	2.7 2.7	2.7 2.7	2.7 2.7	2.7 2.7
HF 2 (v) (a)	6.1 6.1	6.1 6.1	6.1 6.1	6.1 6.1	6.1 6.1	6.0 6.1	6.1 6.1	6.1 6.1	6.1 6.1	2.8 2.7	2.8 2.7	2.7 2.7	2.7 2.7	2.7 2.7

Table B-3 (Continued)

Run No. →	5-F	5-G	5-H	5-I	5-J	5-K	5-L	5-M	5-N	6-A	6-B	6-C	6-D	6-E
Date	7-19-66	7-19-66	7-19-66	7-20-66	7-20-66	7-20-66	7-20-66	7-20-66	7-20-66	7-21-66	7-21-66	7-21-66	7-21-66	7-21-66
Time Begun	12:37	2:35	3:30	8:50	10:10	11:20	12:20	1:35	2:25	9:00	10:10	12:10	1:55	3:00
Dial Zero (in.)	0.05269	0.05269	0.05269	0.05269	0.05269	0.05269	0.05269	0.05269	0.05269	0.04258	0.4258	0.04258	0.04258	0.04258
Dial Reading (in.)	0.10241	0.10241	0.08248	0.06258	0.05805	0.05495	0.05269	0.07248	0.09245	0.19544	0.17540	0.15540	0.13518	0.11540
TC 1 (mv)	8.1878	8.1800	8.1360	8.0474	8.0307	8.0424	8.0356	8.0621	8.1019	11.5063	11.4776	11.4570	11.4918	11.4631
TC 2 (mv)	7.8830	7.8772	7.9015	7.8885	7.8893	7.9127	7.9115	7.8702	7.8388	10.9625	10.9873	11.0294	11.1131	11.1363
TC 3 (mv)	8.3199	8.3119	8.2684	8.1776	8.1563	8.1660	8.1600	8.1881	8.2296	11.6280	11.6017	11.5769	11.6122	11.5832
TC 4 (mv)	8.3056	8.2971	8.2530	8.1629	8.1433	8.1532	8.1470	8.1748	8.2161	11.6076	11.5806	11.5567	11.5934	11.5631
TC 5 (mv)	8.2738	8.2619	8.2288	8.1438	8.1170	8.1262	8.1231	8.1440	8.1768	11.6136	11.5815	11.5466	11.5923	11.5625
TC 6 (mv)	9.1811	9.1630	9.1508	9.1049	9.1021	9.1001	9.0990	9.1030	9.1088	13.3060	13.2899	13.2726	13.2809	13.2832
TC 7 (mv)	-	-	-	-	-	-	-	-	-	-	-	-	-	-
TC 8 (mv)	8.8037	8.7926	8.7932	8.7616	8.7838	8.7835	8.7840	8.7744	8.7688	12.9338	12.9291	12.9388	12.9700	12.9839
TC 9 (mv)	-	-	-	-	-	-	-	-	-	-	-	-	-	-
TC 1 (final)	8.1878	8.1800	8.1349	8.0473	8.0307	8.0416	8.0356	8.0657	8.0990	11.5050	11.4778	11.4565	11.4931	11.4626
TC 2 (final)	7.8833	7.8772	7.9016	7.8883	7.8903	7.9121	7.9111	7.8725	7.8356	10.9625	10.9873	11.0280	11.1142	11.1366
Time Finish	12:45	2:40	3:40	9:00	10:20	11:35	12:30	1:45	2:40	9:13	10:15	12:20	2:00	3:10
HT (v) (a)	0 0	0 0	0 0	0 0	0 0									
HM (v) (a)	9.59 1.1034	9.59 1.1043	9.59 1.1056	9.59 1.1086	9.59 1.1093	9.59 1.1091	9.59 1.1093	9.59 1.1083	9.59 1.1072	8.645 0.9086	8.64 0.9092	8.64 0.9097	8.64 0.9087	8.64 0.9093
HS (v) (a)	0 0	0 0	0 0	0 0	0 0									
HR 1 (v) (a)	1.8 1.6	2.0 1.6	2.0 1.6	2.0 1.6	2.0 1.6	2.0 1.6								
HR 2 (v) (a)	4.4 4.9	4.5 4.9	4.35 4.8	4.1 4.6	3.9 4.3	3.9 4.3	3.9 4.3	4.1 4.6	4.3 4.7	4.2 4.4	3.9 4.1	3.6 3.9	3.4 3.65	3.2 3.4
HR 3 (v) (a)	4.5 5.0	4.5 5.0	4.35 4.7	4.0 4.4	3.9 4.3	3.9 4.3	3.9 4.3	4.1 4.6	4.3 4.7	4.1 4.3	3.9 4.1	3.4 3.0	3.4 3.65	3.2 3.3
HF 1 (v) (a)	- 2.7	- 3.8	- 3.8	- 3.8	- 3.8	- 3.8								
HF 2 (v) (a)	- 2.7	- 3.8	- 3.8	- 3.8	- 3.8	- 3.8								

Table B-3 (Continued)

Run No. →	6-F	6-G	6-H	6-I	6-J	7-A	7-B	7-C	7-D	7-E	7-F	7-G	7-H	7-I
Date	7-21-66	7-22-66	7-22-66	7-22-66	7-22-66	7-25-66	7-25-66	7-25-66	7-25-66	7-25-66	7-26-66	7-26-66	7-26-66	7-26-66
Time Begun	3:55	11:20	12:20	1:10	3:30	11:10	12:35	2:10	3:20	4:17	10:30	12:05	1:15	3:05
Dial Zero (in.)	0.04258	0.04258	0.04258	0.04258	0.04258	0.00672	0.00672	0.00672	0.00672	0.00672	0.00672	0.00672	0.00672	0.00672
Dial Reading (in.)	0.09541	0.07560	0.05535	0.04535	0.05039	0.12653	0.10650	0.08641	0.06636	0.04628	0.02657	0.01661	0.01162	0.02163
TC 1 (mv)	11.4312	11.3900	11.3670	11.3427	11.3306	22.976	22.949	22.929	22.934	22.914	22.881	22.853	22.854	22.864
TC 2 (mv)	11.1613	11.1736	11.2101	11.2173	11.1923	22.492	22.509	22.533	22.580	22.612	22.639	22.640	22.660	22.634
TC 3 (mv)	11.5516	11.5136	11.4910	11.4636	11.4467	23.139	23.107	23.090	23.095	23.084	23.063	23.041	23.036	23.043
TC 4 (mv)	11.5310	11.4908	11.4680	11.4413	11.4266	23.116	23.081	23.061	23.066	23.050	23.024	22.996	22.992	23.002
TC 5 (mv)	11.5316	11.4959	11.4838	11.4548	11.4289	23.159	23.118	23.096	23.096	23.089	23.077	23.064	23.065	23.068
TC 6 (mv)	13.2789	13.2767	13.2655	13.2579	13.2336	24.170	24.242	24.236	24.225	24.224	24.212	24.204	24.194	24.190
TC 7 (mv)	-	-	-	-	-	-	-	-	-	-	-	-	-	-
TC 8 (mv)	12.9912	12.9998	12.9936	12.9919	12.9759	24.041	24.048	24.057	24.074	24.089	24.068	24.062	24.063	24.053
TC 9 (mv)	-	-	-	-	-	-	-	-	-	-	-	-	-	-
TC 1 (final)	11.4316	11.3900	11.3676	11.3435	11.3310	22.975	22.947	22.930	22.935	22.915	22.887	22.853	22.853	22.864
TC 2 (final)	11.1620	11.1734	11.2110	11.2175	11.1935	22.492	22.510	22.535	22.581	22.613	22.639	22.659	22.634	
Time Finish	4:05	11:25	12:32	1:15	3:35	11:20	12:45	2:20	3:25	4:22	10:40	12:10	1:25	3:10
HT (v) (a)	0 0													
HM (v) (a)	8.64 0.9101	8.64 0.9112	8.64 0.9116	8.64 0.9121	8.64 0.9126	9.58 0.7888	9.58 0.7893	9.58 0.7894	9.58 0.7894	9.58 0.7896	9.58 0.7901	9.58 0.7906	9.58 0.7907	9.58 0.7907
HS (v) (a)	0 0													
HR 1 (v) (a)	2.0 1.6	2.0 1.6	2.0 1.6	2.0 1.6	2.0 1.6	1.8 1.05	1.8 1.05	1.8 1.05	1.8 1.05	1.8 1.05	1.4 0.8	1.0 0.2	0 0	0 0
HR 2 (v) (a)	2.9 3.1	2.7 2.7	2.4 2.5	2.1 2.2	2.2 2.2	3.1 3.0	2.3 2.3	2.0 1.7	1.5 1.2	1.0 0.5	0 0	0 0	0 0	0 0
HR 3 (v) (a)	2.9 3.1	2.8 2.8	2.5 2.5	2.1 2.1	2.1 2.1	3.1 3.0	2.3 2.3	2.0 1.8	1.5 1.2	0.1 0.5	0 0	0 0	0 0	0 0
HF 1 (v) (a)	- 3.8	- 3.8	- 3.8	- 3.8	- 3.8	- 6.2								
HF 2 (v) (a)	- 3.8	- 3.8	- 3.8	- 3.8	- 3.8	- 6.2	- 6.2	- 6.2	- 6.2	- 6.2	- 6.1	- 6.1	- 6.1	- 6.1

Table B-3 (Continued)

Run No. →	11-N	11-O	11-P	11-Q	11-R	11-S	11-T	11-U	11-V	11-W	11-X	11-Y	11-Z	11-AA
Date	8-8-66	8-8-66	8-8-66	8-10-66	8-10-66	8-10-66	8-10-66	8-10-66	8-10-66	8-10-66	8-10-66	8-10-66	8-10-66	8-10-66
Time Begun	9:40	10:40	11:20	9:00	10:15	11:10	12:00	12:50	1:35	2:25	3:30	4:10	4:57	6:40
Dial Zero (in.)	0.01540	0.01540	0.01540	0.01540	0.01540	0.01540	0.01540	0.01540	0.01540	0.01540	0.01540	0.01540	0.01540	0.01540
Dial Reading (in.)	0.07055	0.06458	0.05878	0.05435	0.05168	0.04671	0.04232	0.03826	0.03449	0.03072	0.02675	0.02270	0.02132	0.01954
TC 1 (mv)	22.963	22.970	22.959	23.067	23.068	23.058	23.056	23.052	23.056	23.047	23.027	23.018	23.012	23.027
TC 2 (mv)	22.610	22.627	22.626	22.764	22.778	22.781	22.789	22.795	22.811	22.810	22.800	22.820	22.816	22.836
TC 3 (mv)	23.131	23.134	23.123	23.222	23.227	23.222	23.219	23.216	23.220	23.213	23.198	23.194	23.191	23.202
TC 4 (mv)	23.103	23.101	23.091	23.197	23.198	23.190	23.189	23.185	23.189	23.179	23.163	23.157	23.153	23.165
TC 5 (mv)	23.132	23.127	23.122	23.221	23.224	23.220	23.223	23.222	23.227	23.221	23.212	23.214	23.213	23.224
TC 6 (mv)	24.230	24.221	24.219	24.277	24.277	24.276	24.276	24.273	24.272	24.269	24.264	24.260	24.262	24.264
TC 7 (mv)	-	-	-	-	-	-	-	-	-	-	-	-	-	-
TC 8 (mv)	24.050	24.049	24.046	24.143	24.145	24.140	24.137	24.141	24.149	24.152	24.149	24.152	24.151	24.164
TC 9 (mv)	-	-	-	-	-	-	-	-	-	-	-	-	-	-
TC 1 (final)	22.962	22.970	22.959	23.067	23.066	23.057	23.056	23.052	23.057	23.045	23.026	23.018	23.009	23.026
TC 2 (final)	23.609	22.626	22.626	22.764	22.777	22.780	22.790	22.796	22.812	22.809	22.800	22.820	22.815	22.836
Time Finish	9:45	10:45	11:25	9:05	10:25	11:16	12:10	1:00	1:45	2:35	3:35	4:17	5:07	6:45
HF (v) (a)	0 0	0 0	0 0	0 0	0 0	0 0	0 0	0 0	0 0	0 0	0 0	0 0	0 0	0 0
FM (v) (a)	9.60 0.7899	9.60 0.7900	9.60 0.7903	9.595 0.7881	9.595 0.7881	9.595 0.7881	9.59 0.7879	9.585 0.7878	9.585 0.7879	9.585 0.7880	9.585 0.7881	9.585 0.7881	9.585 0.7881	9.585 0.7878
HS (v) (a)	0 0	0 0	0 0	0 0	0 0	0 0	0 0	0 0	0 0	0 0	0 0	0 0	0 0	0 0
HR 1 (v) (a)	1.7 1.05	1.7 1.05	1.7 1.05	1.8 1.05	1.8 1.05	1.8 1.05	1.8 1.05	1.3 0.8	1.3 0.8	0 0	0 0	0 0	0 0	0 0
HR 2 (v) (a)	1.1 0.8	1.0 0.5	1.0 0.5	<1.0 0.3	<1.0 0.3	<1.0 0.2	<1.0 0.1	0 0						
HR 3 (v) (a)	1.2 0.9	1.0 0.5	1.0 0.5	<1.0 0.3	<1.0 0.3	<1.0 0.2	<1.0 0.1	0 0						
HF 1 (v) (a)	6.2 6.2	6.2 6.2	6.2 6.2	6.2 6.2	6.2 6.2	6.2 6.2	6.2 6.2	6.2 6.2	6.2 6.2	6.2 6.2	6.2 6.2	6.2 6.2	6.2 6.2	6.2 6.2
HF 2 (v) (a)	6.2 6.2	6.2 6.2	6.2 6.2	6.2 6.2	6.2 6.2	6.2 6.2	6.2 6.2	6.2 6.2	6.2 6.2	6.2 6.2	6.2 6.2	6.2 6.2	6.2 6.2	6.2 6.2

Table B-3 (Continued)

Run No. +	11-BB	11-CC	12-A	12-B	12-C	12-D	12-E	12-F	12-G	12-H	12-I	12-J	12-K	12-L
Date	8-10-66	8-10-66	8-10-66	8-10-66	8-10-66	8-10-66	8-10-66	8-11-66	8-11-66	8-11-66	8-11-66	8-11-66	8-11-66	8-11-66
Time Begun	7:23	8:05	8:55	9:35	10:15	10:50	11:35	8:40	9:56	10:45	11:35	12:25	1:20	2:30
Dial Zero (in.)	0.01540	0.01540	0.01540	0.01540	0.01540	0.01540	0.01540	0.01540	0.01540	0.01540	0.01540	0.01540	0.01540	0.01540
Dial Reading (in.)	0.01742	0.01532	0.02336	0.03125	0.03511	0.03908	0.04301	0.04691	0.05095	0.05481	0.05870	0.06461	0.07063	0.07652
TC 1 (mv)	23.014	23.005	23.009	23.021	23.026	23.029	23.043	23.094	23.085	23.085	23.087	23.087	23.087	23.086
TC 2 (mv)	22.837	22.829	22.805	22.791	22.785	22.780	22.782	22.822	22.809	22.805	22.801	22.795	22.791	22.784
TC 3 (mv)	23.198	23.185	23.188	23.194	23.196	23.198	23.207	21.257	23.251	23.251	23.252	23.250	23.248	23.248
TC 4 (mv)	23.157	23.146	23.148	23.158	23.162	23.165	23.176	23.225	23.219	23.220	23.220	23.219	23.219	23.219
TC 5 (mv)	23.222	23.217	23.207	23.204	23.203	23.201	23.211	23.259	23.252	23.252	23.251	23.250	23.249	23.251
TC 6 (mv)	24.266	24.265	24.261	24.256	24.254	24.254	24.261	24.298	24.293	24.291	24.287	24.286	24.279	24.278
TC 7 (mv)	-	-	-	-	-	-	-	-	-	-	-	-	-	-
TC 8 (mv)	24.159	24.150	24.137	24.128	24.125	24.123	24.124	24.163	24.149	24.143	24.140	24.134	24.133	24.132
TC 9 (mv)	-	-	-	-	-	-	-	-	-	-	-	-	-	-
TC 1 (final)	23.014	23.003	23.009	23.021	23.026	23.030	23.043	23.092	23.086	23.087	23.085	23.086	23.087	23.086
TC 2 (final)	22.836	22.829	22.805	22.791	22.784	22.780	22.782	22.821	22.809	22.807	22.800	22.795	22.792	22.784
Time Finish	7:28	8:10	9:00	9:40	10:20	10:55	11:40	8:55	10:05	10:55	11:45	12:30	1:30	2:40
HT {v}	0	0	0	0	0	0	0	0	0	0	0	0	0	0
{a}	0	0	0	0	0	0	0	0	0	0	0	0	0	0
HM {v}	9.585 0.7878	9.585 0.7881	9.585 0.7869	9.585 0.7871	9.585 0.7871	9.585 0.7869	9.585 0.7869	9.585 0.7870						
{a}	0	0	0	0	0	0	0	0	0	0	0	0	0	0
HS {v}	0	0	0	0	0	0	0	0	0	0	0	0	0	0
{a}	0	0	0	0	0	0	0	0	0	0	0	0	0	0
HR 1 {v}	0	0	0	0	0	0	1.8	1.8	1.8	1.8	1.8	1.8	1.8	1.8
{a}	0	0	0	0	0	0	1.0	1.0	1.0	1.0	1.0	1.0	1.0	1.0
HR 2 {v}	0	0	0	0	0	0	0	<1.0 0.15	<1.0 0.2	<1.0 0.3	<1.0 0.4	<1.0 0.5	<1.0 0.6	<1.0 0.7
{a}	0	0	0	0	0	0	0	0.15	0.3	0.4	0.5	0.6	0.7	1.0
HR 3 {v}	0	0	0	0	0	0	0	<1.0 0.15	<1.0 0.3	<1.0 0.4	<1.0 0.5	<1.0 0.6	<1.0 0.7	<1.0 0.8
{a}	0	0	0	0	0	0	0	0.15	0.3	0.4	0.5	0.6	0.7	1.0
HF 1 {v}	-	-	-	-	-	-	-	-	-	-	-	-	-	-
{a}	6.2	6.2	6.2	6.2	6.2	6.2	6.2	6.2	6.2	6.2	6.2	6.2	6.2	-
HF 2 {v}	6.2	6.2	6.2	6.2	6.2	6.2	6.2	6.2	6.2	6.2	6.2	6.2	6.2	-
{a}	6.2	6.2	6.2	6.2	6.2	6.2	6.2	6.2	6.2	6.2	6.2	6.2	6.2	-

Table B-3 (Continued)

Run No. →	12-M	12-N	12-O	12-P	12-Q	12-R	12-S	12-T
Date	8-11-66	8-11-66	8-11-66	8-11-66	8-11-66	8-11-66	8-11-66	8-11-66
Time Begun	3:50	4:40	5:28	6:55	7:40	8:40	9:30	10:10
Dial Zero (in.)	0.01540	0.01540	0.01540	0.01540	0.01540	0.01540	0.01540	0.01540
Dial Reading (in.)	0.08221	0.08820	0.09413	0.10025	0.11000	0.11773	0.12558	0.13344
TC 1 (mv)	23.097	23.102	23.107	23.102	23.114	23.141	23.147	23.157
TC 2 (mv)	22.781	22.781	22.779	22.761	22.754	22.742	22.734	22.720
TC 3 (mv)	23.257	23.262	23.266	23.267	23.270	23.285	23.296	23.305
TC 4 (mv)	23.228	23.233	23.238	23.236	23.244	23.266	23.276	23.283
TC 5 (mv)	23.264	23.269	23.271	23.270	23.276	23.288	23.300	23.313
TC 6 (mv)	24.281	24.286	24.286	24.289	24.289	24.291	24.295	24.298
TC 7 (mv)	-	-	-	-	-	-	-	-
TC 8 (mv)	24.129	24.128	24.127	24.112	24.102	24.097	24.091	24.085
TC 9 (mv)	-	-	-	-	-	-	-	-
TC 1 (final)	23.096	23.102	23.107	23.102	23.115	23.142	23.147	23.157
TC 2 (final)	22.781	22.781	22.779	22.760	22.754	22.742	22.734	22.720
Time Finish	3:52	4:45	5:30	7:00	7:45	8:45	9:35	10:15
HT (v) (a)	0 0							
HM (v) (a)	9.60 0.7876	9.60 0.7876	9.59 0.7873	9.59 0.7872	9.59 0.7872	9.59 0.7871	9.59 0.7871	9.59 0.7871
HS (v) (a)	0 0							
HR 1 (v) (a)	1.8 1.0							
HR 2 (v) (a)	1.8 1.5	1.6 1.58	1.6 1.58	1.8 1.8	1.9 1.9	2.05 2.05	2.35 2.35	2.7 2.7
HR 3 (v) (a)	1.8 1.5	1.6 1.6	1.6 1.6	1.85 1.85	1.95 1.95	2.15 2.15	2.3 2.3	2.65 2.65
HF 1 (v) (a)	- -	- -	- -	6.2 6.2	6.2 6.2	6.2 6.2	6.2 6.2	6.2 6.2
HF 2 (v) (a)	- -	- -	- -	6.2 6.2	6.2 6.2	6.2 6.2	6.2 6.2	6.2 6.2

Table B-4. Experimental Data for Helium Using Apparatus II-A

Run No. →	1-A	1-B	1-C	1-D	1-E	1-F	1-G	1-H	1-I	1-J	1-K	2-A	2-B	2-C
Date	12-20-66	12-21-66	12-21-66	12-21-66	12-21-66	12-21-66	12-21-66	12-21-66	12-21-66	12-21-66	12-21-66	12-28-66	12-28-66	12-28-66
Time Begun	2:15	8:35	9:28	10:30	11:30	12:30	1:20	2:28	3:18	3:50	4:05	12:00	12:35	1:15
Dial Zero (in.)	0.01470	0.01470	0.01470	0.01470	0.01470	0.01470	0.01470	0.01470	0.01470	0.01470	0.01470	0.01930	0.01930	0.01930
Dial Reading (in.)	0.01470	0.01864	0.02258	0.02660	0.03047	0.03437	0.03830	0.04227	0.05411	0.09352	0.13292	0.01928	0.02325	0.02716
TC 1 (mv)	1.2203	1.2326	1.2382	1.2326	1.2369	1.2459	1.2543	1.2546	1.2685	1.3039	1.3286	4.3631	4.3708	4.3789
TC 2 (mv)	1.1836	1.1875	1.1823	1.1673	1.1621	1.1619	1.1603	1.1513	1.1406	1.1168	1.0979	4.2535	4.2415	4.2306
TC 3 (mv)	1.2377	1.2491	1.2534	1.2467	1.2493	1.2569	1.2667	1.2680	1.2813	1.3111	1.3352	4.4300	4.4353	4.4397
TC 4 (mv)	1.2341	1.2482	1.2531	1.2477	1.2516	1.2606	1.2695	1.2695	1.2829	1.3182	1.3425	4.4246	4.4316	4.4386
TC 5 (mv)	1.2335	1.2391	1.2381	1.2301	1.2291	1.2340	1.2399	1.2369	1.2363	1.2381	1.2386	4.4352	4.4319	4.4296
TC 6 (mv)	6.8867	6.8118	6.8156	6.8085	6.8000	6.7969	6.8000	6.7998	6.7951	6.7939	—	23.340	23.343	23.338
TC 7 (mv)	6.7335	6.6807	6.6792	6.6649	6.6519	6.6459	6.6466	6.6381	6.6314	6.6203	—	23.236	23.229	23.216
TC 8 (mv)	6.0896	6.0501	6.0463	6.0291	6.0096	5.9991	5.9915	5.9762	5.9676	5.9515	—	22.696	22.683	22.667
TC 9 (mv)	1.2362	1.2426	1.2395	1.2294	1.2266	1.2297	1.2316	1.2262	1.2230	1.2166	1.2095	4.3416	4.3354	4.3303
TC 1 (final)	1.2186	1.2328	1.2350	1.2326	1.2364	1.2463	1.2537	1.2542	1.2690	1.3047	1.3295	4.3633	4.3701	4.3791
TC 2 (final)	1.1816	1.1877	1.1793	1.1672	1.1619	1.1625	1.1597	1.1508	1.1406	1.1153	1.0922	4.2535	4.2408	4.2309
Time Finish	2:35	8:41	9:40	10:40	11:40	12:50	1:30	2:40	3:30	4:00	4:35	12:05	12:48	1:28
HT (v) (a)	2.59 —	2.59 —	2.59 —	2.59 —	2.59 —	2.59 —	2.87 —	3.14 —	3.87 —	4.48 —	5.22 —	0.0 0.0	0.0 0.0	0.0 0.0
HM (v) (a)	11.14 1.4129	11.14 1.4107	11.14 1.4094	11.14 1.4110	11.14 1.4105	11.14 1.4105	11.14 1.4072	11.14 1.4069	11.14 1.4085	11.15 1.3990	11.16 1.3951	20.19 1.806	20.19 1.806	20.19 1.805
HS (v) (a)	0.0 0.0	0.0 0.0	0.0 0.0	0.0 0.0										
HR 1 (v) (a)	2.0 1.6	2.0 1.6	2.0 1.6	2.0 1.6	2.0 1.7	2.5 1.6	2.5 1.6	2.5 1.6						
HR 2 (v) (a)	3.2 3.0	3.4 3.2	3.4 3.2	3.4 3.2	3.4 3.2	3.7 3.4	4.0 3.9	4.0 3.8	4.0 3.8	4.0 3.8	4.0 3.8	0.0 0.0	0.0 0.0	0.0 0.0
HR 3 (v) (a)	9.8 8.7	9.9 8.7	9.9 8.7	9.9 8.7	9.9 8.8	9.9 8.8	9.9 8.8	9.9 8.7	9.9 8.7	9.9 8.7	9.9 8.7	0.0 0.0	0.0 0.0	1.3 0.5
HF 1 (v) (a)	20.2 2.0	57.4 6.3	57.4 6.3	57.4 6.3										
HF 2 (v) (a)	13.5 1.3	13.6 1.3	13.6 1.3	13.6 1.3	13.5 1.3	13.5 1.3	13.5 1.3	13.6 1.3	13.6 1.3	13.6 1.3	13.6 1.3	54.5 5.9	54.5 5.9	54.5 5.9

Table B-4 (Continued)

Run No. →	2-D	2-E	2-F	2-G	2-H	2-I	2-J	2-K	2-L	2-M	2-N
Date	12-28-66	12-28-66	12-28-66	12-29-66	12-29-66	12-29-66	12-29-66	12-29-66	12-29-66	12-29-66	12-29-66
Time Begun	2:05	2:55	3:50	8:40	10:30	11:30	12:50	1:35	2:50	3:55	5:20
Dial Zero (in.)	0.01930	0.01930	0.01930	0.01930	0.01930	0.01930	0.01930	0.01930	0.01980	0.01930	0.01850
Dial Reading (in.)	0.03112	0.03510	0.03890	0.04288	0.04688	0.05064	0.05478	0.05869	0.09780	0.13732	0.01850
TC 1 (mv)	4.3841	4.3998	4.4141	4.4101	4.4295	4.4428	4.4450	4.4505	4.5299	4.6069	4.3784
TC 2 (mv)	4.2171	4.2152	4.2086	4.1867	4.1900	4.1840	4.1662	4.1533	4.0950	4.0212	4.2630
TC 3 (mv)	4.4437	4.4579	4.4725	4.4686	4.4868	4.5000	4.5065	4.5121	4.5859	4.6719	4.44447
TC 4 (mv)	4.4437	4.4602	4.4732	4.4694	4.4890	4.4995	4.5049	4.5096	4.5872	4.6644	4.4364
TC 5 (mv)	4.4271	4.4379	4.4513	4.4442	4.4564	4.4694	4.4726	4.4764	4.5339	4.6204	4.4457
TC 6 (mv)	23.324	23.330	23.352	23.345	23.352	23.387	23.397	23.402	23.516	23.714	-
TC 7 (mv)	23.197	23.201	23.221	23.184	23.199	23.220	23.215	23.213	23.276	23.427	-
TC 8 (mv)	22.636	22.621	22.612	22.551	22.556	22.538	22.514	22.488	22.410	22.351	-
TC 9 (mv)	4.3249	4.3332	4.3402	4.3291	4.3414	4.3454	4.3452	4.3420	4.3649	4.3922	4.3497
TC 1 (final)	4.3833	4.4008	4.4132	4.4110	4.4300	4.4440	4.4449	4.4500	4.5298	4.6046	4.3759
TC 2 (final)	4.2163	4.2156	4.2078	4.1878	4.1906	4.1799	4.1655	4.1528	4.0950	4.0209	4.2615
Time Finish	2:15	3:07	4:00	8:50	10:37	12:17	1:01	1:46	3:00	4:08	5:40
HT (v) (a)	0.62 -	0.96 -	1.50 -	1.98 -	2.48 -	2.77 -	2.97 -	3.11 -	3.50 -	3.50 -	0.0 0.0
HM (v) (a)	20.19 1.804	20.19 1.803	20.19 1.802	20.18 1.802	20.18 1.800	20.19 1.797	20.19 1.747	20.19 1.796	20.19 1.786	20.19 1.777	20.19 1.804
HS (v) (a)	0.0 0.0										
HR 1 (v) (a)	2.5 1.6										
HR 2 (v) (a)	0.9 0.5	2.0 1.4	3.2 2.6	3.1 2.5	3.1 2.5	4.2 3.3	4.2 3.3	5.1 4.2	7.6 6.2	10.0 9.2	-
HR 3 (v) (a)	1.9 1.0	3.4 2.7	4.6 3.6	5.0 4.1	5.9 4.8	6.5 5.2	7.0 6.3	7.5 6.0	10.0 8.0	10.0 9.8	-
HF 1 (v) (a)	57.5 6.3	57.5 6.3	57.4 6.3	-							
HF 2 (v) (a)	54.5 5.9	54.5 5.9	54.4 5.9	54.5 6.0	54.4 5.9	54.4 5.9	54.4 6.0	54.4 6.0	54.4 6.0	54.4 6.0	-

Table B-5. Experimental Data for Vacuum Using Apparatus III-B

Run →	1-A	1-B	1-C	1-D	2-A	2-B	2-C	2-D	3-A	3-B	3-C	3-D
Date	1-20-67	1-20-67	1-20-67	1-20-67	1-24-67	1-24-67	1-24-67	1-24-67	5-24-67	5-24-67	5-24-67	5-24-67
Time Begun	2:10	2:45	3:15	3:55	8:45	9:40	11:20	2:25	12:40	1:30	3:55	4:17
Dial Zero (in.)	0.00917	0.00917	0.00917	0.00917	0.01600	0.01600	0.01600	0.01600	0.01000	0.01000	0.01079	0.1079
Dial Reading (in.)	0.12590	0.08782	0.04859	0.02838	0.0548	0.09480	0.13417	0.03528	0.02968	0.06905	0.05018	0.08963
TC 1 (mv)	0.6298	0.6295	0.6295	0.6296	4.4860	4.4860	4.4856	4.4837	8.3780	8.3826	8.2059	8.2079
TC 2 (mv)	0.4763	0.4770	0.4747	0.4760	4.2279	4.2278	4.2266	4.2270	7.5811	7.5785	7.7469	7.7469
TC 3 (mv)	0.6291	0.6290	0.6291	0.6295	4.4971	4.4962	4.4957	4.4934	8.5336	8.5356	8.2831	8.2829
TC 4 (mv)	0.6304	0.6301	0.6302	0.6304	4.4982	4.4979	4.4981	4.4948	8.5394	8.5415	8.2719	8.2730
TC 5 (mv)	0.6380	0.6394	0.6371	0.6363	4.5573	4.5545	4.5523	4.5526	8.2179	8.2165	8.2951	8.2949
TC 6 (mv)	-	-	-	-	23.421	23.408	23.399	23.382	8.4225	8.4215	8.4499	-
TC 7 (mv)	-	-	-	-	23.156	23.143	23.135	23.128	8.1614	8.1594	8.2714	-
TC 8 (mv)	-	-	-	-	22.461	22.428	22.401	22.435	7.6730	7.6720	7.8571	-
TC 9 (mv)	0.6040	0.6050	0.6032	0.6030	4.4533	4.4504	4.4487	4.4496	7.9869	7.9835	8.0843	8.0825
TC 1 (final)	0.6295	0.6295	0.6293	0.6295	4.4860	4.4858	4.4859	4.4836	8.3795	8.3830	8.2051	8.2073
Tc 2 (final)	0.4762	0.4770	0.4753	0.4757	4.2279	4.2278	4.2269	4.2279	7.5820	7.5801	7.7469	7.7450
Time Finish	2:17	2:50	3:28	4:00	-	10:10	11:25	2:35	12:50	1:40	4:05	4:25
HT (v) (a)	2.11 -	2.11 -	2.11 -	2.11 0.0	0.0 0.0	0.13 -	0.41 -	0.27 -	14.5 -	14.5 -	0.0 0.0	0.0 0.0
HM (v) (a)	2.08 0.2979	2.08 0.2978	2.08 0.2978	2.08 0.2977	8.105 0.7292	8.100 0.7280	8.085 0.7269	8.100 0.7296	20.25 1.412	20.25 1.412	12.00 0.848	12.00 0.848
HS (v) (a)	0.0 0.0	0.0 0.0	0.0 0.0	0.0 0.0	0.0 0.0	0.0 0.0	0.0 0.0	0.0 0.0	0.0 0.0	0.0 0.0	0.0 0.0	0.0 0.0
HR 1 (v) (a)	4.4 4.1	4.4 4.1	4.4 4.1	4.4 4.1	0.0 0.0	0.0 0.0	0.0 0.0	0.0 0.0	10.0 9.8	10.0 9.8	10.0 9.8	10.0 9.8
HR 2 (v) (a)	4.9 5.0	4.9 5.0	4.8 4.9	4.6 4.7	0.0 0.0	0.0 0.0	0.0 0.0	0.0 0.0	8.9 7.1	8.9 7.1	9.0 7.1	9.0 7.1
HR 3 (v) (a)	6.7 7.0	6.7 7.0	6.6 7.0	6.7 7.0	0.0 0.0	0.0 0.0	0.0 0.0	0.0 0.0	8.1 7.0	8.1 7.0	8.2 7.0	8.2 7.0
HF 1 (v) (a)	0.0 0.0	0.0 0.0	0.0 0.0	0.0 0.0	57.4 6.4	57.4 6.4	57.5 6.4	57.4 6.4	83.5 9.2	83.5 9.2	83.5 9.2	83.5 9.2
HF 2 (v) (a)	0.0 0.0	0.0 0.0	0.0 0.0	0.0 0.0	54.6 6.0	54.6 6.0	54.6 6.0	54.7 6.0	78.0 8.6	78.0 8.6	78.0 8.6	78.0 8.6

72

Table B-6. Experimental Data for HTS Using Apparatus II-B

Run No. →	1-A	1-B	1-C	1-D	1-E	1-F	1-G	1-H	1-I	1-J	1-K	1-L
Date	2-7-67	2-7-67	2-7-67	2-7-67	2-7-67	2-7-67	2-7-67	2-8-67	2-8-67	2-8-67	2-8-67	2-8-67
Time Begun	9:10	9:25	10:40	1:05	2:10	3:10	4:00	8:45	10:00	10:40	11:25	1:25
Dial Zero (in.)	0.00172	0.00172	0.00172	0.00172	0.00172	0.00172	0.00172	0.00172	0.00172	0.00172	0.00172	0.00172
Dial Reading (in.)	0.00172	0.00563	0.00960	0.01352	0.01743	0.02142	0.02537	0.02930	0.03334	0.03720	0.04115	0.08049
TC 1 (mv)	4.5465	4.5598	4.5681	4.5734	4.5759	4.5852	4.5943	4.5980	4.5995	4.6049	4.6083	4.6663
TC 2 (mv)	4.4152	4.4122	4.4019	4.3846	4.3777	4.3750	4.3700	4.3672	4.3613	4.3570	5.3515	4.2920
TC 3 (mv)	4.6469	4.6543	4.6680	4.6794	4.6867	4.6919	4.7008	4.7065	4.7080	4.7120	4.7131	4.7667
TC 4 (mv)	4.6484	4.6569	4.6665	4.6755	4.6815	4.6903	4.6970	4.7050	4.7070	4.7120	4.7141	4.7699
TC 5 (mv)	4.6196	4.6215	4.6310	4.6457	4.6638	4.6832	4.6971	4.7017	4.7010	4.7044	4.7024	4.7351
TC 6 (mv)	23.248	23.243	23.256	23.301	23.329	23.374	—	23.455	23.455	23.454	23.449	23.511
TC 7 (mv)	23.136	23.127	23.139	23.161	23.197	23.239	—	23.280	23.279	23.274	23.266	23.309
TC 8 (mv)	22.251	22.221	22.199	22.158	22.141	22.125	—	22.092	22.086	22.076	22.056	21.958
TC 9 (mv)	4.5401	4.5391	4.5434	4.5505	4.5604	4.5733	4.5800	4.5843	4.5810	4.5839	4.5813	4.5913
TC 1 (final)	4.5465	4.5534	4.5630	4.5704	4.5773	4.5847	4.5895	4.5985	4.5995	4.6052	4.6084	4.6669
TC 2 (final)	4.4152	4.4039	4.3957	4.3848	4.3787	4.3745	4.3662	4.3672	4.3615	4.3575	4.3507	4.2926
Time Finish	9:20	10:37	11:35	1:35	2:30	3:30	4:20	8:55	10:10	10:55	11:35	1:35
HT (v) (a)	4.18 —	4.47 —	5.02 —	4.90 —	4.0 —	1.95 —	1.00 —	0.98 —	0.98 —	0.98 —	0.98 —	2.96 —
HM (v) (a)	19.62 1.720	19.64 1.720	19.64 1.719	19.64 1.717	19.64 1.714	19.60 1.711	19.60 1.710	19.64 1.712	19.64 1.712	19.64 1.712	19.64 1.712	19.64 1.703
HS (v) (a)	0.0 0.0											
HR 1 (v) (a)	7.6 5.0	7.6 5.0	7.6 5.0	7.6 5.0	7.6 5.0	7.5 5.0	7.5 5.0	7.5 5.0	7.5 5.0	7.5 5.0	7.5 5.0	6.0
HR 2 (v) (a)	2.1 1.6	2.5 2.1	3.6 3.0	4.7 4.0	6.0 5.0	6.8 5.8	7.5 6.3	7.4 6.4	7.4 6.4	7.5 6.4	7.5 6.4	9.6 8.2
HR 3 (v) (a)	2.0 1.5	2.4 2.0	3.5 3.0	4.5 3.9	5.6 4.9	6.5 5.8	7.1 6.2	6.9 6.2	7.0 6.2	7.3 6.5	7.3 6.5	9.2 8.2
HF 1 (v) (a)	57.6 6.4	57.5 6.4	57.5 6.4	57.5 6.4	57.5 6.4	57.5 6.4						
HF 2 (v) (a)	54.7 5.9	54.7 5.9	54.7 5.9	54.7 5.9	54.7 5.9	54.7 6.0						

Table B-6 (Continued)

Table B-7. Experimental Data for Helium Using Apparatus II-B

Run No. →	1-A	1-B	1-C	1-D	1-E	1-F	1-G	1-H	1-I	1-J
Date	1-25-67	1-25-67	1-25-67	1-25-67	1-25-67	1-25-67	1-25-67	1-25-67	1-25-67	1-25-67
Time Begun	10:10	12:00	12:50	1:25	3:35	5:00	5:30	6:40	8:02	8:40
Dial Zero (in.)	0.01870	0.01870	0.01870	0.01870	0.01870	0.01870	0.01870	0.01870	0.01870	0.01870
Dial Reading (in.)	0.01870	0.02255	0.02654	0.03052	0.03432	0.03840	0.04234	0.04620	0.09735	0.13690
TC 1 (mv)	4.4683	4.4799	4.4881	4.5012	4.5117	4.5210	4.5354	4.5419	4.6247	4.6744
TC 2 (mv)	4.3472	4.3374	4.3241	4.3131	4.3037	4.2881	4.2835	4.2658	4.1780	4.1283
TC 3 (mv)	4.5453	4.5544	4.5701	4.5798	4.5928	4.6063	4.6191	4.6302	4.7040	4.7559
TC 4 (mv)	4.5461	4.5579	4.5680	4.5775	4.5928	4.6031	4.6146	4.6254	4.7063	4.7548
TC 5 (mv)	4.5300	4.5305	4.5341	4.5438	4.5687	4.5843	4.5991	4.6159	4.6521	4.6791
TC 6 (mv)	23.069	23.065	23.060	23.071	23.130	23.162	23.199	23.235	—	—
TC 7 (mv)	22.976	22.961	22.948	22.945	22.987	23.001	23.028	23.051	—	—
TC 8 (mv)	22.201	22.184	22.156	22.111	22.088	22.026	21.995	21.966	—	—
TC 9 (mv)	4.4575	4.4569	4.4576	4.4631	4.4800	4.4855	4.4926	4.5039	4.5099	4.5150
TC 1 (final)	4.4666	4.3380	4.4872	4.4993	4.5118	4.5197	4.5311	4.5429	4.6259	4.6750
TC 2 (final)	4.3442	4.5544	4.3236	4.3110	4.3038	4.2870	4.2763	4.2666	4.1782	4.1278
Time Finish	11:25	12:15	1:00	2:15	3:45	5:10	6:05	6:55	8:10	8:55
HT (v) (a)	2.77 —	2.90 —	3.58 —	3.38 —	2.95 —	3.00 —	3.00 —	2.72 —	3.52 —	4.2 —
HM (v) (a)	20.16 1.786	20.14 1.783	20.13 1.789	20.19 1.786	20.22 1.785	20.19 1.783	20.22 1.781	20.22 1.781	20.19 1.768	20.19 1.760
HS (v) (a)	— —									
HR 1 (v) (a)	2.6 1.7									
HR 2 (v) (a)	0.0 0.0	0.0 0.0	1.0 0.5	2.1 1.7	3.8 3.3	5.3 4.6	6.0 5.2	6.7 5.8	8.2 7.0	9.5 8.0
HR 3 (v) (a)	2.0 1.5	2.0 1.5	3.0 2.7	4.0 3.6	5.5 5.0	6.2 5.5	6.9 6.1	7.6 6.8	8.8 7.8	9.8 8.5
HF 1 (v) (a)	57.5 6.4									
HF 2 (v) (a)	54.7 6.0									

Table B-7 (Continued)

Table B-8 (Continued)

Table B-8 (Continued)

Run No. →	2-P	2-Q	3-A	3-B	3-C	3-D	3-E	3-F	3-G	3-H	3-I	3-J
Date	5-19-67	5-19-67	5-23-67	5-23-67	5-23-68	5-23-67	5-23-67	5-23-67	5-23-67	5-23-67	5-23-67	5-23-67
Time Begun	7:40	8:40	12:25	1:35	2:20	3:00	4:00	4:40	6:28	7:35	9:05	10:15
Dial Zero (in.)	0.00234	0.00234	0.00633	0.00633	0.00633	0.00633	0.00633	0.00633	0.00750	0.00750	0.00750	0.00750
Dial Reading (in.)	0.01416	0.00234	0.00633	0.01027	0.01425	0.01825	0.02210	0.02601	0.00750	0.01144	0.03118	0.05475
TC 1 (mv)	8.1979	8.1028	8.1030	8.1484	8.1796	8.2087	8.2262	8.2427	8.1037	8.1496	8.2658	8.3008
TC 2 (mv)	7.7653	7.8632	7.8478	7.7939	7.7706	7.7476	7.7300	7.7201	7.8509	7.7932	7.6983	7.6490
TC 3 (mv)	8.3361	8.2475	8.2752	8.3156	8.3489	8.3731	8.3920	8.4133	8.2754	8.3151	8.4323	8.4686
TC 4 (mv)	8.3365	8.2547	8.2829	8.3206	8.3536	8.3749	8.3935	8.4121	8.2832	8.3210	8.4318	8.4681
TC 5 (mv)	8.1798	8.1743	8.1882	8.1785	8.1797	8.1774	8.1834	8.1928	8.1846	8.1780	8.2101	8.2291
TC 6 (mv)	8.3456	-	8.3689	8.3620	8.3615	8.3624	8.3644	8.3720	8.3596	8.3649	8.3851	8.3977
TC 7 (mv)	-	-	8.2012	8.1831	8.1788	8.1716	8.1721	8.1753	8.1982	8.1841	8.1863	8.1838
TC 8 (mv)	--	-	7.8540	7.8236	7.8215	7.7945	7.7857	7.7757	7.8533	7.8222	7.7687	7.7296
TC 9 (mv)	8.0121	8.0379	8.0399	8.0205	8.0157	8.0081	8.0080	8.0106	8.0384	8.0190	8.0176	8.0149
TC 1 (final)	8.1940	8.1030	8.1029	8.1475	8.1842	8.2069	8.2261	8.2453	8.1031	8.1470	8.2645	8.3027
TC 2 (final)	7.7640	7.8650	7.8480	7.7955	7.7695	7.7456	7.7296	7.7152	7.8500	7.7936	7.6992	7.6485
Time Finish	8:00	9:00	12:35	1:50	2:42	3:30	4:10	5:15	6:40	7:55	9:20	10:32
HF (v) (a)	10.0 -	4.0 -	6.50 -	9.20 -	10.5 -	11.5 -	12.0 -	12.5 -	7.00 -	9.2 -	12.5 -	13.0 -
HM (v) (a)	20.25 1.425	20.22 1.429	20.25 1.429	20.25 1.426	20.25 1.425	20.25 1.423	20.25 1.422	20.25 1.420	20.25 1.428	20.25 1.425	20.25 1.418	20.25 1.416
HS (v) (a)	0.0 0.0											
HR 1 (v) (a)	10.0 9.8											
HR 2 (v) (a)	3.8 3.0	0.0 0.0	1.8 1.0	2.7 2.0	3.2 2.6	3.8 3.0	4.7 3.7	5.6 4.5	1.8 1.0	2.7 2.0	6.9 5.5	8.9 7.0
HR 3 (v) (a)	3.5 3.0	0.0 0.0	1.7 1.0	2.4 2.0	3.0 2.6	3.5 3.0	4.3 3.7	5.2 4.5	1.6 1.0	2.5 2.0	6.5 5.5	8.2 7.1
HF 1 (v) (a)	83.5 9.2											
HF 2 (v) (a)	78.1 8.6	78.1 8.6	78.0 8.6									

67

Table B-9. Experimental Data for Vacuum Using Apparatus III-B

Run No. →	1-A	1-B	1-C	2-A	2-B	2-C	3-A	3-B	3-C	3-D	3-E	3-F
Date	4-29-68	4-30-68	4-30-68	5-14-68	5-14-68	5-14-68	5-20-69	5-20-69	5-20-69	5-21-69	5-21-69	5-21-69
Time Begun	3:20	8:30	11:00	9:05	10:48	2:45	12:30	3:55	4:15	9:05	10:00	1:15
Dial Zero (in.)	0.00550	0.00550	0.00550	0.00350	0.00350	0.00350	0.00950	0.00950	0.00950	0.00950	0.00950	0.00950
Dial Reading (in.)	0.04592	0.8440	0.12364	0.04287	0.08221	0.08185	0.11795	0.11695	0.09665	0.09630	0.03629	0.00950
TC 1 (mv)	4.73500	4.72734	4.73272	4.92576	4.92231	4.67598	4.41962	4.63630	4.63410	4.64323	4.63913	4.47694
TC 2 (mv)	4.44768	4.44014	4.44248	4.04408	4.04184	4.28115	3.85608	3.85880	3.85735	3.86968	3.87027	3.90316
TC 3 (mv)	4.74724	4.74000	4.75778	4.97487	4.96879	4.69932	4.43611	4.67283	4.67104	4.68082	4.67722	4.54451
TC 4 (mv)	4.74866	7.74165	1.74813	4.97698	4.96909	4.70045	4.43380	4.67246	4.66938	4.68060	4.67640	4.54355
TC 5 (mv)	4.58635	4.57100	4.57520	4.28821	4.28609	4.41272	4.44541	4.47043	4.46990	4.48101	4.48098	4.45886
TC 6 (mv)	-	-	-	-	-	-	4.8364	4.8493	-	4.8587	4.8594	4.8434
TC 7 (mv)	-	-	-	-	-	-	4.4934	4.4959	-	4.5061	4.5067	4.4952
TC 8 (mv)	-	-	-	-	-	-	4.2363	4.2171	-	4.2165	4.2163	4.2120
TC 9 (mv)	4.53910	4.52630	4.53068	4.20146	4.19896	4.36646	4.23274	4.24624	-	4.25692	4.25759	4.24112
TC 1 (final)	4.73725	4.72807	4.73331	4.92582	4.92173	4.68346	4.42003	4.63527	4.63340	4.64332	4.63892	4.47597
TC 2 (final)	4.44500	4.43790	4.44256	4.04376	4.04201	4.27715	3.85644	3.85770	3.85735	3.86980	3.87051	3.90290
Time Finish	3:55	8:55	11:15	9:25	11:02	4:07	12:42	4:10	4:20	9:15	10:12	1:25
HT (v) (a)	9.2 -	9.2 -	10.06 -	7.23 -	7.22 -	5.28 -	0.0050 -	7.5620 -	7.5620 -	7.5603 -	7.5564 -	4.5639 -
HM (v) (a)	10.08 0.9600	10.10 0.9615	10.08 0.9603	15.98 1.485	15.98 1.486	11.06 1.053	6.9554 0.6812	10.5635 1.0132	10.5635 1.0132	10.6186 0.0178	10.6156 1.0180	10.5596 1.0229
HS (v) (a)	0.0 0.0	0.0 0.0	0.0 0.0	0.0 0.0	0.0 0.0	0.0 0.0	0.0 0.0	0.0 0.0	0.0 0.0	0.0 0.0	0.0 0.0	0.0 0.0
HR 1 (v) (a)	10.0 10.0	10.0 10.0	10.0 10.0	10.0 10.0	10.0 10.0	10.0 10.0	10.0 10.0	10.0 10.0	10.0 10.0	10.0 10.0	10.0 10.0	10.0 10.0
HR 2 (v) (a)	0.0 0.0	0.0 0.0	0.0 0.0	0.0 0.0	0.0 0.0	0.0 0.0	0.0 0.0	0.0 0.0	0.0 0.0	0.0 0.0	0.0 0.0	0.0 0.0
HR 3 (v) (a)	0.0 0.0	0.0 0.0	0.0 0.0	0.0 0.0	0.0 0.0	0.0 0.0	0.0 0.0	0.0 0.0	0.0 0.0	0.0 0.0	0.0 0.0	0.0 0.0
HF 1 (v) (a)	45.8 5.0	45.8 5.0	45.8 5.0	44.6 4.8	44.6 4.8	44.6 4.8	58.0 6.4	58.6 6.4	58.6 6.4	58.1 6.4	58.1 6.4	58.1 6.4
HF 2 (v) (a)	46.1 5.0	46.1 5.0	46.1 5.0	45.2 4.8	45.3 4.8	45.3 4.8	55.5 6.0	55.5 6.0	55.5 6.0	55.5 6.0	55.5 6.0	55.5 6.0

Table B-9 (Continued)

Run No. →	3-G	3-H	3-I	3-J	3-K	3-L	3-M	3-N	3-O	3-P	3-Q
Date	5-22-69	5-22-69	5-22-69	3-22-69	5-26-69	5-26-69	5-26-69	5-27-69	5-27-69	5-28-69	5-28-69
Time Begun	9:45	11:25	1:17	4:05	12:01	1:15	3:15	11:10	1:45	9:11	11:50
Dial Zero (in.)	0.00900	0.00900	0.00900	0.00900	0.00895	0.00895	0.00895	0.00945	0.00920	0.00950	0.00950
Dial Reading (in.)	0.0170	0.05725	0.11550	0.00902	0.01642	0.09345	0.00895	0.00945	0.00920	0.09660	0.09680
TC 1 (mv)	5.07218	5.07337	5.06542	4.81593	5.65625	5.65577	5.32091	5.27146	5.25189	4.61445	4.55459
TC 2 (mv)	3.86710	3.86620	3.86782	3.95608	3.83283	3.83880	3.98725	3.94277	3.96323	3.87430	3.87881
TC 3 (mv)	5.16607	5.16756	5.15535	4.96167	5.84771	5.84995	5.60207	5.56454	5.55558	4.65053	4.54622
TC 4 (mv)	5.16560	5.16626	5.15710	4.96193	5.84800	5.84842	5.60160	5.55708	5.54145	4.64809	4.58102
TC 5 (mv)	4.53827	4.53936	4.53954	4.51708	4.61330	4.62100	4.58947	4.54929	4.55472	4.47105	4.46870
TC 6 (mv)	4.9001	4.9024	4.9028	4.8846	4.9417	4.9508	4.9356	4.9035	4.9075	4.8381	4.8384
TC 7 (mv)	4.5121	4.5135	4.5137	4.5062	4.94957	4.5018	4.4949	4.4580	4.4692	4.4993	4.5024
TC 8 (mv)	4.1751	4.1755	4.1765	4.1811	4.0726	4.0770	4.0835	4.0555	4.0702	4.2164	4.2269
TC 9 (mv)	4.28540	4.28535	4.28538	4.27500	4.31032	4.31508	4.30093	4.25694	4.26563	4.25313	4.25284
TC 1 (final)	5.07257	5.07318	5.06542	4.81437	4.65585	5.65605	5.32134	5.27178	5.25191	4.61555	4.55466
TC 2 (final)	3.86675	3.86667	3.86784	3.95620	3.83322	3.83936	3.98926	3.94499	3.96301	3.87811	3.87902
Time Finish	10:05	11:35	1:25	4:15	12:13	1:30	3:30	11:22	1:55	9:30	12:00
HT (v) (a)	14.0865 —	14.0875 —	13.8571 —	11.1933 —	21.3285 —	21.3137 —	18.4127 —	18.4555 —	18.4450 —	7.4767 —	0.0 0.0
HM (v) (a)	16.2273 1.4942	16.2106 1.4925	16.1944 1.4918	16.2247 1.5150	23.3177 2.0372	23.3179 2.0369	23.6104 2.0923	23.5360 2.0920	23.5118 2.0917	10.6360 1.0216	10.6317 1.0266
HS (v) (a)	0.0 0.0										
HR 1 (v) (a)	10.0 10.0										
HR 2 (v) (a)	0.0 0.0										
HR 3 (v) (a)	0.0 0.0										
HF 1 (v) (a)	58.0 6.4	58.0 6.4	58.1 6.4	58.1 6.4	58.1 6.4	58.1 6.4	58.0 6.4	58.0 6.4	58.0 6.4	58.0 6.4	58.0 6.4
HF 2 (v) (a)	55.5 6.0	55.5 6.0	55.4 6.0	55.4 6.0	55.3 5.9	55.4 5.9	55.4 5.9	55.7 6.0	55.7 6.0	55.7 6.0	55.7 6.0

T8

Table B-9 (Continued)

Run No. →	3-R	3-S	3-T	4-A	4-B	4-C	4-D	4-E	4-F	4-G	4-H
Date	5-28-69	5-29-69	5-29-69	6-16-69	6-17-69	6-17-69	6-24-69	6-25-69	6-25-69	6-27-69	6-27-69
Time Begin	-	9:45	3:20	3:40	9:40	3:35	3:45	8:35	3:05	1:15	3:25
Dial Zero (in.)	0.00950	0.00950	0.00950	0.07605	0.07605	0.07605	0.07630	0.07630	0.07665	0.07660	0.07660
Dial Reading (in.)	0.10020	0.10050	0.10251	0.13400	0.08408	0.07605	0.12088	0.08175	0.07665	0.11920	0.07878
TC 1 (mv)	4.46714	4.44503	4.25802	2.85182	2.85970	2.27650	1.98446	1.99560	1.50110	2.02568	2.03860
TC 2 (mv)	3.87826	3.87370	3.87468	0.53666	0.53118	0.60441	0.42329	0.42756	0.44636	0.52970	0.52553
TC 3 (mv)	-	4.41243	4.24505	2.89315	2.90084	2.38276	1.98752	1.99685	1.53108	2.02824	2.03982
TC 4 (mv)	-	4.46458	4.26154	2.89347	2.90054	2.38000	1.98796	1.99767	1.53098	2.02849	2.04102
TC 5 (mv)	-	4.35515	4.29844	0.64295	0.63487	0.58655	0.45202	0.45457	0.43473	0.54016	0.53558
TC 6 (mv)	-	4.6587	4.5820	0.4748	0.4645	0.4362	0.3567	0.3541	0.3411	0.4259	0.4186
TC 7 (mv)	-	4.4249	4.3970	0.4484	0.4386	0.4188	0.3578	0.3490	0.3419	0.4332	0.4262
TC 8 (mv)	-	4.1910	4.1883	0.3714	0.3633	0.3574	0.3117	0.3088	0.3087	0.3933	0.3870
TC 9 (mv)	-	4.18170	4.14887	0.58747	0.57949	0.56751	0.43198	0.43507	0.43708	0.52599	0.52172
TC 1 (final)	4.46714	4.44514	4.25888	2.85187	2.85953	2.27379	1.98557	1.99570	1.50063	2.02634	2.03908
TC 2 (final)	3.87826	3.87349	3.87794	0.53641	0.53072	0.60330	0.42311	0.42716	0.44627	0.52921	0.52505
Time Finish	-	10:05	3:33	3:50	9:55	3:50	4:00	8:45	3:15	1:30	3:45
HT (v) (a)	0.0 0.0	0.0 0.0	0.0 0.0	15.0712 -	15.0703 -	12.2091 -	10.2909 -	10.2909 -	8.3677 -	10.3345 -	10.3265 -
HM (v) (a)	-	10.6699 1.0392	6.9100 0.6854	13.9510 1.5564	13.9445 1.5542	13.8940 1.6368	8.9272 1.1078	8.9287 1.1063	8.8922 1.1732	8.9403 1.1038	8.9460 1.1028
HS (v) (a)	0.0 0.0	0.0 0.0	0.0 0.0	0.0 0.0	0.0 0.0	0.0 0.0	0.0 0.0	0.0 0.0	5.6 2.6	5.6 2.6	
HR 1 (v) (a)	10.0 10.0	- -	- -	0.0 0.0	0.0 0.0	0.0 0.0	0.0 0.0	0.0 0.0	0.0 0.0	0.0 0.0	0.0 0.0
HR 2 (v) (a)	0.0 0.0	0.0 0.0	0.0 0.0	0.0 0.0	0.0 0.0	0.0 0.0	0.0 0.0	0.0 0.0	0.0 0.0	0.0 0.0	0.0 0.0
HR 3 (v) (a)	0.0 0.0	0.0 0.0	0.0 0.0	0.0 0.0	0.0 0.0	0.0 0.0	0.0 0.0	0.0 0.0	0.0 0.0	0.0 0.0	0.0 0.0
HF 1 (v) (a)	58.0 6.4	58.0 6.4	58.0 6.4	0.0 0.0	0.0 0.0	0.0 0.0	0.0 0.0	0.0 0.0	0.0 0.0	0.0 0.0	0.0 0.0
HF 2 (v) (a)	55.7 6.0	55.6 6.0	55.6 6.0	0.0 0.0	0.0 0.0	0.0 0.0	0.0 0.0	0.0 0.0	0.0 0.0	0.0 0.0	0.0 0.0

Table B-10. Experimental Data for Helium Using Apparatus III-B

Run No. →	1-A	1-B	1-C	1-D	1-E	1-F	2-A	2-B	2-C	2-D	2-E
Date	5-15-68	5-15-68	5-15-68	5-15-68	5-15-68	5-15-68	5-16-68	5-16-68	5-16-68	5-16-68	5-16-68
Time Begun	10:55	11:15	1:20	2:33	3:25	4:12	10:27	11:15	12:40	1:36	3:00
Dial Zero (in.)	0.00150	0.00150	0.00150	0.00150	0.00150	0.00150	0.00150	0.00150	0.00150	0.00150	0.00150
Dial Reading (in.)	0.00308	0.02135	0.04092	0.08040	0.11964	0.00540	0.00544	0.00741	0.00938	0.01339	0.02120
TC 1 (mv)	4.46667	4.48898	4.48682	4.49993	4.50992	4.45916	4.49062	4.48898	4.49031	4.49150	4.49906
TC 2 (mv)	4.46918	4.49654	4.44759	4.43296	4.42322	4.46272	4.49814	4.49654	4.49340	4.49142	4.48580
TC 3 (mv)	4.4900	4.5166	4.5072	4.5172	4.5290	4.4835	4.5136	4.5166	4.5197	4.5216	4.5232
TC 4 (mv)	4.4899	4.5162	4.5072	4.5181	4.5284	4.4821	4.5154	4.5162	4.5193	4.5210	4.5231
TC 5 (mv)	4.4684	4.4922	4.4658	4.4644	4.4649	4.4601	4.4943	4.4922	4.4910	4.4908	4.4901
TC 6 (mv)	-	-	-	-	-	-	-	-	-	-	-
TC 7 (Mv)	-	-	-	-	-	-	-	-	-	-	-
TC 8 (mv)	-	-	-	-	-	-	-	-	-	-	-
TC 9 (mv)	4.46867	4.4639	4.4606	4.4559	4.4536	4.4596	4.4955	4.4926	4.4914	4.4906	4.4887
TC 1 (final)	4.46680	4.47514	4.4869	4.49920	4.50952	4.45946	4.48793	4.48843	4.49118	4.4938	4.4984
TC 2 (final)	4.47327	4.4579	4.44765	4.43255	4.42278	4.46265	4.49756	4.49626	4.49395	4.49091	4.48534
Time Finish	11:37	12:30	1:35	2:50	3:40	4:30	10:50	11:30	1:00	1:55	3:17
HT (v) (a)	3.58	3.70	3.89	4.09	4.30	3.63	3.61	3.71	3.75	3.79	3.80
HM (v) (a)	11.00 1.067	11.00 1.066	11.00 1.066	11.00 1.065	11.00 1.064	11.00 1.067	11.00 1.064	11.00 1.064	11.00 1.064	11.00 1.064	11.00 1.064
HS (v) (a)	0.0 0.0										
HR 1 (v) (a)	10.0 10.0										
HR 2 (v) (a)	0.0 0.0										
HR 3 (v) (a)	0.0 0.0										
HF 1(v) (a)	44.5 4.8	44.5 4.8	44.6 4.8	44.5 4.8	44.5 4.8						
HR 2 (v) (a)	45.1 4.8	45.1 4.8	45.2 4.8	45.1 4.8	45.1 4.8						

Table B-10 (Continued)

Run No. →	3-A	3-B	3-C	3-D	3-E	3-F	3-G	3-H	3-I	3-J
Date	5-21-68	5-21-68	5-21-68	5-21-68	5-21-68	5-22-68	5-22-68	5-22-68	5-22-68	5-23-68
Time Begun	9:55	12:20	1:55	3:25	4:10	9:40	11:45	2:15	4:05	9:15
Dial Zero (in.)	0.00085	0.00085	0.00085	0.00085	0.00085	0.00085	0.00085	0.00085	0.00085	0.00035
Dial Reading (in.)	0.00275	0.00473	0.00676	0.00873	0.01264	0.02060	0.04012	0.07940	0.11899	0.00873
TC 1 (mv)	0.69932	0.70271	0.71024	0.70857	0.71978	0.73624	0.77943	0.83894	0.88340	0.72427
TC 2 (mv)	0.66788	0.66340	0.65895	0.65483	0.64751	0.62570	0.59132	0.54510	0.51077	0.65789
TC 3 (mv)	0.7721	0.7776	0.7836	0.7844	0.7974	0.8100	0.8475	0.9081	0.9515	0.7986
TC 4 (mv)	0.7696	0.7736	0.7813	0.7829	0.7947	0.8068	0.8454	0.9052	0.9476	0.7965
TC 5 (mv)	0.5991	0.5996	0.5994	0.5999	0.6016	0.5956	0.5973	0.6043	0.6112	0.6044
TC 6 (mv)	-	-	-	-	-	-	-	-	-	-
TC 7 (mv)	-	-	-	-	-	-	-	-	-	-
TC 8 (mv)	-	-	-	-	-	-	-	-	-	-
TC 9 (mv)	0.6075	0.6062	0.6048	0.6038	0.6031	0.5928	0.5850	0.5767	0.5720	0.6080
TC 1 (final)	0.69833	0.70311	0.70920	0.70883	0.71988	0.73643	0.77725	0.83896	0.88346	0.72426
TC 2 (final)	0.66797	0.66353	0.65892	0.65476	0.64772	0.62563	0.59138	0.54496	0.51077	0.65790
Time Finish	10:15	12:36	2:10	3:35	4:25	9:50	12:00	2:30	4:15	9:20
HT (v) (a)	2.86 -	2.89 -	2.90 -	2.92 -	2.99 -	3.03 -	3.22 -	3.49 -	3.68 -	2.95 -
HM (v) (a)	15.12 2.237	15.12 2.234	15.12 2.233	15.12 2.232	15.12 2.228	15.15 2.225	15.18 2.213	15.21 2.194	15.24 2.180	15.15 2.231
HS (v) (a)	0.0 0.0									
HR 1 (v) (a)	0.0 0.0									
HR 2 (v)	0.0	0.0	0.0	0.0	0.0	0.0	0.0	0.0	0.0	0.0
HR 3 (v)	0.0	0.0	0.0	0.0	0.0	0.0	0.0	0.0	0.0	0.0
HF 1 (v) (a)	0.0 0.0									
HF 2 (v) (a)	0.0 0.0									

Table B-11. Experimental Data for HTS Using Apparatus III-B

Run No. +	1-A	1-B	1-C	1-D	1-E	1-F	1-G	1-H	1-I	1-J	1-K	1-L	1-M	1-N
Date	7-16-68	7-16-68	7-16-68	7-16-68	7-16-68	7-16-68	7-17-68	7-17-68	7-17-68	7-17-68	7-17-68	7-18-68	7-18-68	7-18-68
Time Begun	10:10	11:10	12:25	1:40	2:45	3:55	9:15	10:50	12:17	2:25	3:57	8:30	10:25	12:42
Dial Zero (in.)	0.00400	0.00400	0.00400	0.00400	0.00400	0.00400	0.0400	0.00400	0.00400	0.00400	0.00400	0.00400	0.00400	0.00400
Dial Reading (in.)	0.00560	0.00794	0.00991	0.01188	0.01582	0.02370	0.03150	0.04337	0.06310	0.12212	0.02370	0.02375	0.02755	0.00560
TC 1 (mv)	4.4224	4.4270	4.4323	4.4374	4.4459	4.4585	4.4795	4.4847	4.5054	4.5707	4.4734	4.4671	4.4712	4.4219
TC 2 (mv)	4.3036	4.2995	4.2974	4.2953	4.2941	4.2933	4.3004	4.3019	4.2930	4.2775	4.3084	4.2983	4.2988	4.3039
TC 3 (mv)	4.5248	4.5289	4.5358	4.5407	4.5492	4.5621	4.5811	4.5880	4.6050	4.6696	4.5756	4.5676	4.5718	4.5234
TC 4 (mv)	4.5250	4.5299	4.5357	4.5407	4.5497	4.5619	4.5811	4.5869	4.6054	4.6717	4.5740	4.5686	4.5728	4.5236
TC 5 (mv)	4.5013	4.5008	4.5020	4.5030	4.5062	4.5102	4.5232	4.5258	4.5305	4.5502	4.5252	4.5164	4.5181	4.5012
TC 6 (mv)	4.639	-	4.637	-	4.637	4.637	4.650	4.651	4.653	4.662	4.654	4.644	4.646	4.637
TC 7 (mv)	4.585	-	4.583	-	4.583	4.583	4.597	4.598	4.598	4.604	4.600	4.593	4.594	4.585
TC 8 (mv)	4.409	-	4.406	-	4.405	4.405	4.416	4.416	4.413	4.414	4.417	4.414	4.414	4.409
TC 9 (mv)	4.4126	4.4117	4.4125	4.41305	4.4156	4.4184	4.4308	4.4329	4.4354	4.4481	4.4333	4.4247	4.4262	4.4126
TC 1 (final)	4.4210	4.4266	4.4323	4.4375	4.4470	4.4588	4.4798	4.4843	4.5042	4.5722	4.4722	4.4674	4.4714	4.4216
TC 2 (final)	4.3024	4.2986	4.2970	4.2953	4.2947	4.2935	4.3006	4.3018	4.2931	4.2802	4.3074	4.2982	4.2987	4.3036
Time (finish)	10:25	11:25	12:40	1:55	3:01	4:00	9:30	11:00	12:40	2:50	4:10	8:43	10:35	12:52
HT {v} (a)	4.00 -	4.30 -	4.70 -	4.90 -	5.20 -	5.64 -	5.92 -	6.13 -	6.63 -	8.35 -	5.63 -	5.63 -	5.73 -	3.96 -
HM {v} (a)	17.56 1.692	17.56 1.692	17.56 1.690	17.60 1.690	17.58 1.689	17.58 1.688	17.60 1.685	17.58 1.686	17.60 1.685	17.60 1.678	17.62 1.689	17.62 1.689	17.60 1.689	17.60 1.694
HS {v} (a)	0.0 0.0													
HR 1 {v} (a)	9.2 5.0	9.0 5.0	9.0 5.0	9.0 5.0	9.0 5.0	9.0 5.0	9.0 5.0							
HR 2 {v} (a)	4.0 2.2													
HR 3 {v} (a)	3.7 2.1													
HF 1 {v} (a)	54.8 6.0													
HF 2 {v} (a)	53.6 5.8	53.7 5.8												

CO
U1

Table B-11 (Continued)

Run No. →	1-0	2-A	2-B	2-C	2-D	2-E	2-F	2-G	2-H	3-A	3-B	3-C	3-D	3-E
Date	7-18-68	7-19-68	7-19-68	7-19-68	7-19-68	7-19-68	7-22-68	7-22-68	7-22-68	7-24-68	7-25-68	7-26-68	7-29-68	7-30-68
Time Begun	2:05	10:55	12:35	1:50	2:55	4:00	9:45	2:05	3:30	10:30	9:05	9:20	10:30	9:35
Dial Zero (in.)	0.00400	0.00380	0.00380	0.00380	0.00380	0.00380	0.00380	0.00380	0.00380	0.00380	0.00380	0.00380	0.00380	0.00380
Dial Reading (in.)	0.00800	0.00538	0.00774	0.00971	0.01168	0.01562	0.01565	0.02350	0.03132	0.06611	0.10677	0.04800	0.03192	0.8483
TC 1 (mv)	4.4257	2.5149	2.5217	2.5268	2.5307	2.5381	2.5426	2.5562	2.5695	0.8166	0.8409	0.8175	0.8129	0.8383
TC 2 (mv)	4.2987	2.4157	2.4164	2.4162	2.4152	2.4139	2.4178	2.4140	2.4112	0.7568	0.7565	0.7691	0.7740	0.7655
TC 3 (mv)	4.5277	2.5980	2.6050	2.6097	2.6142	2.6213	2.6253	2.6391	2.6527	0.8479	0.8704	0.8473	0.8423	0.8665
TC 4 (mv)	4.5277	2.5984	2.6050	2.6099	2.6142	2.6214	2.6253	2.6386	2.6518	0.8486	0.8714	0.8477	0.8422	0.8671
TC 5 (mv)	4.5003	2.5308	2.5339	2.5363	2.5380	2.5404	2.5445	2.5493	2.5536	0.8041	0.8172	0.8117	0.8131	0.8210
TC 6 (mv)	4.635	2.612	2.614	2.618	2.618	2.618	2.625	2.626	2.628	0.894	0.903	0.908	0.915	0.905
TC 7 (mv)	4.584	2.603	2.603	2.606	2.606	2.606	2.613	2.613	2.614	0.888	0.892	0.902	0.908	0.901
TC 8 (mv)	4.407	2.472	2.474	2.473	2.473	2.483	2.483	2.480	—	0.850	0.849	0.865	0.869	0.863
TC 9 (mv)	4.4110	2.4744	2.4768	2.4785	2.4745	2.4812	2.4851	2.4881	2.4910	0.7806	0.7904	0.7886	0.7905	0.7954
TC 1 (final)	4.4256	2.5154	2.5219	2.5269	2.5310	2.5385	2.5427	2.5566	2.5697	0.8167	0.8409	0.8172	0.8123	0.8385
TC 2 (final)	4.2986	2.4161	2.4164	2.4162	2.4155	2.4142	2.4180	2.4144	2.4113	0.7568	0.7565	0.7689	0.7735	0.7659
Time Finish	2:15	11:15	12:50	2:05	3:10	4:15	10:08	2:20	—	10:45	9:20	9:35	10:50	9:45
HT {v} (a)	4.27	6.12	6.28	2.32	6.44	6.55	6.56	6.85	7.15	4.38	4.92	3.98	3.80	4.44
HM {v} (a)	17.60 1.694	15.96 1.836	15.96 1.836	15.96 1.835	15.96 1.834	15.96 1.832	15.96 1.831	15.94 1.829	15.94 1.826	9.50 1.399	9.52 1.398	9.48 1.396	9.47 1.396	9.46 1.389
HS {v} (a)	0.0 0.0	0.0 0.0	0.0 0.0	0.0 0.0	0.0 0.0	0.0 0.0								
HR 1 {v} (a)	9.0 5.0	9.2 5.0	5.8 3.2	5.8 3.2	5.8 3.2	5.8 3.2	5.8 3.2							
HR 2 {v} (a)	4.0 2.2	5.0 2.9	2.9 1.4	3.0 1.5	3.0 1.5	3.1 1.6	3.3 1.7							
HR 3 {v} (a)	3.7 2.1	6.8 4.2	6.8 4.2	6.8 4.2	6.8 4.1	6.8 4.1	6.8 4.1	6.8 4.1	6.8 4.1	2.3 1.0	2.3 1.1	2.3 1.1	2.3 1.1	2.4 1.1
HF 1 {v} (a)	54.8 6.0	36.1 3.8	19.0 2.0	19.0 2.0	19.0 2.0	19.0 2.0	19.0 2.0							
HF 2 {v} (a)	53.7 5.8	35.5 3.8	35.5 3.8	35.5 3.8	35.5 3.8	35.5 3.8	35.6 3.8	35.6 3.8	35.6 3.8	19.2 2.0	19.0 2.0	19.0 2.0	19.0 2.0	19.0 2.0

88

Table B-12. Reduced Experimental Data for H₂O Using Apparatus I-A

Run No.	Specimen			Guard Factor, G	Shunting Factor, F	Heat Flux, Q/A (W cm ⁻²)	Thermal Resistance, ΔT/(Q/A) (°C cm ² W ⁻¹)
	Thickness, ΔX (cm)	Temperature, T _{avg} (°C)	Temperature Drop, ΔT (°C)				
1-A	0.5122	22.8	16.66	<0.05	1.000	0.200	83.3
1-B	0.3861	18.4	13.04	<0.05	1.000	0.201	64.9
1-C	0.2773	29.4	13.04	<0.05	1.000	0.299	43.6
1-D	0.1301	29.6	6.84	<0.05	1.000	0.300	22.8
1-E	0.0502	28.6	4.53	<0.05	1.000	0.301	15.0
1-F ^a	0.2512	46.5	19.34	<0.05	1.000	0.451	42.9
1-G ^a	0.1246	45.2	11.12	<0.05	1.000	0.453	24.5
1-H ^a	0.0625	44.6	6.86	<0.05	1.000	0.456	15.0
1-I ^a	0.0315	44.5	4.72	<0.05	1.000	0.448	10.5
2-A	0.3805	52.2	26.55	<0.05	1.000	0.452	58.7
2-B	0.3679	52.7	26.48	<0.05	1.000	0.452	58.6
2-C	0.2414	51.9	18.99	<0.05	1.000	0.455	41.7
2-D	0.1137	50.7	10.54	<0.05	1.000	0.460	22.9
3-A	0.3740	37.7	20.89	<0.05	1.000	0.350	59.7
3-B	0.2460	37.9	14.74	<0.05	1.000	0.352	41.9
3-C	0.1701	38.4	10.82	<0.05	1.000	0.352	30.7

^aThese data used to calculate k for Run 1.

Table B-13. Reduced Experimental Data for Hg Using Apparatus I-A

Run No.	Specimen			Guard Factor, G	Shunting Factor, F	Heat Flux, Q/A (W cm ⁻²)	Thermal Resistance, ΔT/(Q/A) (°C cm ² W ⁻¹)
	Thickness, ΔX (cm)	Temperature, T _{avg} (°C)	Temperature Drop, ΔT (°C)				
1-A	0.4946	60.2	6.99	<0.05	1.000	0.634	11.03
1-B	0.2408	60.8	5.10	<0.05	1.000	0.634	8.04
1-C	0.2401	60.9	5.33	<0.05	1.000	0.669	7.97
1-D	0.1130	60.5	4.33	<0.05	1.000	0.669	6.47
1-E	0.0568	58.8	3.86	<0.05	1.000	0.670	5.76
2-A	0.2418	61.2	4.93	<0.05	1.000	0.668	7.38
2-B	0.1180	61.2	4.02	<0.05	1.000	0.667	6.03
2-C	0.3810	61.4	6.04	<0.05	1.000	0.668	9.04
2-D	0.2419	60.4	4.96	<0.05	1.000	0.662	7.47
2-E	0.1142	60.4	4.07	<0.05	1.000	0.664	6.12
2-F	0.0147	60.4	3.38	<0.05	1.000	0.666	5.08

Table B-14 (continued)

Run No.	Specimen			Guard Factor, G	Shunting Factor, F	Heat Flux, Q/A (W cm ⁻²)	Thermal Resistance, ΔT/(Q/A) (°C cm ² W ⁻¹)
	Thickness, ΔX (cm)	Temperature, T _{avg} (°C)	Temperature Drop, ΔT (°C)				
11-Z	0.0150	553.2	4.56	<0.01	1.000	0.127	35.8
11-AA	0.0105	553.6	4.47	<0.01	1.000	0.127	35.1
11-BB	0.0051	553.5	4.19	<0.01	1.000	0.127	32.9
11-CC	0.0000	553.4	4.09	<0.01	1.000	0.127	32.2
12-A	0.0202	553.1	4.80	<0.01	1.000	0.127	37.6
12-B	0.0403	553.1	5.41	<0.01	1.000	0.127	42.5
12-C	0.0500	553.1	5.69	<0.01	1.000	0.127	44.8
12-D	0.0601	553.1	5.88	<0.01	1.000	0.127	46.3
12-E	0.0701	553.2	6.14	<0.01	1.000	0.127	48.3
12-F	0.0800	554.1	6.38	<0.01	1.000	0.127	50.2
12-G	0.0903	554.0	6.52	<0.01	1.000	0.127	51.2
12-H	0.1000	554.0	6.59	<0.01	1.000	0.127	51.8
12-I	0.1100	554.0	6.71	<0.01	1.000	0.127	52.6
12-J	0.1249	553.9	6.85	<0.01	1.000	0.127	53.7
12-K	0.1402	553.9	6.94	<0.01	1.000	0.127	54.6
12-L	0.1551	553.8	7.11	<0.01	1.000	0.127	55.9
12-M	0.1698	553.9	7.41	<0.01	1.000	0.127	58.1
12-N	0.1875	553.8	7.55	<0.01	1.000	0.127	59.2
12-O	0.2000	553.8	7.72	<0.01	1.000	0.127	60.7
12-P	0.2160	553.6	8.05	<0.01	1.000	0.127	63.3
12-Q	0.2400	553.6	8.49	<0.01	1.000	0.127	66.8
12-R	0.2600	553.8	9.41	<0.01	1.000	0.127	74.0
12-S	0.2800	553.8	9.72	<0.01	1.000	0.127	76.4
12-T	0.3000	553.8	10.28	<0.01	1.000	0.127	80.8

Table B-20. Reduced Experimental Data for Vacuum Using Apparatus III-B

Run No.	Thickness, ΔX (cm)	Specimen Temperature, T_{avg} (°C)	Temperature Drop, ΔT (°C)	Guard Factor, G	Shunting Factor, F	Heat Flux, Q/A (W cm ⁻²)	Thermal Resistance, $\Delta T/(Q/A)$ (°C cm ² W ⁻¹)
1-A	0.1027	537.3	28.14	0.54	0.787	0.1306	215.5
1-B	0.2004	537.0	27.94	0.56	0.781	0.1296	215.6
1-C	0.3001	536.5	27.93	0.58	0.775	0.1287	217.0
2-A	0.1000	526.7	85.97	0.74	0.740	0.295	291.4
2-B	0.2000	526.4	85.73	0.74	0.740	0.295	290.6
2-C	0.2000	526.2	39.36	0.69	0.755	0.148	265.9
3-A	0.2755	500 ^a	57.50	-0.017	1.010	0.082	701.3
3-B	0.2729		79.33	0.247	0.886	0.163	486.7
3-C	0.2214		78.99	0.247	0.886	0.163	484.6
3-D	0.2205		78.52	0.247	0.886	0.163	481.7
3-E	0.0680		78.01	0.247	0.886	0.163	478.6
3-F	0.0000		58.17	0.141	0.927	0.171	340.2
3-G	0.0208		121.18	0.485	0.805	0.340	356.4
3-H	0.1226		121.25	0.485	0.805	0.333	364.1
3-I	0.2705		120.25	0.480	0.805	0.333	361.1
3-J	0.0000		86.26	0.440	0.820	0.346	249.3
3-K	0.0189		181.33	0.610	0.766	0.624	290.6
3-L	0.2146		180.77	0.610	0.766	0.624	289.7
3-M	0.0000		132.53	0.610	0.766	0.649	204.2
3-N	0.0000		132.53	0.620	0.766	0.649	204.2
3-O	0.0000		128.24	0.620	0.766	0.649	197.6
3-P	0.2212		75.26	0.630	0.766	0.142	530.0
3-Q	0.2212		68.94	0.230	0.893	0.142	485.5
3-R	0.2304		60.08	0.120	0.936	0.178	337.5
3-S	0.2311		58.43	0.100	0.945	0.180	324.6
3-T	0.2362		38.66	0.110	1.060	0.090	429.6
4-A	0.1472	200 ^b	319.78	0.95	0.599	0.223	1434.0
4-B	0.0204		321.64	0.96	0.596	0.221	1455.3
4-C	0.0000		191.93	1.01	0.579	0.226	849.2
4-D	0.1132		157.73	0.98	0.580	0.099	1593.2
4-E	0.0139		158.36	0.98	0.580	0.098	1615.9
4-F	0.0000		90.99	1.01	0.570	0.102	892.1
4-G	0.1082		158.29	0.99	0.575	0.097	1631.8
4-H	0.0055		160.08	0.99	0.573	0.097	1650.3

^aNormalized to 500°C.^bNormalized to 200°C.

Table B-21. Reduced Experimental Data for Helium Using Apparatus III-B

Run No.	Specimen		Guard Factor, G	Shunting Factor, F	Heat Flux, Q/A (W cm ⁻²)	Thermal Resistance, ΔT/(Q/A) (°C cm ² W ⁻¹)
	Thickness, ΔX (cm)	Temperature, T _{avg} (°C)				
1-A	0.0040	525.2	-0.65	1.00	0.997	0.200
1-B	0.0504	524.9	1.73	1.00	0.969	0.195
1-C	0.1001	524.9	3.94	0.67	0.924	0.186
1-D	0.2004	524.8	6.70	0.62	0.857	0.172
1-E	0.3001	524.8	8.72	0.64	0.806	0.162
1-F	0.0099	524.4	-0.32	1.00	0.993	0.200
2-A	0.0100	527.5	-0.97	1.00	0.993	0.200
2-B	0.0150	527.4	-0.79	1.00	0.992	0.199
2-C	0.0200	527.4	-0.28	1.00	0.990	0.199
2-D	0.0302	527.4	0.29	1.00	0.975	0.196
2-E	0.0500	527.4	1.31	0.75	0.978	0.197
3-A	0.0048	105.4	4.13	1.70	0.991	0.574
3-B	0.0099	105.4	5.38	1.6	0.986	0.572
3-C	0.0150	105.6	6.84	1.5	0.981	0.568
3-D	0.0200	105.2	7.36	1.4	0.975	0.563
3-E	0.0299	105.5	9.81	1.3	0.961	0.555
3-F	0.0502	105.1	15.07	1.2	0.930	0.536
3-G	0.0997	105.6	25.29	0.96	0.875	0.502
3-H	0.1997	106.7	40.00	0.83	0.760	0.431
3-I	0.3001	107.4	50.71	0.77	0.675	0.383
3-J	0.0213	106.6	9.03	1.4	0.973	0.562

Table B-22. Reduced Experimental Data for HTS Using Apparatus III-B

Run No.	Specimen		Guard Factor, G	Shunting Factor, F	Heat Flux, Q/A (W cm ⁻²)	Thermal Resistance, ΔT/(Q/A) (°C cm ² W ⁻¹)
	Thickness, ΔX (cm)	Temperature, T _{avg} (°C)				
1-A	0.0040	514.3	11.98	0.12	1.000	0.510
1-B	0.0100	514.4	12.93	0.12	0.999	0.510
1-C	0.0150	514.6	13.67	0.14	0.998	0.509
1-D	0.0200	514.7	14.36	0.15	0.997	0.509
1-E	0.0300	515.2	15.38	0.17	0.995	0.506
1-F	0.0500	515.7	16.69	0.19	0.988	0.502
1-G	0.0698	517.1	18.10	0.21	0.980	0.499
1-H	0.1000	517.4	18.44	0.22	0.969	0.493
1-I	0.1500	518.0	21.33	0.24	0.944	0.480
1-J	0.3000	520.7	29.50	0.30	0.854	0.432
1-K	0.0500	517.1	16.65	0.19	0.988	0.504
1-L	0.0500	516.4	17.08	0.19	0.988	0.504
1-M	0.0598	516.6	17.45	0.20	0.985	0.503
1-N	0.0041	514.4	11.92	0.10	1.000	0.510
1-O	0.0102	514.3	12.83	0.12	0.999	0.510
2-A	0.0040	316.2	10.79	0.37	0.998	0.502
2-B	0.0100	316.6	11.47	0.38	0.998	0.501
2-C	0.0150	317.0	12.04	0.38	0.997	0.501
2-D	0.0200	317.1	12.55	0.38	0.996	0.500
2-E	0.0300	317.4	13.51	0.39	0.994	0.499
2-F	0.0301	317.8	13.55	0.39	0.994	0.499
2-G	0.0500	318.4	15.45	0.40	0.988	0.494
2-H	0.0699	319.0	17.21	0.41	0.980	0.489
3-A	0.1005	119.4	7.88	0.48	0.977	0.223
3-B	0.2040	120.9	11.10	0.47	0.934	0.212
3-C	0.0540	120.1	6.36	0.46	0.990	0.225
3-D	0.0137	120.1	5.11	0.43	0.997	0.227
3-E	0.1506	121.2	9.55	0.45	0.958	0.216

APPENDIX C

PRECISION AND ERROR ANALYSIS

The general form of the equation used to determine the thermal conductivity in this investigation is Eq. (9), rearranged as

$$k = x \left\{ \frac{Q'/A}{\left[\left(\frac{\Delta T}{F} \right)_x - \left(\frac{\Delta T}{F} \right)_o \right]} - \frac{16}{3} \bar{n}^2 \sigma T^3 \left(\frac{Y}{\tau} \right)_x \right\} , \quad (C-1)$$

where the measured heat flux, Q'/A , is assumed to be constant during the measurements and the specimen thickness is $x \equiv \Delta x$.

By taking the total derivative of Eq. (C-1) and rearranging terms, the change in k due to a change in any of the quantities in Eq. (C-1) is

$$\begin{aligned} \frac{dk}{k} &= \frac{dx}{x} + \frac{Q'/A}{JK} \left[\frac{d(Q'/A)}{Q'/A} \right] - \frac{Q'/A}{JK^2} \left(\frac{\Delta T}{F} \right)_x \left(\frac{d \Delta T_x}{\Delta T_x} - \frac{dF_x}{F_x} \right) + \\ &\quad \frac{Q'/A}{JK^2} \left(\frac{\Delta T}{F} \right)_o \left(\frac{d \Delta T_o}{\Delta T_o} - \frac{dF_o}{F_o} \right) - \frac{L}{J} \left[\frac{2dn}{n} + \frac{3dT}{T} + \frac{d(Y/\tau)}{Y/\tau} \right] , \end{aligned} \quad (C-2)$$

where

J = quantity enclosed by braces in Eq. (C-1),

K = quantity enclosed by brackets in Eq. (C-1), and

$L = (16/3) \bar{n}^2 \sigma T^3 (Y/\tau)_x$.

By using certain approximations, Eq. (C-2) can be simplified to express quantities more readily measured,

$$w \equiv \left[\frac{\Delta T}{F(Q'/A)} \right]_o ,$$

$$h_r = \frac{16}{3} \bar{n}^2 \sigma T^3 (Y/\tau)_x \underset{\tau \rightarrow 0}{=} 4\bar{n}^2 \sigma T^3 ,$$

and

$$\Delta T_x = \Delta T_{sx} + \Delta T_o ,$$

$$(\Delta T_s/F)_x = \frac{Q'/A}{(k/x) + \epsilon h_r} ,$$

$$\tau = \frac{k}{\epsilon h_r} x .$$

In the present studies, the heat shunting was usually small so that F_x and F_o can be assumed to be unity in the weighting functions. Furthermore, the error in $Y_{\tau, \epsilon}/\tau$ can be evaluated as

$$\frac{d(Y/\tau)}{Y/\tau} = \left(\frac{\tau}{Y} \frac{dY}{d\tau} - 1 \right) \left(\frac{dk}{k} + \frac{dx}{x} \right) + \frac{\epsilon}{Y} \frac{dY}{d\epsilon} \frac{de}{\epsilon} .$$

Finally, the total error in the conductivity would be approximately,

$$\frac{dk}{k} = \frac{dx}{x} + [(1 + \epsilon h_r x)/k] \left\{ \frac{d(Q'/A)}{Q'/A} - \frac{d\Delta T_{sx}}{\Delta T_{sx}} + \frac{dF_x}{F_x} + w[(k/x) + \epsilon h_r] x \right. \\ \left(\frac{dF_x}{F_x} - \frac{dF_o}{F_o} \right) - \left(\frac{\epsilon h_r x}{k + \epsilon h_r x} \right) \left[\left(\frac{2dn}{n} + \frac{3dT}{T} \right) + \left(\frac{\tau}{Y} \frac{dY}{d\tau} - 1 \right) x \right. \\ \left. \left(\frac{dk}{k} + \frac{dx}{x} \right) + \left(\frac{\epsilon}{Y} \frac{dY}{d\epsilon} \frac{de}{\epsilon} \right) \right] \right\} . \quad (C-3)$$

The magnitude or the error in the conductivity is dependent on the specimen thickness. Some of the uncertainties increase and others decrease with a change in specimen thickness. Therefore, there should be an optimum thickness that would minimize the errors associated with it. The errors are also dependent on the magnitude of the thermal conductivity, the fixed resistance, and ϵh_r .

The error in the conductivity measurements now considered refers to the apparatus model III-B for various values of x , k , ϵh_r , and $\Delta T/F(Q'/A)$ observed in the present studies.

Using the accuracy limits listed in Table 2 and the tolerance limits shown in Figs. A-1 and A-2, the error terms appearing in Eq. (C-3) can be determined as follows:

Temperature level

$dT/T = \pm 0.2\%$ (published error for Pt vs Pt-10% Rh thermocouple)

The potentiometer and other temperature measuring errors can be neglected in comparison with the thermocouple error.

Temperature differences

$d\Delta T = (\Delta T/T) dT$, or $d\Delta T/\Delta T = dT/T = \pm 0.2\%$ (Pt vs Pt-10% Rh thermocouple)

Measured heat flux

$$Q'/A = 4EVI/(\pi D^2) = 4EV(V_1/\Omega)/(\pi D^2) ,$$

$$\frac{d(Q'/A)}{Q'/A} = \frac{dE}{E} + \frac{dV}{V} - \frac{d\Omega}{\Omega} - \frac{2dD}{D} + \frac{dV_1}{V_1} ,$$

$$dV/V = dV_1/V_1 = \pm(10)(0.01) = \pm 0.1\% \text{ (maximum error)},$$

$$d\Omega/\Omega = \pm 0.04\%,$$

$$dD/D = \pm(0.005 \times 100)/3.25 = \pm 0.15,$$

$$dE/E = \pm(0.25 \times 100)/60 = 0.42\% \text{ (uncertainty in heater wire length} \\ \text{= } \pm 0.25 \text{ in.}).$$

Another uncertainty in the heat flux is the axial heat loss across the air gap between the main and guard heaters:

$$(Q/A)_L = \left(\frac{k_{air}}{x} + \frac{\epsilon_{Pt} h_r}{3} \right) \Delta T \\ = (6.3k_{air} + 0.03h_r) \Delta T \text{ and } d(Q/A)_L = (6.3k_{air} + 0.03h_r) d \Delta T$$

but

$$d \Delta T = T dT/T ;$$

therefore,

$$\frac{d(Q/A)_L}{Q'/A} = \left(\frac{6.3k_{air} + 0.03h_r}{Q'/A} \right) T (\pm 0.20\%)$$

Finally,

$$\frac{d(Q'/A)}{Q'/A} = (\pm 0.42\%) + (\pm 0.2\%) - (\pm 0.04\%) - (\pm 0.30\%) \\ + \frac{(6.3k_{air} + 0.03h_r)}{Q'/A} T (\pm 0.20\%) .$$

Average refractive index

$$\bar{n} = \pm(0.2 \times 100)/1.5 = \pm 13\% \text{ (estimated from the HTS measurements)} \\ = 0.0\% \text{ } (\bar{n} = 1.000 \text{ for argon and helium}).$$

Radiation function

The expression for Y/τ is quite complex [Eq. (8)]; fortunately, for $\epsilon = 0.5$ and $\tau < 5$, Y/τ is very nearly a constant and for $\tau > 10$ is very nearly equal to $1/\tau$. Thus, the error in Y/τ due to an uncertainty in τ can be neglected, except in the narrow interval $5 < \tau > 10$. Furthermore, the maximum value of the term $\epsilon dY/Yd\epsilon \approx 1$, so that the error in Y/τ is primarily due to the uncertainty in the surface emissivity of the upper and lower plates.

Surface emissivity

$$d\epsilon/\epsilon = \pm(0.05 \times 100)/0.45 = \pm 11.1\% \text{ (estimated from the vacuum measurements, see Chapter 5).}$$

Specimen thickness

Dial indicator:

$$dx/x = \pm(0.00005)(2.54) \times 100/x = \pm 0.013\%/x .$$

Thermal expansion:

Although a fused quartz rod was used to minimize thermal expansion effects in the mobile piston assembly, it was not practical to make a dual quartz rod dial indicator system. The uncertainty caused by the thermal expansion difference of stainless steel from that of fused quartz is estimated to be

$$dx/x = \pm 0.5 [\alpha L(\Delta T_{sx}/2)] = \pm 0.5 [(20 \times 10^{-6})(25)/2] \Delta T_{sx} \\ = \pm 0.013 T_{sx}\% \text{ or } dx/x = \pm 0.013 [(Q'/A)/k + \epsilon h_r x]\% ,$$

where

α = coefficient of linear expansion, $^{\circ}\text{C}^{-1}$,

L = length of cylinder component of the conductivity cell, cm.

Heat shunting factor

$$\frac{dF_x}{F_x} = \frac{d(1 - F_x)}{F_x},$$

$$(1 - F_x) \propto G^{0.8} \propto U_2^{0.8} \quad [\text{Eq. (23)}],$$

$$\frac{d(1 - F_x)}{1 - F_x} = 0.8 (dU_2/U_2).$$

The dominant resistance in the heat-transfer coefficient, U_2 , measurement is the air gap (Fig. 1). The major uncertainty in determining this resistance is the emissivity. Therefore,

$$dU_2/U_2 = d\epsilon/\epsilon.$$

Thus,

$$\frac{dF_x}{F_x} = \pm \frac{(1 - F_x)}{F_x} \frac{d(1 - F_x)}{1 - F_x} = \pm \frac{(1 - F_x)}{F_x} 0.8d\epsilon/\epsilon$$

[$d\epsilon/\epsilon = \pm 0.1 \times 100/0.4 = \pm 25\%$ (estimated for the air gap)]. Thus

$$dF_x/F_x = \pm 20 (1 - F_x)/F_x \%.$$

Summation of errors

All the uncertainties now combined in Eq. (C-3) yields

$$\begin{aligned} \frac{dk}{k} (\%) &= \pm 0.013 \left(\frac{1}{x} + \frac{Q'/A}{k + \epsilon h_r x} \right) + \left(\frac{k + \epsilon h_r x}{k} \right) \{ (\pm 0.42) + (\pm 0.2) - (\pm 0.4) \} \\ &\quad - (\pm 0.3) + \left(\frac{(6.3k_{\text{air}} + 0.03h_r)T}{Q'/A} - 1 \right) (\pm 0.2) + [\pm 20(1 - F_x)/F_x] \end{aligned}$$

(continued)

$$+ w \frac{k + \epsilon h_r x}{x} [\pm 20 (1/F_x - 1/F_o)] \\ - \frac{\epsilon h_r x}{k + \epsilon h_r x} [(\pm 13) + (\pm 0.6) + (\pm 11)] \}$$

The standard error in the conductivity was calculated as a function of x , k , and ϵh_r with $Q'/A = 0.5 \text{ W cm}^{-2}$, $\epsilon = 0.5$, and $w = 20^\circ\text{C cm}^2 \text{ W}^{-1}$ where the standard error is defined as

$$\frac{dk}{k} = \left[\sum_n (\text{error})_n^2 \right]^{1/2}$$

In Fig. C-1, the error calculated using Eqs. (C-3) and (C-4) is shown plotted as a function of the specimen thickness for various values of the specimen conductivity. The error is most sensitive to the magnitude of the specimen conductivity. The primary source of error in the low conductivity measurements at small thicknesses is the uncertainty in the specimen thickness; however, at large thicknesses and for transparent

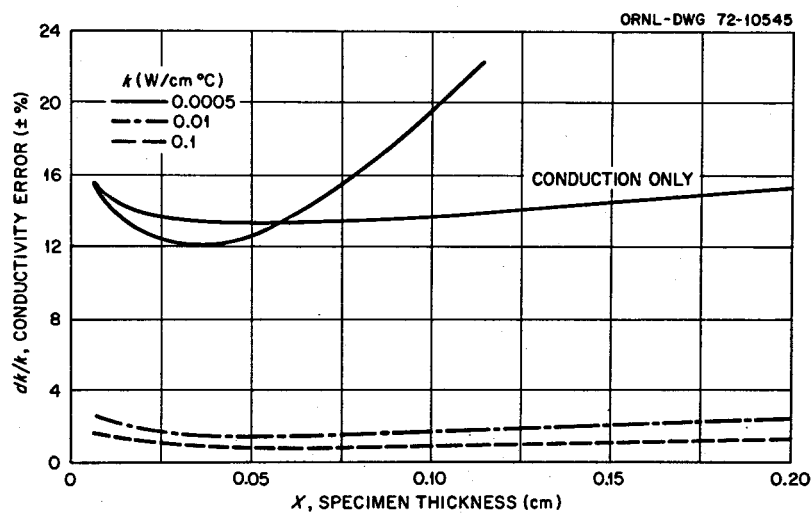
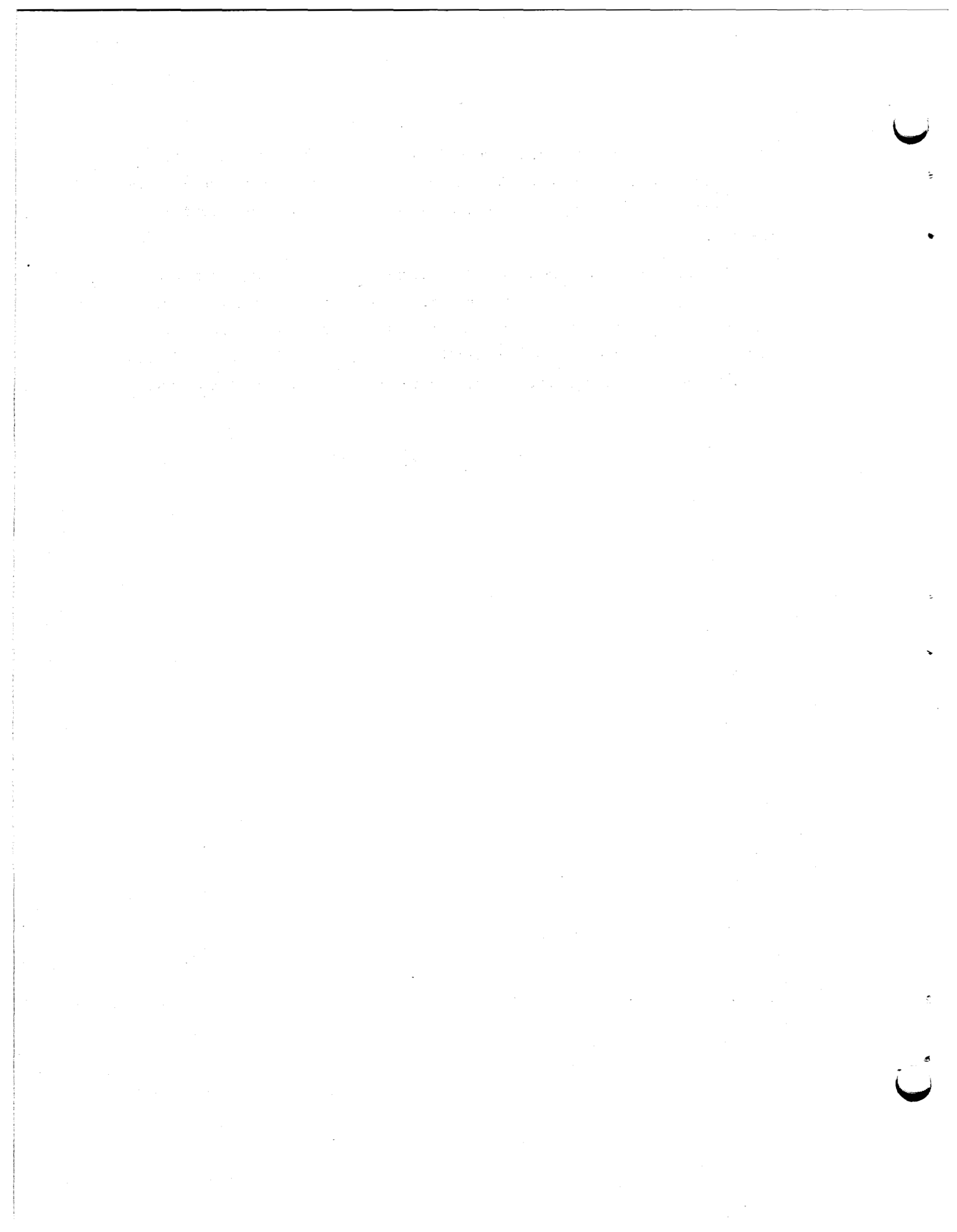


Fig. C-1. Estimated error in the conductivity measurements for the Apparatus III-B vs specimen thickness at an average specimen temperature of 600°C for various specimen conductivities. Radiation assumed ($\epsilon = 0.5$, $\bar{n} = 1.0$, $\bar{K} = 0$) except as noted.

specimens, the uncertainty in the emissivity and index of refraction cause the principal errors. The uncertainty in the temperature measurements comprises the primary source of errors in the high conductivity measurements.

The minimum error from Fig. C-1 occurs in the vicinity of $x = 0.05$ cm. Consequently, most of the experimental data were taken for specimen thicknesses of less than 0.1 cm. A plot of the estimated error limits as a function of specimen conductivity for a specimen thickness of 0.05 cm is shown in Fig. 22, Chapter 6, for the maximum and standard error, where

$$(dk/k)_{\max} = \sum_n (\text{error})_n .$$



INTERNAL DISTRIBUTION

- | | |
|--------------------------|--|
| 1. L. G. Alexander | 75. C. G. Lawson |
| 2. J. L. Anderson | 76. D. B. Lloyd |
| 3. C. F. Baes | 77. J. D. Lore (Y-12) |
| 4. S. E. Beall | 78. M. I. Lundin |
| 5. E. S. Bettis | 79. R. N. Lyon |
| 6. W. A. Bird | 80. H. G. MacPherson |
| 7. E. G. Bohlmann | 81. R. E. MacPherson |
| 8. R. B. Briggs | 82. H. E. McCoy |
| 9. R. H. Chapman | 83. D. L. McElroy |
| 10. S. J. Claiborne, Jr. | 84. L. E. McNeese |
| 11-40. J. W. Cooke | 85. J. R. McWherter |
| 41. W. B. Cottrell | 86. A. S. Meyer |
| 42. F. L. Culler | 87. C. A. Mills |
| 43. J. H. DeVan | 88. A. J. Miller |
| 44. J. R. DiStefano | 89. S. L. Milora |
| 45. S. J. Ditto | 90. W. R. Mixon |
| 46. W. P. Eatherly | 91. J. P. Moore |
| 47. D. M. Eissenberg | 92. R. L. Moore |
| 48. J. R. Engle | 93. S. E. Moore |
| 49. D. E. Ferguson | 94. E. L. Nicholson |
| 50. L. M. Ferris | 95. A. M. Perry |
| 51. M. H. Fontana | 96-97. M. W. Rosenthal |
| 52. A. P. Fraas | 98. J. P. Sanders |
| 53. W. Fulkerson | 99. W. K. Sartory |
| 54. R. B. Gallaher | 100. Dunlap Scott |
| 55. W. R. Gambill | 101. Myrtleen Sheldon |
| 56. W. R. Grimes | 102. J. D. Sheppard |
| 57. A. G. Grindell | 103. M. J. Skinner |
| 58. H. W. Godbee | 104. I. Spiewak |
| 59. T. G. Godfrey | 105. D. A. Sundberg |
| 60. R. H. Guymon | 106. R. E. Thoma |
| 61. P. N. Haubenreich | 107. D. G. Thomas |
| 62. R. B. Heimdal | 108. D. B. Trauger |
| 63. R. E. Helms | 109. J. L. Wantland |
| 64. R. F. Hibbs (Y-12) | 110. A. M. Weinberg |
| 65. H. W. Hoffman | 111. J. R. Weir |
| 66. P. P. Holz | 112. J. C. White |
| 67. W. R. Huntley | 113. G. D. Whitman |
| 68. P. R. Kasten | 114. R. P. Wichner |
| 69. J. J. Keyes, Jr. | 115. R. K. Williams |
| 70. O. H. Klepper | 116. H. C. Young |
| 71. T. G. Kollie | 117-119. Central Research Library |
| 72. A. I. Krakoviak | 120. Y-12 Document Reference Section |
| 73. T. S. Kress | 121-142. Laboratory Records Department |
| 74. J. W. Krewson | 143. Laboratory Records (RC) |

EXTERNAL DISTRIBUTION

- 144. R. U. Acton, Division 5322, Sandia Laboratories, P. O. Box 5800, Albuquerque, NM 87115
- 145. J. L. Bates, Hanford Engineering Development Laboratory, P. O. Box 1970, Richland, WA 99352
- 146. K. H. Bode, Physikalisch-Technische Bundesanstalt, Bundesallee 100, 33 Braunschweig, Germany
- 147. W. L. Carroll, National Bureau of Standards, Washington, DC 20234
- 148. B. C. Chu, Intern Business Machines Corp., Systems Development Division, Poughkeepsie, NY 12601
- 149. J. G. Cooke, National Research Council of Canada, Ottawa, Canada
- 150. D. F. Cope, AEC-OSR
- 151. G. L. Denman, Air Force Materials Laboratory, Wright-Patterson Air Force Base, OH 45433
- 152. C. T. Ewing, U. S. Naval Research Laboratory, Code G130, Washington, DC 20390
- 153. D. R. Flynn, Noise Section, National Bureau of Standards, Washinton, DC 20234
- 154. M. J. Laubitz, National Research Council of Canada, Ottawa, Canada
- 155. Kermit Laughon, AEC-OSR
- 156. W. Leindenfrost, Mechanical Engineering Department, Purdue University, Lafayette, IN 47901
- 157. P. E. Liley, TPRC, Purdue University, Lafayette, IN 47901
- 158. A. Lunden, Department of Physics, Chalmers University of Technology, Gothenburg S, Sweden
- 159. Tadashi Makita, Kyoto Technical University, Matsugasaki, Sakyo-Ku, Kyoto, Japan
- 160. J. Matolich, Jr., Battelle Memorial Institute, 505 King Ave., Columbus, OH 43201
- 161. E. McLaughlin, Chemical Engineering Department, Louisiana State University, Baton Rouge, LA 70803
- 162. M. L. Minges, Air Force Materials Laboratory, Wright-Patterson Air Force Base, OH 45433
- 163-164. MSBR Program Manager, AEC-Washington
- 165. K. K. Nangia, Heat Transfer Research, Inc., Alhambra, CA 91800
- 166. W. A. Plummer, Corning Glass Works, Corning, NY 80210
- 167. J. D. Plunkett, Department of Metallurgy, University of Denver, Denver, CO 80200
- 168. H. Poltz, PTB, Braunschweig, Germany
- 169. R. W. Powell, PRC, Purdue University, Lafayette, IN 47901
- 170. M. J. Rice, General Electric R&D Division, P. O. Box 8, Schenectady, NY 12301
- 171. J. T. Schreimpft, Naval Research Laboratory, Code 6330, Washington, DC 20390
- 172. R. M. Scroggins, AEC-Washington
- 173. M. Shaw, AEC-Washington
- 174. R. E. Taylor, TPRC, Purdue University, Lafayette, IN 47901
- 175. R. P. Tye, Dynatech R/D Company, 99 Erie Street, Cambridge, MA 02129

176. J. E. S. Venart, Department of Mechanical Engineering, University of Calgary, Calgary, Alberta, Canada
177. J. T. R. Watson, National Engineering Laboratory, East Kilbride, Glasgow, Scotland
178. A. E. Wechsler, A. D. Little Corporation, 20 Acron Park, Cambridge, MA 02141
179. G. K. White, C.S.I.R.O., Division of Physics, National Standards Laboratory, Sydney, Australia 2008
180. Patent Office, AEC, ORO
- 181-183. Directorate of Licensing, USAEC, Washington, DC 20545
- 184-185. Directorate of Regulatory Standards, USAEC, Washington, DC 20545
- 186-202. Manager, Technical Information Center, AEC
203. Research and Technical Support Division, AEC, ORO
- 204-418. Given distribution as shown in TID-4500 under Reactor Technology category (including 25 copies - NTIS)